

DENITRIFICATION BIOREMEDIATION: AMELIORATING EXCESSIVE N LOADING  
BY PUTTING MICROBES TO WORK

By

CASEY ADAM SCHMIDT

A DISSERTATION PRESENTED TO THE GRADUATE SCHOOL  
OF THE UNIVERSITY OF FLORIDA IN PARTIAL FULFILLMENT  
OF THE REQUIREMENTS FOR THE DEGREE OF  
DOCTOR OF PHILOSOPHY

UNIVERSITY OF FLORIDA

2011

© 2011 Casey Adam Schmidt

To my saintly wife Jennifer I would like to primarily dedicate this work. Though the journey has left me weary and my innocence decayed, you are a beacon of salvation in my universe.

“For small creatures such as we, the vastness is bearable only through love”  
Carl Sagan.

## ACKNOWLEDGMENTS

I would like to thank my wife Jennifer who has sacrificed enormously on my behalf and I will spend a lifetime repaying the debt. To my parents, who have been immeasurably kind and supportive of my endeavors. I would like to thank the agencies that funded this research, the Florida Department of Environmental Protection and the Florida Department of Agriculture and Consumer Services. I would particularly like to thank Mike Thomas at FDEP for supporting this project. I would like to thank Todd Stephens at the Holly Factory for being an incredibly supportive and willing participant in this research. Thanks to my advisor Mark Clark for being a mentor and eventually a friend. Although you understandably like to keep your fingers in projects to make sure they're successful, I'm glad you eventually came to trust me and give me some amazing opportunities for research. While I came to Florida as an aquatic ecologist, you helped me in becoming a wetland biogeochemist for a few years and using this experience as a bootstrap to becoming an ecological engineer. I can sum up my feelings on your guidance with the following quote: "I may not have gone where I intended to go, but I have ended up where I needed to be" – Douglas Adams. I would like to thank Dr. Jawitz for continued friendly and productive criticism, guidance, support and manuscript review. It gives one great confidence to have one's work thought highly by a respected professor. I would like to thank the rest of my committee Dr. Inglett, Cohen and Yeager for their guidance. This work wouldn't have been nearly as successful without Patrick Moran's persistence, diligence and dogged insistence on calling technical support at any opportunity. I would like to thank Ryan TenBroeck, Cody Smith and Ryan Hood for among other things, frequently siphoning sediments from above my weirs after the frequent Florida storms. The lab staff at the WBL including Yu Wang and Gavin Wilson

has contributed significantly towards this project. Mihai Giurcanu has been tremendously helpful in teaching me a semesters worth of statistics in two meetings. Lastly and most importantly, I would like to thank David Sutton (EMT) and my bicycle helmet, for without them this *work of staggering genius* wouldn't have been completed.

## TABLE OF CONTENTS

	<u>page</u>
ACKNOWLEDGMENTS.....	4
LIST OF TABLES.....	8
LIST OF FIGURES.....	9
LIST OF ABBREVIATIONS.....	11
ABSTRACT.....	12
CHAPTER	
1 GENERAL INTRODUCTION AND STATEMENT OF PROBLEM.....	14
Nitrogen in the Environment.....	14
Nitrogen from Agriculture.....	15
Nitrogen Aquatic Ecosystem Impacts.....	15
Denitrification.....	16
Limits to Denitrification in the Environment.....	19
Site Overview.....	20
Denitrification Bioreactors.....	22
Objectives and Hypotheses.....	26
2 EFFICACY OF A DENITRIFICATION WALL TO TREAT CONTINUOUSLY HIGH NITRATE LOADS.....	30
Background.....	30
Materials and Methods.....	32
Site Location and Construction.....	32
Denitrification wall Efficiency Measurements.....	34
Media Sampling.....	38
Media Characterization.....	39
Media Denitrification Rate.....	40
Statistical Analyses.....	42
Results and Discussion.....	43
Groundwater Hydrology.....	43
Nitrogen Concentrations in Well Transects.....	47
Media Potential Denitrification Rate.....	53
Microbial Biomass Carbon and Total Carbon.....	55
Total Carbon Mass Balance.....	56
Summary and Recommendations.....	58

3	EVALUATION OF A DENITRIFICATION WALL TO REDUCE SURFACE WATER NITROGEN LOADS .....	60
	Background.....	60
	Materials and Methods.....	61
	Site Location and Construction.....	61
	Surface Water Monitoring.....	62
	Results and Discussion.....	66
	Stream Oxygen Depletion .....	66
	Surface Water N Loading Reduction .....	68
	Nitrogen in groundwater versus surface water .....	73
	Summary of results.....	75
	Nitrogen load treatment costs .....	76
4	MODELING THE EFFECTS OF TEMPERATURE, HYDRAULICS AND MEDIA PHYSICO-CHEMICAL PROPERTIES ON DENITRIFICATION BIOREACTOR PERFORMANCE .....	77
	Background.....	77
	Materials and Methods.....	80
	Mesocosm Installation .....	80
	Media Physical Properties .....	85
	Media Hydraulic Conductivity .....	85
	Water Sampling and Analysis.....	86
	Media Sampling and Analysis .....	86
	Total Carbon and Carbon Quality .....	87
	Microbial Biomass Carbon.....	88
	Media Denitrification Rate .....	88
	Particle Surface Area .....	89
	Statistical and Data Analysis Methods .....	89
	Results.....	91
	Hydraulic Conductivity .....	91
	Dissolved Organic Carbon and Total Kjeldahl Nitrogen export.....	93
	Reaction Order .....	97
	Denitrification Rate .....	99
	Carbon Quality Transformations.....	108
	Predictors of Denitrification Rate .....	114
	Summary .....	120
5	CONCLUSIONS AND RECOMMENDATIONS .....	122
	Summary of Research .....	122
	Recommendations and Guidelines .....	125
	LIST OF REFERENCES .....	133
	BIOGRAPHICAL SKETCH.....	141

## LIST OF TABLES

<u>Table</u>	<u>page</u>
2-1	The hydraulic conductivity (Ksat) of the denitrification wall (center) and undisturbed soils upgradient (up) and downgradient (down) of the wall. .... 43
2-2	Groundwater velocity, flow length and detention time within the denitrification wall wells for Transects 1 - 3 (T1 - T3). .... 46
2-3	Influent NO <sub>3</sub> concentrations and percent NO <sub>3</sub> reduction values from the upgradient well to the center and downgradient wells. .... 50
2-4	Volumetric nitrate removal rates in May and July for the three transects (T1 – T3) ..... 51
3-1	Dissolved oxygen concentration (DO) and dissolved organic carbon (DOC) within receiving surface waters. .... 67
4-1	A summary of the bioreactor media treatments. .... 83
4-2	A statistical analysis on the hydraulic conductivity mean and rate of change (slope) from varying the wood volume and particle size. .... 93
4-3	Results from the first order decay model of dissolved organic carbon (DOC) over time for the treatments. .... 96
4-4	A statistical analysis of the effects on total Kjeldahl N (TKN) export rate from varying the wood volume, type and particle size. .... 96
4-5	A statistical analysis of the effects on nitrate reduction rate (Equation 4-2) from varying the wood volume, type and particle size. .... 103
4-6	A comparison of actual and predicted nitrate removal rates of other denitrification walls based on the model created in this study. .... 108
4-7	Changes of neutral detergent fiber (NDF), hemicellulose, cellulose, lignin and carbon within the study. .... 113
4-8	Correlations between measured predictors and nitrate reduction rate ( $\text{g m}^{-3} \text{d}^{-1}$ ) as determined from Equation 4-2 over all temperatures. .... 115
4-9	Parameters of the multiple regression model predicting nitrate removal rates as a function of temperature and media physicochemical properties. .... 120
5-1	A design guideline table relating the volumetric nitrate reduction rate ( $\text{g m}^{-3} \text{d}^{-1}$ ) to the groundwater temperature for three wood volumes measured. .... 130

## LIST OF FIGURES

<u>Figure</u>		<u>page</u>
1-1	Site location images for the property where the research occurred. ....	21
1-2	An orthophotograph of the focal agricultural property overlain with three-year average surface and groundwater N concentrations. ....	22
1-3	A diagram of a typical denitrification wall. ....	25
2-1	An orthophotograph delineating the land-use, denitrification wall location and streams at the study site. ....	33
2-2	Diagrams of the well transects within the denitrification wall. ....	35
2-3	A diagram of the soil and denitrification wall media collection locations. ....	39
2-4	Porewater velocities and direction at three depths within the denitrification wall center wells. ....	45
2-5	Dissolved organic C concentration in the upgradient, center and downgradient wells over time. ....	47
2-6	The concentrations of nitrate and total Kjeldahl N (TKN) over time within the upgradient, center and downgradient wells for all three transects. ....	48
3-1	A diagram of soil and water table elevation measured before the wall was installed and the approximate location of the wall. ....	62
3-2	Map of the denitrification wall, contributing edge of field perimeter, elevation and N load sampling stations at the treatment and control streams. ....	63
3-3	The correlation between discharge and N concentration between the control and treatment stream. ....	69
3-4	N concentration, load and hydrology values for the treatment and control stream before and after wall implementation. ....	72
4-1	A diagram of the continuous-flow mesocosm experiment used to test the impact of various treatments on nitrate removal rates. ....	82
4-2	A particle size analysis of the different wood media showing the percentages of wood mass within a given particle diameter range. ....	84
4-3	The saturated hydraulic conductivity for all treatments (wood volume, wood type and wood size) averaged over all sampling times. ....	92

4-4	Actual and modeled data for dissolved organic carbon (DOC) export rate per volume of bioreactor media over time for all treatments. ....	94
4-5	Figures demonstrating the zero order reaction kinetics of denitrification in this experiment.....	98
4-6	The nitrate reduction rate as a function of groundwater temperature for all the mesocosms treatments. ....	101
4-7	The results of the ANCOVA model comparing nitrate reduction rates across a range of temperatures. ....	104
4-8	Figures detailing the goodness of fit between the actual and predicted nitrate reduction rates of the ANCOVA statistical model. ....	106
4-9	Carbon quantity and quality values of the bioreactor media and changes in these values in the duration of the study. ....	110
4-10	A photograph of the bioreactor effluent from the first sampling indicating the dark color of the hardwood treatment. ....	112
4-11	Graphs detailing the accuracy of the multiple regression model.....	119
5-1	Design guidelines relating the time required to completely remove influent NO <sub>3</sub> concentrations as a function of groundwater temperature. ....	131

## LIST OF ABBREVIATIONS

BOD	Biological oxygen demand
D <sub>25</sub>	The particle diameter below which 25% of the sample is finer by mass.
D <sub>50</sub>	The particle diameter below which 50% of the sample is finer by mass, which is the mean diameter.
D <sub>75</sub>	The particle diameter below which 75% of the sample is finer by mass.
DEA	Denitrification enzyme activity
DNRA	Dissimilatory nitrate reduction to ammonium
DO	Dissolved oxygen
DOC	Dissolved organic carbon
$K_{sat}$	Saturated hydraulic conductivity
LOI	Loss on ignition
MBC	Microbial biomass carbon
NDF	Neutral detergent fiber
PRB	Permeable reactive barrier
TKN	Total Kjeldahl nitrogen
TOC	Total organic carbon

Abstract of Dissertation Presented to the Graduate School  
of the University of Florida in Partial Fulfillment of the  
Requirements for the Degree of Doctor of Philosophy

DENITRIFICATION BIOREMEDIATION: AMELIORATING EXCESSIVE N LOADING  
BY PUTTING MICROBES TO WORK

By

Casey Adam Schmidt

December 2011

Chair: Mark Clark

Major: Soil and Water Science

Nitrate contamination in groundwater and surface waters draining agricultural lands is a continuing problem. Denitrification walls are a permeable reactive barrier constructed by introducing an organic C amendment in contact with flowing groundwater to stimulate denitrification and reduce nitrate concentrations. In this study, a 55 m long, 1.7 m wide and 1.8 m deep denitrification wall was installed in a container-plant nursery within the watershed of the Santa Fe River, Florida. The denitrification wall was located adjacent to the headwaters of a stream draining the property in order to target an area where groundwater was focused. Due to the proximal stream, porewater velocity within the wall was relatively rapid ( $1.7 \text{ m day}^{-1}$ ) with shorter detention times (1.7 – 1.9 days) than other denitrification walls, although the entire influent nitrate load was reduced for a total N reduction of  $220 \pm 54 \text{ kg yr}^{-1}$ . Maximum nitrate removal rates per volume of media ( $4.9 - 5.5 \text{ g-N per m}^{-3} \text{ d}^{-1}$ ) were higher than other sand-sawdust walls with no significant declines in total media C observed over the 18-month study. This indicates the potential to sustainably treat groundwater even with high nitrate loading rates. Nitrate load reductions were even greater within the targeted downgradient stream, which declined by approximately 65% ( $345 \text{ kg yr}^{-1}$ ) thus indicating

the extended impact of the denitrification wall beyond the immediate boundaries. This extended impact was inauspiciously confirmed when dissolved oxygen (DO) levels at the headwaters of the receiving stream declined from approximately 2.3 to a low of 1.2 mg L<sup>-1</sup> for approximately 50 days, then stabilized at previous levels. This DO reduction was driven by an increased biological oxygen demand due to C leaching from the freshly installed sawdust. As a result of the success of this denitrification wall, a continuous groundwater flow mesocosm study was implemented. The objective of this study was to parameterize denitrification wall performance as a function of the physicochemical properties of the media and to develop applicable design guidelines. Groundwater temperature was found to be the most significant driver of denitrification rates, although the total wood volume and hydraulic and physicochemical properties of the bioreactor media such as surface area and carbon bioavailability all influenced rates. Based on these findings a design model was created to guide future denitrification wall construction. This study indicates the significant potential to efficiently and effectively decrease nitrate loading in surface and groundwater draining agricultural lands.

## CHAPTER 1 GENERAL INTRODUCTION AND STATEMENT OF PROBLEM

### **Nitrogen in the Environment**

The total mass of N in the atmosphere, soils, and waters on earth is more than the mass of all other major life-sustaining nutrients (C, P and S) combined (Mackenzie, 1995). But 99% of this N is unavailable to 99% of living organisms because it is present as elemental N, which contains a triple bond that is energetically costly to utilize (Galloway et al., 2003). The demand for this essential nutrient has created a strong selection pressure and several species of N fixing bacteria have evolved to overcome this energetic hurdle. In 1909, with the successful demonstration of the Haber-Bosch process, the triple bond of elemental N was broken by human action, albeit still at a high energetic cost. This breakthrough ushered in an increase in food production to such an extent that it is estimated 40% of the world's population owes their life to the Haber - Bosch process (Smil, 2001). As a result of this technological innovation, humanity has blanketed much of the planet with synthetic N.

In the last few decades US fertilizer consumption has increased 20-fold, and the Haber-Bosch process has now surpassed worldwide bacterial N fixation (Galloway, 2008; Puckett et al., 1995). Human alterations to the N cycle, including fertilizer applications, N-fixing leguminous crops, and the burning of fuels, has doubled the rate of N input to terrestrial systems (Vitousek et al., 1997). Rising demands for food, biofuels and other crops will ensure that N demand will continue to increase in the future. Between 2009 and 2013, world fertilizer demand is projected to increase by 10.9% to 146 Tg, while consumption of N fertilizers in North America alone will increase approximately 6% to 28.6 Tg during the same time frame (FAO, 2008). This

monumental transformation of N from relatively stable atmospheric pools to the landscape will continue to drastically alter the cycling of this essential nutrient.

### **Nitrogen from Agriculture**

Agriculture is the most extensive source of nitrate to groundwater and increases in nitrate within shallow groundwater due to modern agricultural practices have been well documented (Hill, 1983; Anderson and Kristiansen, 1984; Hallberg, 1989; Puckett et al., 1999; Refsgaard et al., 1999; Hudak, 2000; Nolan and Stoner, 2000; Nolan, 2001; Breemen et al., 2002). Yet the efficiency of N applied for crop production is generally low. It is estimated that approximately 33% of N added to agroecosystems is consumed by humans or livestock, while 65% is lost to the atmosphere or aquatic ecosystems (Smil 2001, 2002; Galloway 2003). Additionally it has been estimated that in the United States, farmers typically over fertilize with N by 20 to 38% (Babcock and Blackmer, 1992; Hong et al., 2007; Trachtenberg and Ogg, 1994). As a result of this low efficiency, the highest median concentrations of groundwater nitrate are present beneath agricultural lands (Nolan and Stoner 2000; Freeze and Cherry 1979). The ubiquitous presence of nitrate in shallow groundwater below agricultural lands has impacted some larger regional aquifers at significant concentrations. Concentrations of nitrate exceeding USEPA maximum contaminant levels for drinking water of 10 ppm have been observed in 15% of groundwater samples from 4 of 33 major regional aquifers used for drinking water (Nolan and Stoner, 2000; USEPA, 1996). Minimizing the impact of nitrogen from agricultural effluent will continue to be a pressing concern.

### **Nitrogen Aquatic Ecosystem Impacts**

Elevated nitrate concentrations can modify natural ecosystems in a significant manner at concentrations well below the drinking water standards of 10 mg/L. Within

aquatic ecosystems, elevated N has been implicated in chlorophyll-a increases, decreased water clarity, increased phytoplankton growth, declines in dissolved oxygen, species composition changes, and fish reproductive morphology modifications in freshwater springs (Cowell and Dawes, 2006; Edwards and Guillette, 2007; Edwards et al., 2006; Goolsby and Battaglin, 2000; Quinlan et al., 2008). The dominant paradigm is that N is limiting in coastal marine systems and that P is the limiting in freshwater ecosystems, particularly lakes (Howarth et al., 2000; Rabalais et al., 2001; Schindler, 1977). A dramatic example of the impact of N loading on coastal systems is the annual appearance of hypoxic dead zones in the Gulf of Mexico from distant agricultural effluent (Goolsby and Battaglin, 2000). However, in freshwater ecosystems recent reviews have cast doubt on this paradigm, demonstrating that N and P limitation are equivalent in freshwater lakes and rivers (Elser et al., 2009; Elser et al., 2007; Lewis and Wurtsbaugh, 2008). As a consequence, the effective mitigation of agricultural runoff containing N will continue to be essential to prevent ecological impacts to freshwater and marine ecosystems.

### **Denitrification**

Much of the N applied to the landscape as synthetic fertilizers is returned to the atmosphere via the naturally attenuating process of denitrification. Denitrification occurs as a result of constraints introduced on the dissimilatory metabolism of the microbial community when oxygen becomes depleted. Oxygen respiration provides the greatest amount of energy to the microbial community. Although in environments where oxygen respiration has depleted oxygen as an electron acceptor, alternate electron acceptors such as nitrate can be utilized in the denitrification process to gain energy (Reddy and Delaune, 2008). Denitrifying bacteria are generally facultative aerobic bacteria

commonly present in all soils that possess the adaptive ability to create enzymes for denitrification in the absence of oxygen (Tiedje, 1982). In most instances, denitrification occurs when the presence of organic C induces aerobic decomposition, a process that consumes oxygen. This process is usually represented by Equation 1-1.



In environments with little to no atmospheric contact, this results in net oxygen consumption. Net oxygen consumption is particularly prevalent in continuously saturated environments because oxygen diffusion in water is approximately 10,000 times slower than in air (Reddy and Delaune, 2008). Once dissolved oxygen is consumed, nitrate serves as an alternate electron acceptor in place of more energy-yielding oxygen and the organic C serves as an electron donor. This is a redox reaction represented with glucose as an electron donor as shown below in Equation 1-2.



Denitrification is an energy-yielding process of unique significance since it reduces nitrate to dinitrogen gas ( $\text{N}_2$ ), which is released back in to the atmosphere.

Denitrification is a major component of the N cycle in many ecosystems. Globally, denitrification is ubiquitous in a variety of ecosystems with continental shelf sediments accounting for 44% of global denitrification, followed by terrestrial soils (22%), freshwater systems (groundwater, lakes, rivers) (20%), oceanic oxygen minimum zones (14%) and estuaries (1%) (Seitzinger et al., 2006). The diversity and distribution of microbial species with the denitrifying capacity is greater than any of the other inorganic biotransformations and among the soil biogeochemical process, there are more species with denitrification capacity than any other process (N fixation, DNRA, etc.) except

respiration (Tiedje et al., 1989; Tiedje, 1982). The major denitrifying enzyme nitrite reductase, seems to have evolved twice using different means to achieve the same process, indicating that there has been a strong selection pressure to gain energy from this process in the many anaerobic environments globally (Tiedje et al., 1989). The prevalence of denitrifiers in many ecosystems and the terminal atmospheric end-product ( $N_2$  gas) makes this an important component of N cycling.

Denitrification has been documented as a significant loss mechanism for nitrogen in many agroecosystems. Several researchers have estimated the amount of fertilizer that is denitrified in agroecosystems and the reported results vary from 5-45% (Galloway et al., 2003) and 0-70% with a mean centered around 20-30% (Tiedje 1982). Reviews of the estimates of denitrification in groundwater alone are highly variable as well (Groffman et al., 1989; Nolan, 1999). This variability across landscapes and poor estimation is likely due to climate and drainage differences among sites (Galloway et al., 2003; Nolan and Stoner, 2000). The processing of N across the landscape is quite variable between watersheds and it depends on the presence of organic-rich anaerobic zones such as seepage slopes, wetlands and a strong degree of connectivity between the groundwater and the riparian zone (Bohlke and Denver 1995). Galloway et al. (2003) estimates that along a typical wetland-stream-river network, the cumulative N removal through denitrification may be as much as 30-70% with each ecosystem component only causing 1-20% of the removal. Contrastingly there are well-documented examples such as the Mississippi river basin where N applied as fertilizer is spread for hundreds of miles to coastal regions from areas far removed from the ocean (Goolsby and Battaglin, 2000). As is demonstrated by this far-reaching impact

and the increasing N concentrations documented in many regions, denitrification rates aren't sufficient to protect receiving water bodies and nitrogen pollution has consequently become a critical concern.

### **Limits to Denitrification in the Environment**

The presence of shallow groundwater draining horizontally through surface soils is highly suitable for denitrification due to the close interaction between groundwater and high C riparian areas (Cooper, 1990; Hill, 1996). Therefore, it is likely that there is some denitrification occurring in groundwater that is transported through riparian areas into streams. Even though denitrification is occurring in riparian zones, the effect on overall nitrate concentration is often diluted when the majority of the groundwater does not contact high C riparian zones and is instead transported through sandy vadose zones or less C rich riparian areas (Cooper, 1990; Hill, 1996; Schipper and Cooper, 1993). Additionally, riparian subsoils may not have enough C and/or may not be waterlogged frequently enough to support continuously active denitrifying microbial communities (Lowrance, 1992). Still others have found that the distribution of C in subsoils is so patchy that denitrification only occurs in sparse hotspots of buried C (Addy and Gold et al., 1999; Groffman and Tiedje, 1989; Jacinthe and Groffman, 1998; Parkin, 1987). Still there is a large potential to increase denitrification in contaminated groundwater by increasing the contact with zones of saturation and high soil C before reaching sensitive surface water bodies. The overarching goal of this research will be to determine the feasibility of utilizing groundwater bioremediation to increase denitrification rates in groundwater within agricultural properties to prevent impacts to sensitive receiving water bodies. To achieve this objective, a carbon-amended permeable reactive barrier,

termed a denitrification bioreactor, will be installed within an agricultural property in North-Central Florida.

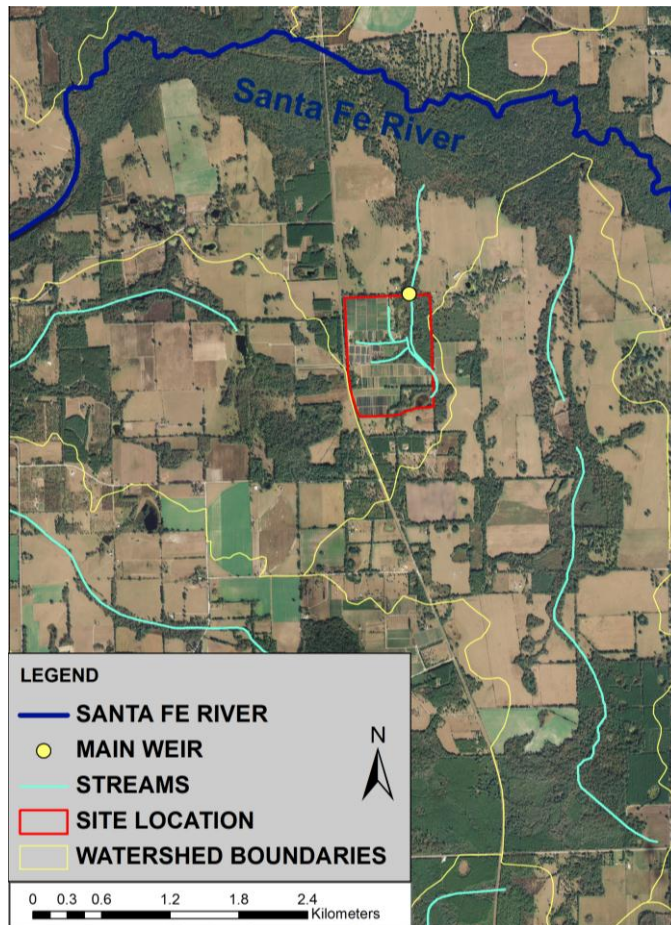
### **Site Overview**

The study area where this research occurred is on a 160-acre container nursery in Alachua Florida, which contains approximately 100,000 – 200,000 containerized plants destined for the commercial landscape market. The property is located within the Santa Fe river watershed, which is a part of the greater Suwannee River Basin located in north-central Florida (Figure 1-1). The Santa Fe River watershed encompasses approximately 3,500 km<sup>2</sup> and flows for 121 km before entering the Suwannee River which ultimately discharges to the Gulf of Mexico. Both the Santa Fe and Suwannee rivers have total maximum daily load (TMDL) restrictions for nitrate (Hallas and Magley, 2008). In addition, the EPA has proposed numeric nutrient criteria for nitrate in Florida's lakes and streams that are one to two orders of magnitude lower than the drinking water standards of 10 mg L<sup>-1</sup> (FDEP, 2009). These regulations require much greater reductions in nitrate loading from agricultural sources within the watershed.

The landowner of the study area has taken precautions to minimize N losses including using precision micro-jet irrigation and controlled-release fertilizer on the property. Recent improvements in irrigation efficiency have reduced the leaching from each container by more than half at this site. These efficiency improvements appear to be reaching a ceiling, and groundwater and surface water concentrations remain quite high (Figure 1-2). As a result of these limitations on fertilizer efficiency improvements, the use of groundwater bioremediation as a supplemental N mitigation technique to treat agricultural effluent will be evaluated on this property.



A



B

Figure 1-1. Site location images for the property where the research occurred. Shown in the figures are a (A) large-scale site location map and a (B) localized aerial photograph of the research site. Map created by author, using publicly available orthophotographs from (ACPA, 2006), watershed boundaries from (FDEP, 1997-98) and streams from (USGS, 2006).

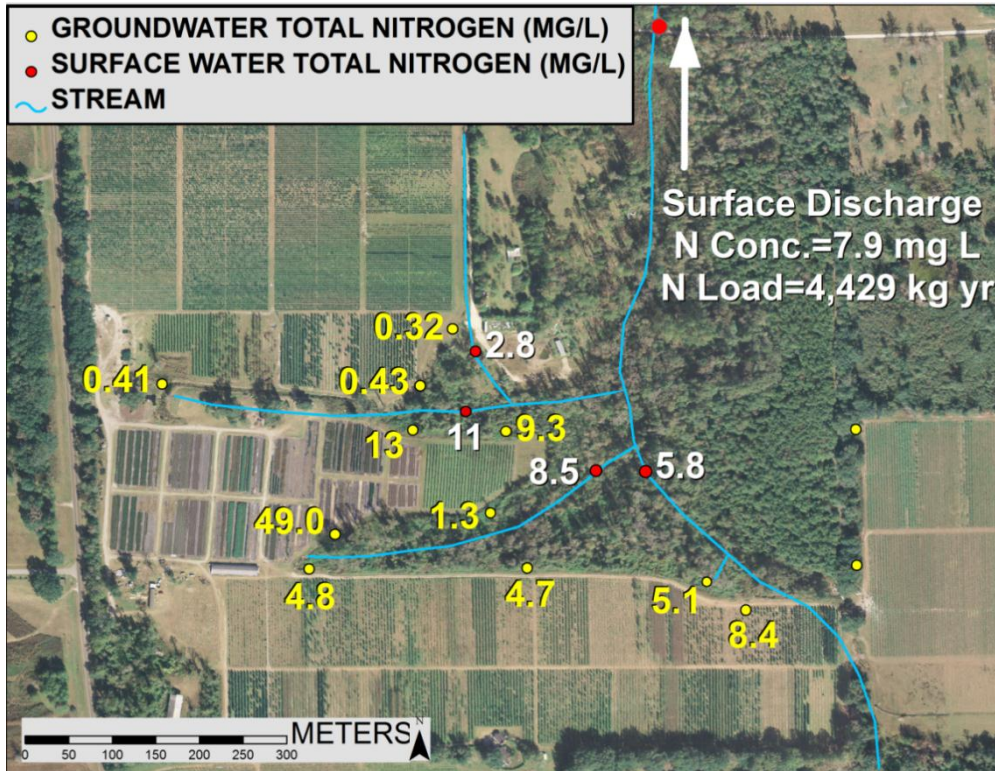


Figure 1-2. An orthophotograph of the focal agricultural property overlain with three-year average surface and groundwater N concentrations. Map created by author, using publicly available orthophotographs from (ACPA, 2006).

### Denitrification Bioreactors

Mitigation of nitrate-contaminated groundwater below agroecosystems presents a difficult problem because the environmental contaminant is diffuse. As a result of this widespread contamination, pragmatically remediating N-contaminated groundwater requires cost-effective, low maintenance systems that can provide long-term treatment over a wide area with minimal impact to production. One method that possibly fits these requirements is a denitrification bioreactor. A denitrification bioreactor is a mitigation strategy that involves introducing an organic C amendment in contact with high nitrate flowing groundwater to create suitable conditions for microbial denitrification. The C amendment serves as an electron donor firstly in aerobic respiration and subsequently

in microbial denitrification. Because these bioreactors take advantage of gravitational flow gradients, it is a low maintenance, passive treatment option.

The successful application of these bioreactors to stimulate nitrogen removal from groundwater was first demonstrated 15 years ago on a pilot-scale for septic system effluent (Robertson and Cherry, 1995). This project demonstrated that bioreactors constructed simply of a combination of sawdust, rye seed and compost have the potential to completely remediate groundwater N concentrations as high as 50 mg L<sup>-1</sup> (Robertson and Cherry, 1995). Although the small-scale of the bioreactor had minimal effect on the total groundwater N pool even immediately downgradient from the bioreactor (Robertson and Cherry, 1995). Shortly after this project a much larger denitrification bioreactor was installed from a mixture of native soils and pine sawdust in New Zealand (Schipper and Vojvodic-Vukovic, 1998). This project demonstrated that microbial denitrification specifically was completely removing N from the groundwater to the atmosphere in these bioreactors (Schipper and Vojvodic-Vukovic, 2000). The sustainability of these treatment systems to continue removing nitrogen from groundwater was first demonstrated after 5 years (Robertson and Cherry, 2000; Schipper and Vojvodic-Vukovic, 2001) and subsequently bioreactors have been shown to continue reducing nitrogen in excess of 60-90% after approximately 15 years (Long et al., 2011, Moorman et al., 2010; Robertson, 2008). Based on these studies, denitrification bioreactors have been shown to be a long-term, maintenance-free treatment system consisting simply of low-cost organic C sources.

These first denitrification bioreactors demonstrated a proof of concept for treating small pockets of groundwater. Pragmatically achieving significant reductions in

contamination as widespread as the Mississippi River basin will require cost-effective and efficient bioreactor designs that will treat large volumes of water. The design of bioreactors takes on many forms, mostly dependent on the hydraulics of the affected influent waters. The two predominant types of denitrification systems are denitrification beds and denitrification walls, both termed bioreactors (Schipper et al., 2010b).

Denitrification walls are traditional permeable reactive barriers (PRBs) inserted vertically into the ground to intercept groundwater flow (Figure 1-3). The first seminal bioreactors would be categorized as denitrification walls (Robertson and Cherry, 1995; Schipper and Vojvodic-Vukovic, 1998). The denitrification process is stimulated in denitrification walls through the mixing of a C substrate within the soil to maintain structure.

Denitrification beds are used in locations where discharges are controlled naturally or through tile-drainage and mostly consist of containerized treatment systems usually of wood-chips alone (Blowes et al., 1994; Robertson et al., 2009; Schipper et al., 2010a). Additionally streambed bioreactors have been used by focusing surface waters below grade through porous media into a reactor zone filled with the wood media and covered by an impermeable surface (Robertson and Merkley, 2009). Nitrate removal rates per media volume within denitrification beds tend to be much higher than denitrification walls owing to the fact that beds often consist of woodchips only, while walls are usually mixed with soils (Schipper et al., 2010b). Additionally because denitrification beds are treating controlled discharges with high denitrification rates, they have the potential to significantly reduce N loads in effluent. This characteristic has shifted much of the research focus towards utilizing denitrification beds. However in many situations, surface soils are well drained, concentrated and controlled discharges are not present

or feasible, nitrate contamination is more diffuse, and mounding of groundwater or manipulation of seepage stream flow may be undesirable or prohibited by law. Under such conditions a long and narrow denitrification wall that passively intercepts flow, but does not appreciably change groundwater flow characteristics is the only suitable option.

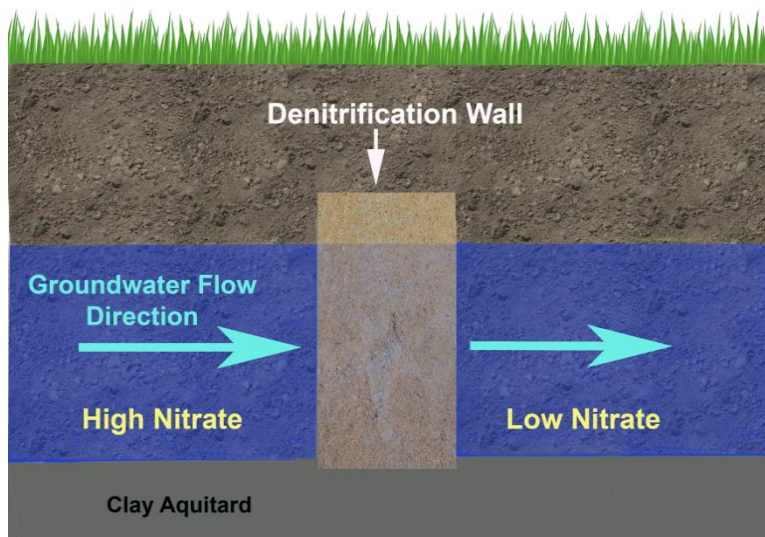


Figure 1-3. A diagram of a typical denitrification wall. Sawdust is usually mixed in to the soil structure, so that denitrification rates of passively flowing groundwater are increased.

In order to pragmatically reduce non-point source N loading from agricultural properties, efficiently sized denitrification walls spread over the landscape need to treat large volumes of groundwater rapidly. This will require transferable knowledge of nitrogen reduction rates and assessment methods to increase treatment volumes by focusing denitrification wall installations. Therefore in this study, the efficacy of a targeted denitrification wall to efficiently and rapidly treat high N loads in groundwater before discharging to surface waters will be assessed on the agricultural property. Secondly, the effect of wood media physicochemical properties on denitrification

bioreactor performance will be parameterized through on-site experimental research to guide future wall design.

### **Objectives and Hypotheses**

To reduce the N concentration in groundwater before discharging to surface waters, the denitrification wall was placed immediately upgradient of a stream headwaters. The headwaters of the stream begins as a significant seepage slope discharge where a decline in surface elevation brings groundwater to the surface. There are advantages and disadvantages to locating a denitrification wall proximal to a significant surface water discharge.

A large magnitude seep likely indicates that high volumes of groundwater from a wide area are directed to this location. While this groundwater focusing will allow for maximizing treatment volume, initial assessments indicate that porewater velocities at this site ( $1.1 \text{ m d}^{-1}$ ) are one to three orders of magnitude higher than other denitrification walls ( $0.007$  to  $0.47 \text{ m day}^{-1}$ ) (Robertson and Cherry, 1995; Schipper and Vojvodic-Vukovic, 2000; Schipper et al., 2005). Based on measured nitrate concentrations and assuming a 50% effective porosity, the denitrification wall would be receiving a loading rate of  $4,400 \text{ mg m}^{-2} \text{ d}^{-1}$ , which is an order of magnitude higher than the New Zealand wall which has loading rates of  $160 - 300 \text{ mg d}^{-1}$ , thus pushing the efficacy of a denitrification wall to the limits (Schipper and Vojvodic-Vukovic, 2000). But this New Zealand wall and many others are likely N-load limited, because nitrogen is depleted rapidly under these low loading conditions and long detention times. It is likely that the denitrifying microbial community is less responsive to concentration alone, but the rate of access to nitrate, which is more a function of nitrate loading rate. Increasing the loading rate on denitrification walls will allow for a more accurate assessment of

maximum nitrate removal rates. One potential problem with high N-loading rates, is that carbon consumption is likely to be higher thus possibly limiting the longevity of the denitrification wall. For denitrification walls to be a pragmatic mitigation approach, they need to not only treat high volumes of groundwater but also to be maintenance-free for at least more than a decade. The ability of a denitrification wall to markedly and sustainably reduce N under high loading conditions was evaluated through a well transect study and the analysis of soil chemical and microbiological properties. The hypotheses and objectives for Chapter 2 are listed in the following text:

- Hypothesis 2-1. Nitrate reduction rates are generally underestimated and will therefore increase in a denitrification wall with high nitrate loads.
- Hypothesis 2-2. Nitrate not transformed to other N forms will be reduced as a result of denitrification.
- Objective 2-1. Determine if rates of C consumption are sufficiently low that the wall will function sustainably for more than a decade under high N-loading

Remediating contaminated groundwater before discharging to surface waters is difficult because exposure pathways to surface waters via seepages, deeper groundwater recharge and the stream vadose zone are difficult to target. Although denitrification walls have been successful in treating relatively localized *groundwater* plumes, no other study has determined if they can be effective as a management practice to meaningfully reduce *surface water* N loads from agricultural properties. In order to pragmatically achieve measurable reductions in surface water nitrogen loads from agricultural properties, denitrification walls need to be scaled to treat significant volumes of water with relatively short detention times. Achieving reductions in surface water N loads will be required for a given nutrient management practice to be

considered successful towards achieving TMDLs and numeric nutrient criteria.

Additionally, the majority of the detrimental impacts from excessive N are expressed in surface waters and not groundwater. The development of assessment techniques for determining the location of denitrification wall installations will aid in the success of this technology. In this study, the use of a denitrification wall adjacent to a significant surface water discharge was evaluated as a technique for targeting treatment to achieve large reductions in surface waters. Therefore, the impact of this denitrification wall at the watershed scale was evaluated. The hypothesis and objective of Chapter 3 are described below:

- Objective 3-1. Determine if targeting a denitrification wall adjacent to surface water discharges can treat disproportionately large groundwater areas
- Hypothesis 3-1. Nitrate loads will decrease in a receiving stream solely as a result of the denitrification wall installation.

For denitrification bioreactors to become endemic to agricultural N management requires generalizable design guidelines. Denitrification bioreactors have been constructed using a variety of media types, concentrations and particle sizes, yet few inferences can be made on the relative success of these different treatments. Additionally more in-depth analyses on the relationships between denitrification rate and groundwater temperatures as well as the physical, chemical and hydraulic properties of a given bioreactor media will need to be quantified for this technology to flourish. To answer these questions, an experiment was conducted to understand the drivers of denitrification rate and parameterize these bioreactors as a function of media physicochemical properties and more pragmatic qualitative metrics. The hypotheses and objectives of Chapter 4 are detailed in the following text:

- Objective 4-1. Infer denitrification wall performance from qualitative and quantitative predictors to guide design
- Hypothesis 4-1. Nitrogen reduction rates will increase with greater wood volume ratios and smaller wood sizes.
- Hypothesis 4-2. Hydraulic conductivity will decrease with declining wood sizes.
- Hypothesis 4-3. Nitrogen reduction rates will be higher in bioreactor media with greater total C content, bioavailable fiber components and surface areas.

In the conclusion (Chapter 5), the results will be summarized and specific recommendations will be made for the use of denitrification walls based on the findings of Chapters 2-4.

## CHAPTER 2 EFFICACY OF A DENITRIFICATION WALL TO TREAT CONTINUOUSLY HIGH NITRATE LOADS

### **Background**

Scaling-up denitrification walls for widespread application to reduce groundwater nitrate requires efficiently maximizing treatment area and volume. The appropriate size of a denitrification wall depends on site-specific conditions such as temperature, influent nitrate concentration and porewater velocity as well as transferable and accurate knowledge of in-situ nitrate removal rates of sand-sawdust mixtures. Nitrate removal rates within denitrification walls vary widely in the literature from 0.014 – 3.6 g-N per m<sup>3</sup> of media per day (Jaynes et al., 2008; Robertson et al., 2000; Schipper et al., 2005; as compiled in Schipper et al., 2010b). This variability is driven in part by differences in the site-specific conditions mentioned. Still, estimates of potential nitrate removal rates may be underestimated due to low N loading and long detention times between sampling locations that causes nitrate to become limiting before sampling occurs. As a result, these estimates of nitrate reduction rate may underestimate the true treatment potential and suggests most denitrification walls are oversized.

One standardized method for inferring nitrate removal rates is to analyze potential denitrification rates of media samples in the laboratory. Potential denitrification rates have been shown to be both over and underestimates of rates measured in the field in different studies (Schipper and Vojvodic-Vukovic, 2000; Schipper et al., 2004; Schipper et al., 2005). This variability owes to the problems with all laboratory methods when field-conditions are to be inferred from spatially diffuse samples. Another method used to infer maximum nitrate removal rates involved temporarily dosing a denitrification wall with elevated nitrate loads in-situ, which yielded mass removal rates of 1.4 g-N m<sup>3</sup> day<sup>-1</sup>

(Schipper et al., 2005). Increasing the N load in this dosing study did increase nitrate reduction rates, nevertheless the authors concluded that in this experiment the denitrification wall was still nitrate limited. Uncertainty still remains in inferring maximum nitrate removal rates in order to effectively size denitrification walls.

One potential method for increasing treatment volume and quantifying maximum N removal rates is to locate the wall adjacent to an area of elevated groundwater flow such as a proximal ditch or in riparian areas where groundwater discharges to surface water. Many previous denitrification walls may be N-load limited. It is likely that the microbial community is less responsive to concentration alone but the rate of access to nitrate, which is a function of loading rate. In this study, a denitrification wall was constructed as an edge-of-field treatment in an area of continuously high groundwater nitrate load. The continuously high nitrate load of this project provides another method to infer maximum nitrate removal rates over long time periods as well as to determine the upper limits of N-loading to denitrification walls. Before construction, monitoring of an adjacent well for 15 months yielded nitrate concentrations of  $8 \text{ mg L}^{-1}$  and groundwater velocities ( $1.1 \text{ m day}^{-1}$ ) one to three orders of magnitude faster than velocities in other denitrification walls ( $0.007$  to  $0.47 \text{ m day}^{-1}$ ) (Robertson and Cherry, 1995; Schipper and Vojvodic-Vukovic, 2000; Schipper et al., 2005). The rapid groundwater velocity is due to a steep hydraulic elevation gradient induced by the close downgradient proximity of a seepage slope, which forms the headwaters of a stream. Based on these high loading rates, the efficacy of denitrification walls to rapidly treat groundwater will be pushed to the limits. Carbon consumption in denitrification walls with high loading rates is expected to be higher, possibly decreasing wall lifespan. For

denitrification walls to be a pragmatic treatment option, they need to be able to significantly reduce N loads over long durations. As a result, the longevity of the denitrification wall will be estimated. The hypotheses of this study are listed in the following text:

- Hypothesis 2-1. Nitrate reduction rates are generally underestimated and will therefore increase in a denitrification wall with high nitrate loads.
- Hypothesis 2-2. Nitrate not transformed to other N forms will be reduced as a result of denitrification.
- Objective 2-1. Determine if rates of C consumption are sufficiently low that the wall will function sustainably for more than a decade under high N-loading

## **Materials and Methods**

### **Site Location and Construction**

The denitrification wall was located at the edge of an agricultural field, adjacent to a small stream, which begins as a significant seepage discharge (Figure 2-1). Soils in the groundwatershed of the denitrification wall range from the excessively well-drained Lake series to the moderately well drained Tavares series (USDA, 1985). Both soils consist of at least 93% sands down to 2 meters with 47% of the sands composed of particles between 0.25-0.5 mm in diameter and 36% composed of particles between 0.1-2.5 mm (USDA, 1985). A clay aquitard consisting of translocated clays (B<sub>t</sub> horizon) and Miocene age clay deposits of the Hawthorne formation are present, 2 - 2.4 m below the surface. Generally, excessive N leaching from the bottom of the plant container drains rapidly through the surface soils and is perched on top of the clay aquitard. This shallow groundwater is transported laterally towards the edge of the property where a relatively sharp decline in elevation forces groundwater to the surface in numerous

seepage slopes. Although, while clay-rich soil horizons are known to limit groundwater movement, this hydrologic evaluation is complicated by the fact that the groundwater was observed to flow rapidly through conduits in the upper portion of these clay horizons.

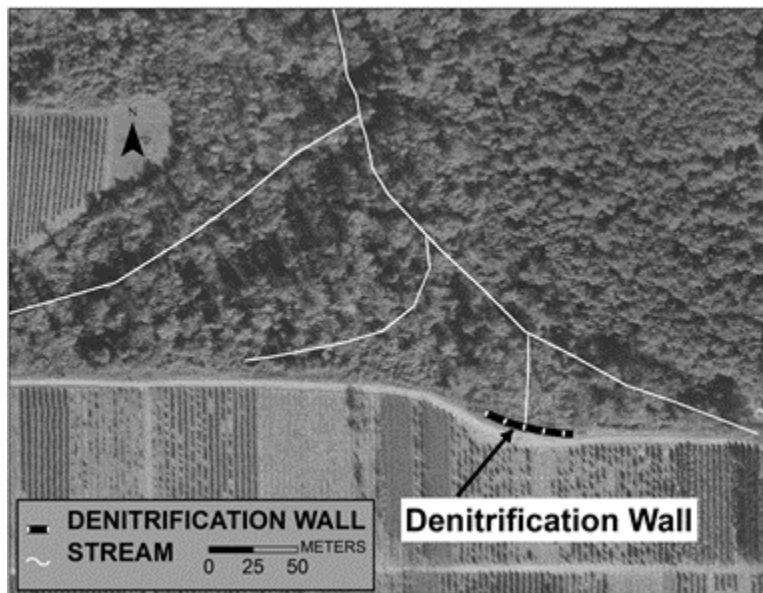


Figure 2-1. An orthophotograph delineating the land-use, denitrification wall location and streams at the study site. Map created by author, using publicly available orthophotographs from (ACPA, 2006)

The denitrification wall was constructed September 30<sup>th</sup>, 2009. The lowest depth of the wall is just below the elevation of the main surface water seep and the shallowest depth was 1.8 m. above that, at a height that for two years had been the highest water table measured. The final dimensions of the wall were 55 m long, 1.7 m wide and 1.8 m deep. A commercially available washed and sieved quartz sand (Edgar Minerals, Inc., Edgar, Florida) with a narrow particle diameter range of 0.106-0.15 mm was mixed with bark-free pine sawdust in a 1:1 ratio by volume. The pine sawdust was relatively coarse with a wide range of particle diameters. The particle diameter, below which 25% of the sample is finer by mass ( $D_{25}$ ), is 1.4 mm, the  $D_{75}$  is 4 mm and the mean particle diameter ( $D_{50}$ ) is 2.5 mm. The sand and sawdust were thoroughly mixed above ground,

and then as soil and groundwater were excavated along the trench, the sand:sawdust media was rapidly placed in the excavated pit to minimize any water intrusion into the trench or sidewall collapse. After construction, subsamples confirmed homogenous organic matter content in the mixed medium.

### **Denitrification wall Efficiency Measurements**

Monitoring wells were installed to the bottom of the denitrification wall in three parallel transects using United States environmental protection agency (USEPA) guidelines (USEPA, 2008) (Figure 2-2). These wells were placed in three parallel transects upgradient, within (center), and downgradient of the denitrification wall to monitor changes in nitrate, dissolved organic C (DOC) and total Kjeldahl N (TKN) as groundwater flows through the wall. Additionally, groundwater temperature, porewater velocity, direction and water table elevation were monitored in the wells.

Water samples were collected within each well weekly for 20 weeks and then monthly thereafter for 660 days after construction. Water samples were collected after purging two well volumes using a submersible pump (Mini Typhoon<sup>®</sup> DTW, Proactive Environmental Products, Bradenton, FL). Samples were collected and either filtered through a 0.45 µm membrane filter (Pall Corporation, Port Washington, NY), then acidified or unfiltered and acidified directly, stored on wet ice and transported to the laboratory. Unfiltered samples were digested using a block digester and analyzed colorimetrically for TKN (EPA Method 351.2) on an autoanalyzer (Seal Analytical, West Sussex, UK). Filtered samples were analyzed for nitrate-nitrite colorimetrically (EPA Method 353.2) after reduction with cadmium on an autoanalyzer (Seal Analytical, West Sussex, UK). Total organic C (TOC) was determined using EPA Method 415.1, after combustion as non-purgable organic C on an infrared gas analyzer (Shimadzu Corp,

Kyoto, Japan). Additionally dissolved oxygen was measured directly in wells using a multi-probe which was moved up and down the well water column during measurement to prevent oxygen consumption (556 MPS, YSI Incorporated, Yellow Springs, Ohio).

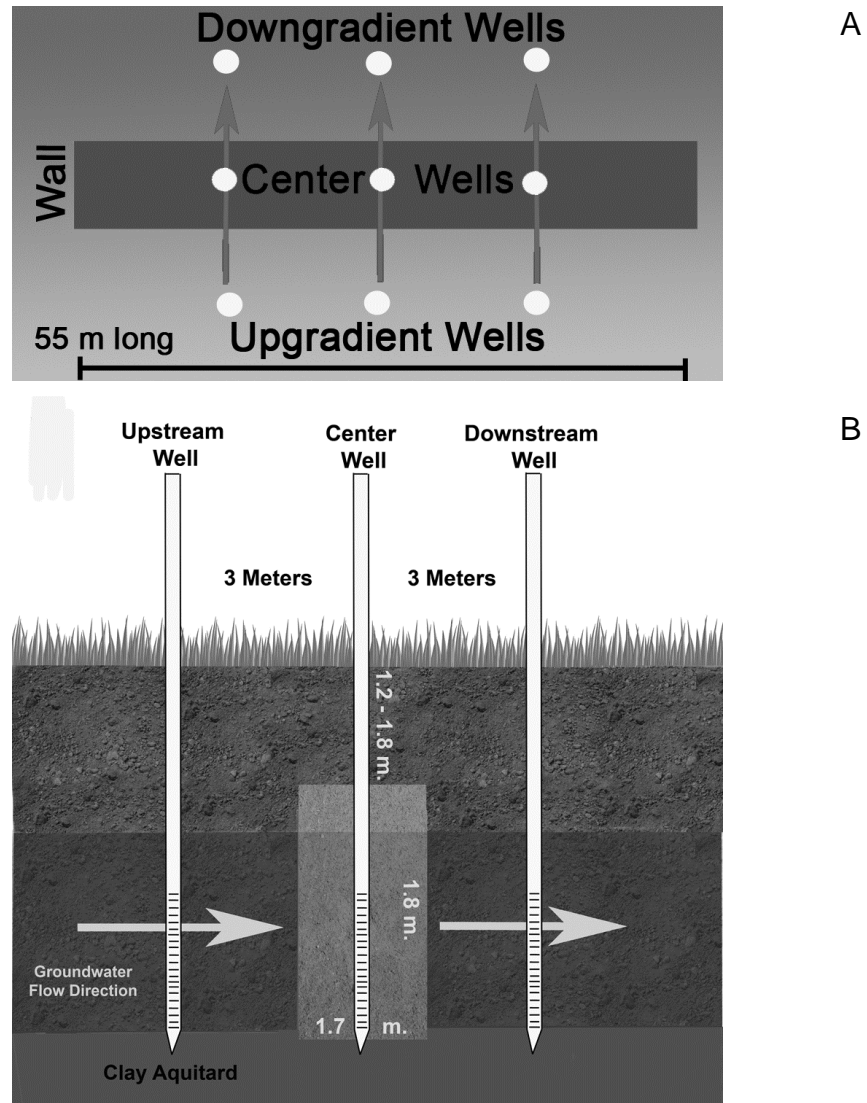


Figure 2-2. Diagrams of the well transects within the denitrification wall. Shown in the figures are a (A) Over view of all three denitrification wall well transects and (B) cross-section view of one well transect.

Effective porosity of the denitrification wall was determined in a laboratory study using recreated cores of sand and sawdust in the same ratios and same bulk density as the denitrification wall in triplicate. The effective porosity measures only the pores that

transmit water (Fetter, 2001). Effective porosity was determined as the fraction of total saturated water volume that drained due to gravity at field capacity (33 kPa) (Ahuja et al., 1984; Timlin et al., 1999). Cores were vacuum saturated in tempe cells (Soil Moisture Equipment Co., Santa Barbara, CA), then allowed to drain to a porous surface for 72 hours. This field capacity measure of effective porosity has been determined as a better predictor of the mobile groundwater volume in denitrification wall media than total porosity (Barkle et al., 2008).

The focusing of groundwater through permeable reactive barriers (PRBs) has been hampered by decreases in hydraulic conductivity due to construction, thus instigating bypass flow (Barkle et al., 2008; Schipper, 2004). The hydraulic conductivity ( $K_{sat}$ ) was therefore determined in all nine wells outside of and within the denitrification wall using the Hvorslev slug-test method described in Equation 2-1 (Fetter, 2001).

$$K_{sat} = \frac{r^2 \ln\left(\frac{L_e}{R}\right)}{2L_e t_{37}} \quad (2-1)$$

In this equation,  $K_{sat}$  is the saturated hydraulic conductivity [ $L T^{-1}$ ],  $r$  is the well casing radius [ $L$ ],  $L_e$  is the length of the well screen [ $L$ ],  $R$  is the borehole radius, and  $t_{37}$  is the time it takes for the water level to fall to 37% of initial change in head. Porewater velocity and direction were measured periodically in wells at 0.4, 0.8 and 1.2 m. from the bottom of the denitrification wall using a heat-pulse flowmeter (GeoFlo Model 40, Kerfoot Technologies, Mashpee, MA). This flowmeter allows direct measurements in wells to more accurately calculate flow direction and porewater velocity, which yields detention times and treatment volumes. When this data is paired with nitrate reductions measured at the same time in well transects, an accurate estimate of N removal rates can be calculated. The direction and velocity readings of the flowmeter are calibrated by

pumping a known velocity and direction in a tank containing the well screen surrounded by the same standard sand filter pack used in the field well installation. This procedure yielded an  $r^2$  for velocity of 0.999 and direction had a standard deviation of  $\pm 2$  degrees around the true value. Heat-pulse groundwater flowmeters have been field-verified as accurate representations of groundwater flow as compared to piezometer gradients with average velocity uncertainties of only  $0.02 - 0.04 \text{ m d}^{-1}$  and direction uncertainties of  $4.9 - 7.4$  degrees (Alden and Munster, 1997). Water level elevations and temperature were measured by pressure transducers placed in the wells (Global Water. Gold River, CA). To provide a confirmation on the groundwater flowmeter results and a more continuous measurement of N load reductions, groundwater discharge was determined using a variation of Darcy's law as described in Equation 2-2.

$$Q = -K \frac{dh}{dt} \frac{A}{\phi} \quad (2-2)$$

In this equation,  $Q$  is the discharge [ $\text{L}^3 \text{T}^{-1}$ ],  $K$  is the hydraulic conductivity of the wall as determined from the slug-test,  $\frac{dh}{dt}$  is the head gradient between the center and downgradient wells as measured hourly from pressure transducers,  $A$  is the vertical area of the denitrification wall and  $\phi$  is the effective porosity as determined from the laboratory core experiment.

Nitrate removal rates within the wells were determined as daily mass nitrate loss per volume of reactor media according to Schipper and Vojvodic-Vukovic (2000) using Equation 2-3.

$$Nr = vA\Delta_n/V_s \quad (2-3)$$

In this equation,  $Nr$  is the nitrate mass removal rate per volume of wall [ $\text{g-N m}^{-3} \text{d}^{-1}$ ],  $v$  is the porewater velocity [ $\text{L T}^{-1}$ ],  $A$  is the cross-sectional area conducting ground water [ $\text{L}^2$ ], calculated as  $A = m^2 \phi$ , where  $\phi$  is effective porosity [ $\text{L}^3 \text{L}^{-3}$ ],  $\Delta_n$  is the decrease in nitrate N concentration [ $\text{M L}^{-3}$ ] and  $V_s$  is the media volume of wall the nitrate travels through [ $\text{L}^3$ ] ( $\text{L}^2 \times$  the travel distance within the wall). Porewater velocity ( $v$ ) and media volume ( $V_s$ ) were determined from velocity and directional readings measured with the groundwater flowmeter.

### **Media Sampling**

Media sampling for microbial biomass C (MBC), bulk density, particle density, total porosity, potential denitrification rate and denitrification enzyme activity (DEA) was conducted on March 28th 2011, 18 months after the denitrification wall installation. Nine media samples were collected along three perpendicular transects within the denitrification wall adjacent to each center well (Figure 2-3). Samples were collected 37 cm apart at the leading edge of groundwater inflow, the midpoint and adjacent to the center wells (Figure 2-3). Three additional samples were collected at the same depths in native soils adjacent to the upgradient wells. Samples analyzed for bulk density, particle density and total porosity analyses were collected with a peat auger (Eljkelkamp Agrisearch Equipment, Giesbeek, Netherlands) and samples for all other analyses were collected with a bucket auger. All samples were collected at depths that have always been below the water table and at least 45 cm below the top of the denitrification wall.

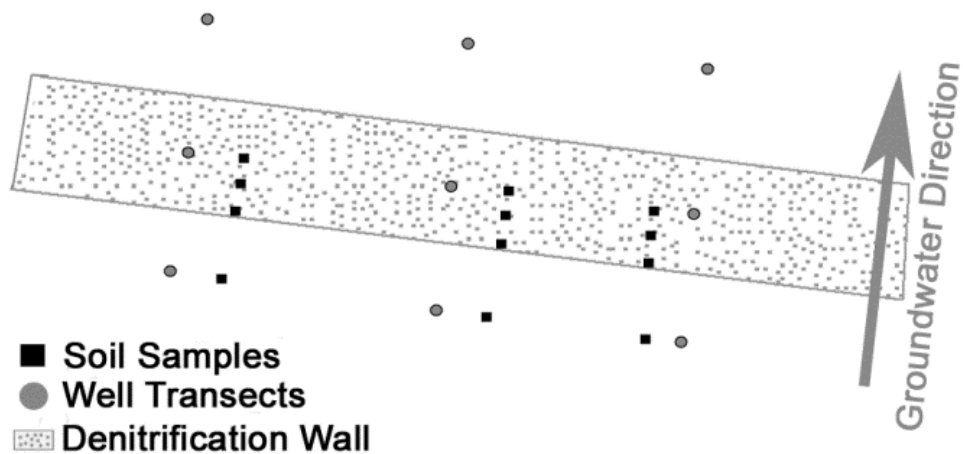


Figure 2-3. A diagram of the soil and denitrification wall media collection locations. Within the denitrification wall samples were collected in a transect. The first sample is collected at the leading edge of the wall, where groundwater first meets the denitrification wall and two samples were collected approximately 37 and 74 cm. further in to the wall.

### Media Characterization

Immediately after media sampling, the gravimetric moisture content was quantified by weighing approximately 50 g of a field-moist subsample in a forced air drying oven at 105°C for 48 hours. Bulk density was calculated as the oven dry weight divided by the volume of sample collected with the peat auger. Particle density was quantified by measuring the volume displacement of water for a known moist media weight for each of the three media samples and reported on a dry-weight basis (Gradwell and Birrell, 1979). Denitrification wall samples were sufficiently saturated and cohesive enough to prevent sawdust particles from floating. Total porosity was measured as  $1 - (\text{Bulk density} \times \text{Particle Density}^{-1})$ . The rest of the moist sample was stored at 4°C for further analysis.

Moist media samples were analyzed for microbial biomass C (MBC) by the 24 hr. chloroform fumigation-extraction method within 4 days (Vance et al., 1987). Samples were extracted with 25 mL of 0.5 M  $K_2SO_4$  and filtered through 2.5  $\mu m$  filter paper (Whatman, Maidstone, UK). Total organic C was measured as described above. MBC was determined as the difference between untreated and chloroform-fumigated media. An extraction efficiency ( $k_{EC}$ ) factor of 0.37 was applied based on previous determinations (Sparling et al., 1990).

To determine changes in sawdust properties with time, the total C and fiber content of media collected from within the denitrification wall 18 months after installation were compared to fresh samples. Oven-dried samples were homogenized and ground with a plant grinder (Thomas Scientific, Swedesboro, NJ). Percentages of neutral detergent fiber (NDF), hemicellulose, cellulose and lignin were determined as mass loss after a sequential neutral detergent-acid digestion technique (Van Soest et al., 1991) within a fiber analyzer (ANKOM, Fairport, New York). Ash content was calculated as the mass loss on ignition after 4 hours in a 550°C muffle furnace. Sub-samples of ground media were further processed using a ball-mill and analyzed for total C and total N using a thermal conductivity detector after dynamic flash combustion (FlashEA<sup>®</sup>1112, Thermo Fisher Scientific, Miami, OK).

### **Media Denitrification Rate**

To place bounds on in-situ denitrification rates, moist media samples were analyzed for potential denitrification rate by simulating the range of conditions the denitrification wall would likely be exposed. All samples were flooded with water collected from the closest upgradient wells ( $NO_3 = 3.8-7.8 \text{ mg L}^{-1}$  and  $DOC = 0.72-1.64 \text{ mg L}^{-1}$ ). Additionally, samples were flooded with water from the center well ( $NO_3 =$

0.05–3.88 mg L<sup>-1</sup> and DOC = 1.6–4.6 mg L<sup>-1</sup>). Lastly, to isolate the impact of DOC on denitrification rates, samples were flooded with high DOC water from the center well (1.6–4.6 mg L<sup>-1</sup>), which was then spiked to the same concentration as the adjacent upgradient well (3.8–7.8 mg L<sup>-1</sup>).

To measure potential denitrification rate, samples were homogenized and approximately 3 g of media was placed in a glass serum bottle that was sealed with a rubber septa and aluminum crimp cap. Subsequently, 5 mL of the aforementioned well water treatments were purged with 99.99% O<sub>2</sub>-free N<sub>2</sub> gas and added to the media. Headspace air was evacuated and replaced with N<sub>2</sub> gas. Then approximately 15% of the headspace N<sub>2</sub> was replaced with acetylene gas (C<sub>2</sub>H<sub>2</sub>) (Balderston et al., 1976; Yoshinari and Knowles, 1977). Bottles were shaken on a longitudinal shaker for one hour and incubated at 22°C, which was the maximum temperature observed in the denitrification wall. Headspace gas was sampled incrementally.

Denitrification enzyme activity (DEA) was measured using the methods outlined in Tiedje (1982) with adaptations by White and Reddy (1999). DEA is a standardized measure that gives a snapshot of the existing pool of denitrifiers in the absence of N or C limitation. DEA was analyzed by adding 2 mL of N<sub>2</sub>-purged deionized water, further purging the headspace with N<sub>2</sub> gas and subsequently adding acetylene as described above. Samples were shaken on a longitudinal shaker for ½ hour to distribute the acetylene gas and then 3 mL of a 56 mg KNO<sub>3</sub>-N L<sup>-1</sup>, 288 mg dextrose C L<sup>-1</sup>, and 2 mg chloramphenicol L<sup>-1</sup> solution were added. Chloramphenicol is added to inhibit the synthesis of new enzymes thus providing a measure only of existing denitrifying enzymes. To determine if N or C was limiting, the above denitrification enzyme activity

procedure was done by excluding the dextrose C-only and then the  $\text{KNO}_3$  only (Schipper and Vojvodic-Vukovic, 1998). Samples were incubated at  $25^\circ\text{C}$  and headspace gas was sampled approximately hourly. All denitrification rates were determined by fitting a least-squares regression line to the cumulative  $\text{N}_2\text{O}$  production over time. Denitrification rates were quantified on a volumetric basis as determined from bulk density measurements.

All headspace samples were analyzed for nitrous oxide production with a gas chromatograph that was equipped with a  $3.7 \times 10^8$  (10mCi)  $^{63}\text{Ni}$  electron capture detector (300C) (Shimadzu GC-14A, Kyoto, Japan). A stainless steel column (1.8 m long by 2 mm i.d.) packed with Poropak<sup>TM</sup> Q (0.177-0.149 mm; 80-100 mesh) was used (Supelco, Bellefonte, PA). Operating temperatures were 120, 30 and  $230^\circ\text{C}$  for the injector, column and detector respectively. Measured values were adjusted to account for  $\text{N}_2\text{O}$  dissolved in the aqueous phase employing Bunsen absorption coefficients (Tiedje, 1982).

### **Statistical Analyses**

A two-way ANOVA was used to screen comparisons for statistical significance. Single pairwise comparisons between denitrification wall and native soils for  $K_{sat}$ , bulk density and porosity were analyzed for statistical significance with a student's t-test. Post-hoc determinations of the statistical significance for multiple pairwise comparisons for nitrate, TKN, DOC, denitrification rate, DEA, MBC and total C between locations was calculated with a Tukey's HSD test. Statistical significance for all tests was determined at an alpha level of 0.05. All statistical analyses were conducted in JMP<sup>®</sup> 8.0 (SAS Institute Inc., Cary, NC).

## Results and Discussion

### Groundwater Hydrology

The saturated hydraulic conductivity ( $K_{sat}$ ) of each denitrification wall transect was 1.3 – 3 times higher than five of the six surrounding wells within those respective transects (Table 2-1). The  $K_{sat}$  within the denitrification wall was higher than all downgradient soils and the upgradient soils for transects 1 and 2, but the hydraulic conductivity of the upgradient soils at transect 3 was higher than any other location. This is possibly due to the penetration of the well through conduits within the clay, which were previously observed rapidly transporting groundwater when the wall was excavated.

Table 2-1. The hydraulic conductivity (Ksat) of the denitrification wall (center) and undisturbed soils upgradient (up) and downgradient (down) of the wall.

	Hydraulic Conductivity (cm d <sup>-1</sup> )		
	Transect		
	1	2	3
Up	34.0	74.9	150
Center	99.8	98.3	83.2
Down	37.7	32.2	32.2

The addition of the denitrification wall media significantly improved the measured properties associated with soil drainage. The average bulk density of the denitrification wall  $\pm 1$  standard deviation (SD) was lower ( $1.13 \pm 0.070$  g cm<sup>-3</sup>, n=3) than the average bulk density of the surrounding soils ( $1.93 \pm 0.15$  g cm<sup>-3</sup>, n=6) and the total porosity of the denitrification wall ( $59.5 \pm 1.6\%$ , n=3) was higher than the surrounding soils ( $22.3 \pm 11\%$ , n=6). The effective porosity of the wall media was  $50.0 \pm 5.3\%$  (n=3) of the total volume.

Barkle et al., 2008 concluded that mixing native soils below the aquifer caused a particle resorting, which reduced the connectivity of pores in a denitrification wall. The sand used in the present study was a commercially available (Edgar Minerals, Inc., Edgar, Florida), sieved, uniform particle-sized sand (0.106-0.15 mm), with a much narrower range in particle sizes than the soils of the Barkle et al. (2008) study. Increasing the diameter and decreasing the range of sand particle sizes increases permeability because these soils are less likely to resort and fill diverse poresizes than soils where fluidized finer particles can clog the pore-space between coarser particles (Fetter, 2001). A mitigation strategy for aquifer sands with a potential to resort upon excavation and mixing could be to import sands/gravels from offsite, although this would increase the cost.

The porewater velocity and direction were measured with the heat-pulse groundwater flowmeter in May and July (Figure 2-4). In general the groundwater travelled perpendicularly through the denitrification wall with a slight curvature towards the main surface water discharge. In both May and July the average porewater velocity was  $1.7 \text{ m day}^{-1}$  (Table 2-2). As expected, these velocities are much faster than groundwater velocities for other denitrification walls ( $0.007\text{-}0.47 \text{ m day}^{-1}$ ) (Schipper and Vojvodic-Vukovic, 2000; Schipper et al., 2005; Robertson and Cherry, 1995). Subsequently, the detention time ( $1.7 - 1.9$  days), which was based on actual flow path through the wall not just average wall width, is also on the lower end of these studies, which reported detention times of 1-10 days (Schipper and Vojvodic-Vukovic, 2001; Schipper et al., 2005) and 10-13 days (Robertson et al., 2000). Based on these measurements with the groundwater flowmeter, the denitrification wall treats

approximately  $8.4 \times 10^4 \text{ L d}^{-1}$ . Discharge was also measured utilizing head gradients between wells which were measured with pressure transducers hourly over 462 days following Equation 2-2. This yields a treatment volume rate of  $10 \times 10^4 \pm 2.8 \times 10^4 \text{ L d}^{-1}$ , which overlaps the measurements of treatment volume directly measured with the groundwater flowmeter.

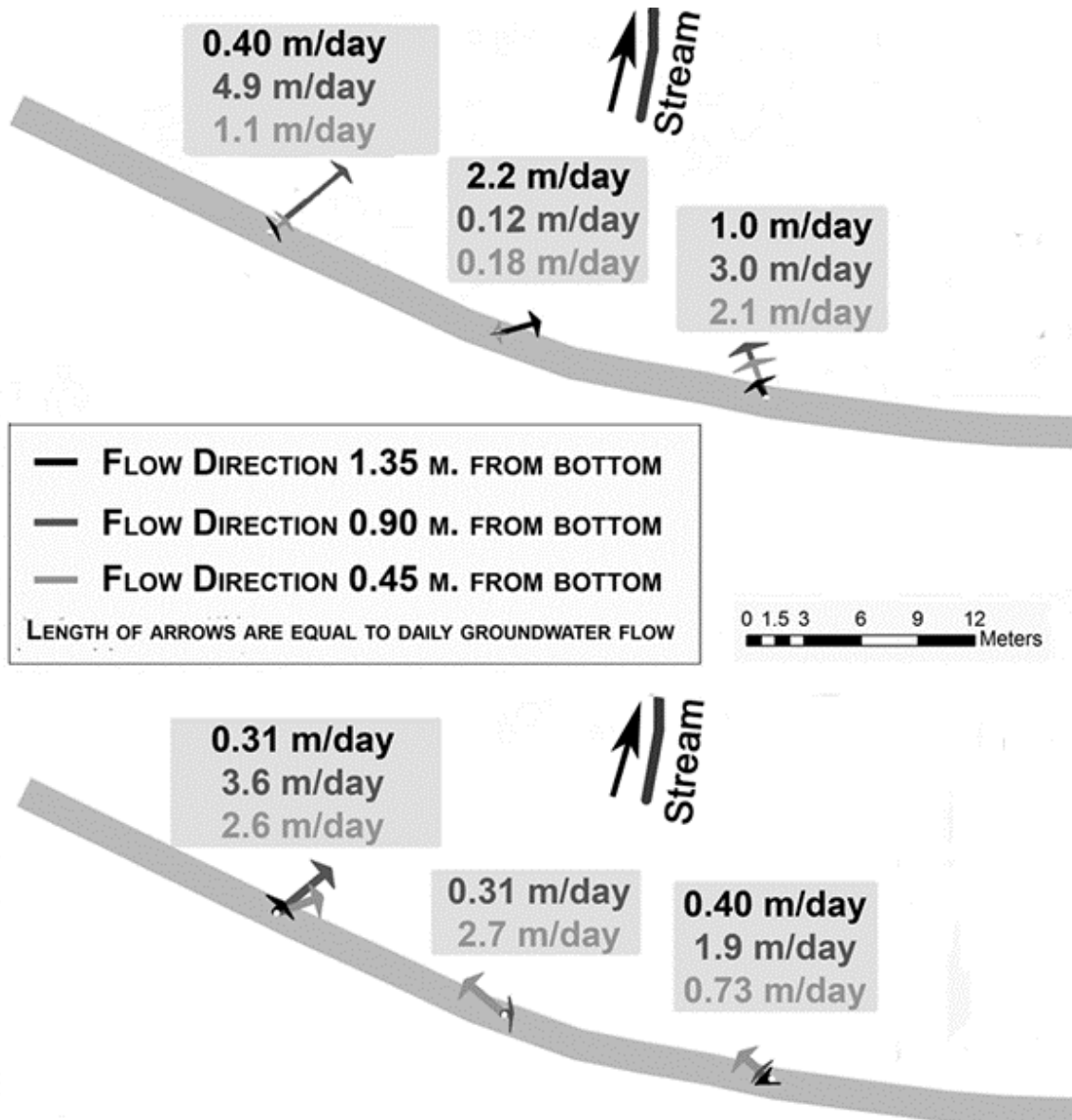


Figure 2-4. Porewater velocities and direction at three depths within the denitrification wall center wells. Values are shown for May at the top and July at the bottom.

The groundwater velocity and direction measured with the groundwater flowmeter were somewhat variable by depth and month. This is likely due to changing water table conditions, heterogeneous native soil horizons present at the site, and the intrusion of a high hydraulic conductivity denitrification wall within the ground. The installation of high hydraulic conductivity PRBs have been shown to cause vertical convergent discharges from the surrounding aquifer into PRBs and variability in groundwater velocities by depth (Benner et al., 2001; Robertson et al., 2005). The groundwater flowmeter only measures net horizontal groundwater movement and could underestimate velocity when significant vertical discharge occurs.

Table 2-2. Groundwater velocity, flow length and detention time within the denitrification wall wells for Transects 1 - 3 (T1 - T3).

	May			July		
	Velocity (m/day)	Flow-length (m)	Detention Time (days)	Velocity (m/day)	Flow-length (m)	Detention Time (days)
T1	2.1	1.9	0.9	1.3	3.0	2.3
T2	0.9	2.8	3.1	1.5	3.6	2.4
T3	2.1	2.1	1.0	2.2	2.1	1.0
Ave	1.7±0.7	2.3±0.5	1.7±1.2	1.7±0.5	2.9±0.8	1.9±0.8

### **Dissolved Organic Carbon Export and Dissolved Oxygen**

In the first sampling event 37 days after denitrification wall installation, dissolved organic C concentration (DOC) was measured at  $34 \pm 5.1$  and  $70 \pm 71$  mg L<sup>-1</sup> (n=3) in the center and downgradient well and after one year concentrations had decreased to  $2.3 \pm 1.1$  and  $2.6 \pm 1.4$  mg L<sup>-1</sup> (n=3) respectively (Figure 2-5). Over the entire sampling period, the influent water in the upgradient well had an average DOC concentration of only  $1.1 \pm 0.66$  mg L<sup>-1</sup> (n=29).

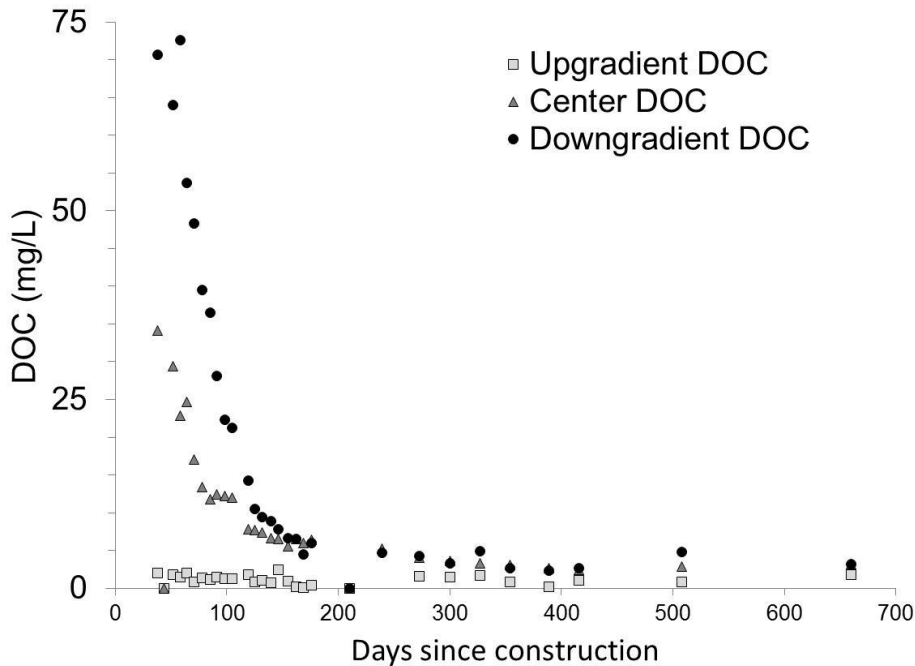


Figure 2-5. Dissolved organic C concentration in the upgradient, center and downgradient wells over time.

### Nitrogen Concentrations in Well Transects

Over the 660 days of sampling, average  $\text{NO}_3$  concentration significantly decreased from  $6.2 \pm 0.65$  to  $1.6 \pm 0.40 \text{ mg L}^{-1}$  ( $n = 30$ ) between the upgradient and downgradient well transects for a 77% average reduction. The  $\text{NO}_3$  reduction between the upgradient and the well within the wall (center) was much greater, with reductions in transects 1, 2 and 3 of 100%, 100% and 75% respectively (Average = 88%) (Figure 2-6). An increase in  $\text{NO}_3$  concentration between wells within the wall (center) and downgradient wells was detected with concentrations doubling from  $0.8 \pm 0.26$  to  $1.6 \pm 0.40 \text{ mg L}^{-1}$  ( $n=30$ ). However, this increase in  $\text{NO}_3$  downgradient is not uniform among the three well transects. The two transects at the ends of the wall had an average  $\text{NO}_3$  increase of ( $1.2 \pm 0.8 \text{ mg L}^{-1}$ ), while the center transect had no increase ( $\sim 0 \text{ mg L}^{-1}$ ). Therefore it is likely that higher  $\text{NO}_3$  concentrations in the outer two transects downgradient of the wall, may be attributed to untreated groundwater bypassing the denitrification wall.

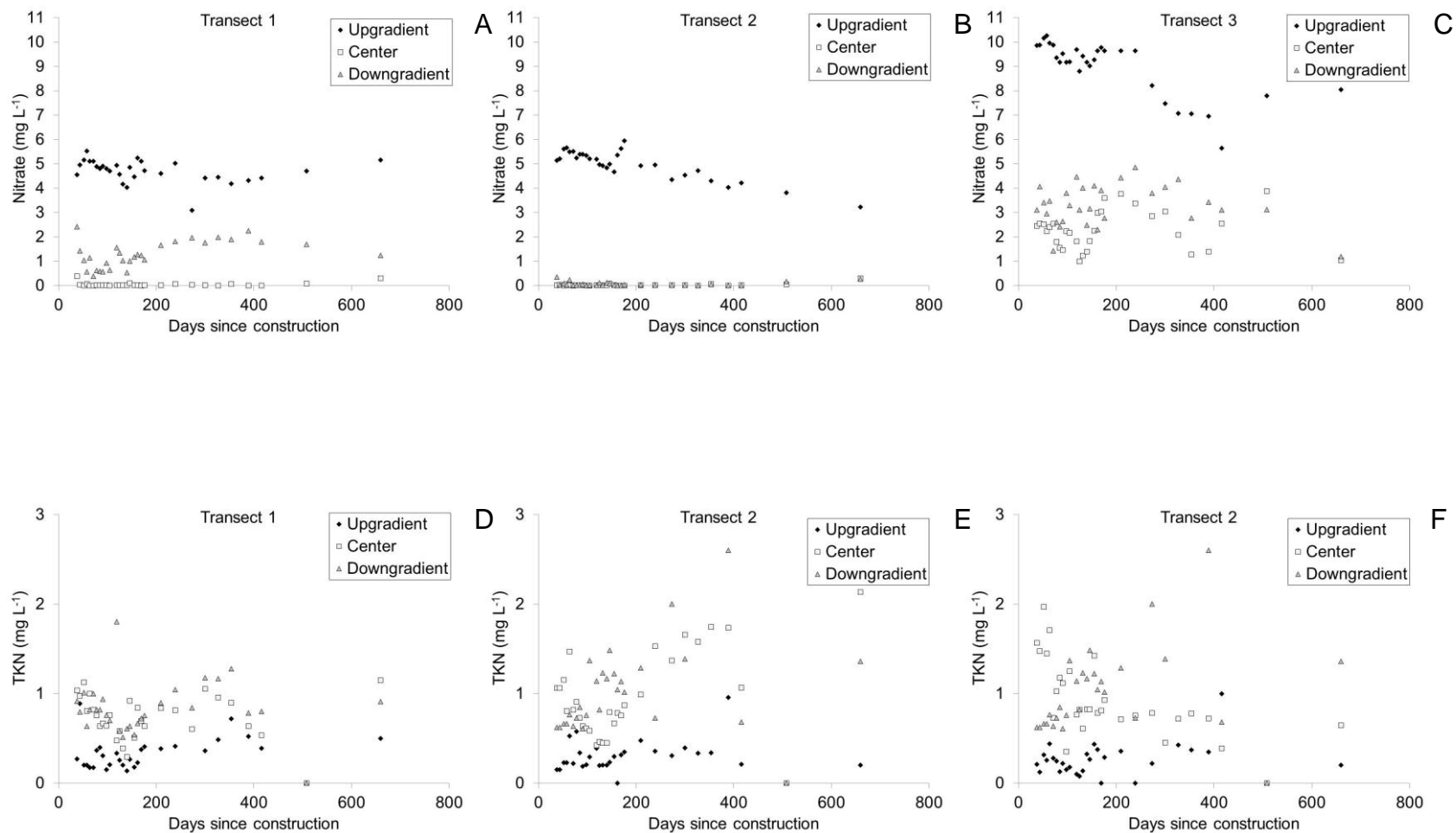


Figure 2-6. The concentrations of nitrate and total Kjeldahl N (TKN) over time within the upgradient, center and downgradient wells for all three transects. Shown in the figures are nitrate concentrations for transects 1-3 (A-C) and TKN concentrations for transects 1-3 (D-F).

Vertical groundwater movement from above and below the wall is possible. During preliminary borehole surveys and denitrification wall construction, groundwater was observed traveling through conduits within the deeper clay aquitard. Water flowing above the wall did not seem to have a negative impact on N reductions. Surprisingly, there was a weak, but significant increase in nitrate removal with increases in groundwater elevation up to 0.7 m above the wall indicating flow above the wall had a positive impact on nitrate removal ( $r^2 = 0.23$ ,  $p < 0.01$ ). Based on hydraulic models using high hydraulic conductivity media, other researchers found that no bypass of waters above the wall occurred until the water table was greater than 2 m above the PRB (Robertson et al., 2005). This is because groundwater converges in to high hydraulic conductivity PRBs. Robertson et al. (2005) have proposed deliberately 'undersizing' the height and depth of denitrification walls even in fluctuating water tables and deeply contaminated aquifers due to the vertical transport of groundwater from above and below the wall

Due to the confounding effect of untreated groundwater in downgradient wells in at least the outer two transects, it is useful to analyze nitrate concentration reductions between the upgradient and center wells. Nitrate reductions varied by transect, partially owing to differing influent concentrations (Table 2-3). When influent concentrations averaged  $5.0 \pm 0.52 \text{ mg L}^{-1}$  ( $n=30$ ) in Transects 1 and 2, nitrate reductions were approximately 100%. Therefore even with rapid groundwater velocities and low detention times, it is likely that nitrate became limited even before reaching the center well in these two transects. Nitrate was still present in the center well of transect 3 which had the highest influent nitrate concentration ( $9.3 \pm 1.2 \text{ mg L}^{-1}$ ), porewater velocity (2.2

m day<sup>-1</sup>) and shortest detention time (0.5 days). Therefore this transects nitrate reduction ( $\Delta[\text{NO}_3] = 6.7 \pm 1.3 \text{ mg L}^{-1}$ ,  $n=30$ ) occurring within a half-day detention time, is a better representation of maximum reduction potentials in this relatively rapid groundwater. Additionally, because nitrate reductions between the upgradient and center well are considerably above 50% for all three transects, it is safe to assume that all nitrate traveling the width of the wall is lost. Based on measurements of treatment volume using the groundwater flowmeter ( $8.4 \times 10^4 \text{ L d}^{-1}$ ) and utilizing head gradients ( $10 \times 10^4 \pm 2.7 \times 10^4$ ), the denitrification wall reduces nitrate load by  $190 \pm 20 \text{ kg yr}^{-1}$  ( $n=2$ ) and  $249 \pm 161 \text{ kg yr}^{-1}$  ( $n=28$ ) respectively utilizing these two methods.

Table 2-3. Influent  $\text{NO}_3$  concentrations and percent  $\text{NO}_3$  reduction values from the upgradient well to the center and downgradient wells. Values are reported for transects 1-3 (T1 – T3) ( $n=29$ ). Values are average  $\pm 1$  standard deviation

	Influent $\text{NO}_3$ conc. ( $\text{mg L}^{-1}$ )	% $\text{NO}_3$ reduction (upgradient to center)	% $\text{NO}_3$ reduction (upgradient to downgradient)
T1	$4.7 \pm 0.46$	$99.5 \pm 1.6$	$74.0 \pm 14$
T2	$5.2 \pm 0.52$	$99.7 \pm 0.43$	$99.0 \pm 9.6$
T3	$9.3 \pm 1.2$	$74.9 \pm 9.7$	$63.0 \pm 12$
Ave	$6.4 \pm 2.5$	$91.3 \pm 14$	$78.7 \pm 18$

The mass nitrate removal rates per volume of reactor media, averaged  $3.35 \text{ g-N m}^{-3} \text{ d}^{-1}$  in May and  $2.95 \text{ g-N m}^{-3} \text{ d}^{-1}$  in July when groundwater flow was measured with the groundwater flowmeter (Table 2-4). The nitrate removal rate of transect 3 (Ave =  $5.18 \text{ g-N m}^{-3} \text{ d}^{-1}$ ) where some nitrate is still present in the center well is likely more representative of actual rates without nitrate limitation. Additionally, transect 3 is receiving the highest nitrate loads due to higher concentrations and groundwater velocities than the other transects. These values are at the upper end of the range of reported nitrate removal rates for other sand-sawdust denitrification walls ( $0.014 - 3.6$

g-N m<sup>-3</sup> d<sup>-1</sup> (Schipper et al., 2010b). The nitrate removal rates measured in this study, indicate the feasibility of a denitrification wall to completely remove nitrate even under the high loading conditions that often occur adjacent to major surface water discharges. Because the microbial community response is likely a function of N-load rather than concentration alone, it is possible that even higher nitrate reduction rates could occur with higher N loads. If this were true, the nitrate reduction rate wouldn't be a constant that is driven by site physicochemical properties alone but would increase as a function of N loading rate. Contrastingly, this high denitrification rate is possibly due to elevated groundwater temperature (average of 19 ± 2.7°C) and greater C additions (Total Media C = 7.4%) than some other studies. Further confirmation of the relationship between temperature and wood volume on nitrate reduction rates would need to be done to place these rates in context. Regardless, the rates measured in this study indicate the greater potential of denitrification walls to effectively treat higher nitrate loading rates than had been previously determined.

Table 2-4. Volumetric nitrate removal rates in May and July for the three transects (T1 – T3)

	May 2010	July 2010
	NO <sub>3</sub> Removal Rate (g N m <sup>-3</sup> d <sup>-1</sup> )	NO <sub>3</sub> Removal Rate (g N m <sup>-3</sup> d <sup>-1</sup> )
T1	3.25	2.00
T2	1.33	1.95
T3	5.46	4.91
Ave	3.35±2.1	2.95±1.7

The total Kjeldahl N (TKN) concentration increased from an average of 0.3 ± 0.12 upgradient of the wall to 0.9 ± 0.25 in the center of the wall to 1.0 ± 0.31 mg L<sup>-1</sup>

downgradient of the wall within all three transects (Figure 2-6). Based on discharges measured from head gradients, this is an annual TKN load increase to downgradient waters of  $28 \pm 17 \text{ kg yr}^{-1}$ . This rise in TKN is possibly associated with DOC leaching, net ammonium ( $\text{NH}_4^+$ ) mineralization (ammonification) or ammonium production as a result of dissimilatory nitrate reduction to ammonium (DNRA). Elevations in ammonium levels generally do not occur in field conditions within denitrification walls (Elgood et al., 2010; Robertson and Cherry, 1995; Schipper and Vojvodic-Vukovic, 1998), although ammonium production and leaching have been observed in mesocosms and in laboratory experiments (Cameron and Schipper, 2010; Greenan et al., 2006). The TKN concentration and export rates were largely constant, whereas the DOC export declined in an exponential fashion and the relationship between the two was weak ( $r^2 = 0.06$ ). This indicates that the TKN was not strongly associated with media leaching and carbon export and is predominantly the result of some continuing biological process such as ammonification or DNRA.

The microbial N pool of the denitrification wall was a small portion of total N lost in groundwater. The total nitrogen content of the denitrification wall media increased from 0.032% to  $0.051 \pm 0.007\%$ , which represents a total microbial N assimilation of  $36 \pm 13 \text{ kg}$  in the 540 days of the study. Net ammonium mineralization (ammonification) occurs when C:N ratios decline below 100 (Reddy and Delaune, 2008). The C:N ratio of the sawdust used in this study initially was approximately 422, which declined in the duration of the study to  $266 \pm 97$ . The high C:N ratio indicates ammonium is likely to be retained in microbial biomass to maintain a microbial C:N ratio of 10:1 and net ammonium immobilization would occur (Reddy and Delaune, 2008). Ammonification is

therefore not a likely source of the TKN increase in groundwater. DNRA occurs in highly reducing environments ( $E_h < 0$  mv) with high electron pressure, which would arise in conditions with high electron donor (sawdust) to electron acceptor (Nitrate) ratios (Reddy and Delaune, 2008). This high electron donor to acceptor ratio is likely to occur in a carbon rich denitrification wall, particularly as the nitrate is depleted. Therefore it is plausible that some of the total nitrate load reduced ( $249 \pm 161$  kg yr<sup>-1</sup>) is not lost to the atmosphere but is instead converted to ammonium, via the DNRA process. TKN is bioavailable and thus can still impact receiving water bodies. Adding TKN to nitrate-N, the total N significantly decreased from  $6.6 \pm 0.6$  mg L<sup>-1</sup> to  $2.6 \pm 0.5$  mg L<sup>-1</sup> (n=29) between the upgradient and downgradient wells for a 62% reduction. Therefore utilizing discharges measured from head gradients, the total N load reduction in groundwater resulting from the denitrification wall is approximately  $220 \pm 54$  kg yr<sup>-1</sup>.

### **Media Potential Denitrification Rate**

Potential denitrification rates and denitrification enzyme activity values (Table 2-5) are well within the range of another study, which analyzed monthly media samples for a year from another denitrification wall (Schipper et al., 2000). Denitrification was not detected in native soils collected adjacent to the denitrification wall. Within the denitrification wall, N<sub>2</sub>O emissions were detected from all media samples collected at the leading edge of the wall flooded with upgradient well water but not consistently detected from any samples collected 37 cm into the wall or with other treatments. Nitrous oxide emissions were sporadically detected from samples collected beyond the leading edge of the wall in transect 3, where some nitrate was present in the center well but not consistently enough to calculate a rate. When media samples were incubated over 59 hours, denitrification was detected in some samples where nitrate but not

chloramphenicol was added indicating the ability of the microbial population to respond to nitrate additions. In a diversion wetland, DEA measured in the laboratory was found to be a strong indicator of the spatial transport of nitrate, even though all soils collected had the same physicochemical properties (Gardner and White, 2010). These results suggests that nitrate becomes rapidly limiting and subsequently the pool of denitrifying enzymes rapidly declines beyond detection. Denitrification was not detected in the dextrose-only treatment but was detected when nitrate alone was added indicating nitrate limitation. Numerically the denitrification rate peaked when both dextrose and nitrate were added indicating a possible co-limitation, although high variability caused the differences to not be statistically significant.

Table 2-5. Potential denitrification rate, denitrification enzyme activity (DEA) and N and C limitation study results of denitrification wall media. Values are reported for all three transects (T1 – T3) as a rate per m<sup>3</sup> of denitrification wall.

	Denitrification rate (g-N m <sup>-3</sup> d <sup>-1</sup> )	DEA (NO <sub>3</sub> & Dextrose) (g-N m <sup>-3</sup> d <sup>-1</sup> )	NO <sub>3</sub> only (g-N m <sup>-3</sup> d <sup>-1</sup> )	Dextrose only (g-N m <sup>-3</sup> d <sup>-1</sup> )
T1	3.00	1.49	0.216	0
T2	3.98	1.49	0.96	0
T3	7.68	3.53	1.70	0
Ave	4.89±2.5	2.17±1.2	0.96±0.7	0

The average potential denitrification rate of media collected from the leading edge of the wall ( $4.89 \pm 2.5$  g-N m<sup>-3</sup> d<sup>-1</sup>,  $n=3$ ) is slightly higher than rates determined from the well transects ( $3.15 \pm 1.70$  g-N m<sup>-3</sup> d<sup>-1</sup>,  $n=6$ ), although the differences are not significant. This indicates that the denitrification process is the likely source of nitrate reductions within the denitrification wall analogous with findings from other studies (Moorman et al., 2010; Schipper et al., 1998). It is notable that the denitrification rate for all treatments at Transect 3 were elevated above the other two transects, mirroring the higher influent N loads and rates of removal measured in the well transects.

The rapid decline in denitrification rate with distance implies that analyses of this type are useful for generalizing fine-scale spatial denitrification dynamics that can not be inferred from nitrate concentration reductions in widely-spaced well transects alone. Nevertheless caution should be taken in the spatial selection of sampling sites to accurately infer denitrification rates. While the results were mixed, in two studies Schipper et al., 2004, 2005 found laboratory estimates of denitrification rate to be underestimates of rates measured in the field. Similar to this study, these authors attributed this to their inability to collect a soil sample at the leading edge of the wall where denitrification rates are greatest due to nitrate limitation beyond. Additionally they inferred that nitrate concentration and thus denitrification rate would be spatially patchy due to variations in hydraulic conductivity and a partitioning of nitrate between mobile and immobile pore spaces. It was expected that the continuously high nitrate loading rate in this wall would minimize this nitrate limitation, although it appears nitrate reductions are limiting denitrifying enzyme formation.

### **Microbial Biomass Carbon and Total Carbon**

The average microbial biomass carbon of denitrification wall media ( $44 \pm 19$  mg C  $\text{kg}^{-1}$ ,  $n=9$ ) was four times higher than native soils ( $10 \pm 12$  mg C  $\text{kg}^{-1}$  soil,  $n=3$ ) both collected at the same depth of approximately 2.3 m. These microbial biomass carbon values are much lower than those reported in Florida wetland surface soils (920-2020 mg C  $\text{kg}^{-1}$  soil), Florida fertilized surface soils (72-988 mg C  $\text{kg}^{-1}$  soil), or another denitrification wall (260-445 mg C  $\text{kg}^{-1}$  soil) but were greater than those collected in a riparian aquifer soil collected at 0.6-1.55 m depth (39.2 - 41.5 mg C  $\text{kg}^{-1}$ ) (Grierson et al., 1999; Jacinthe et al., 2003; Long et al., 2011; White and Reddy, 2003; Schipper et al., 2004). The low background MBC of native soils collected adjacent to the wall attests

to the limitations on biological activity from continuously inundated soils at this depth. The addition of sawdust and inert sand increased the microbial biomass four-fold, which while still low is sufficient for rapid denitrification. No significant difference was observed by groundwater travel distance for microbial biomass carbon..

The total carbon concentration in the wall declined from  $84 \pm 7.4 \text{ kg m}^{-3}$  to  $79 \pm 12.3 \text{ kg m}^{-3}$  (n=9) 18 months after wall installation. This represents a 5% decline, but due to high variability the differences were not statistically significant. Schipper and Vojvodic-Vukovic (1998) also found no significant difference in total carbon after one-year of operation in a denitrification wall with a lower nitrate loading rate. This implies that the carbon consumption rate does not measurably decline more rapidly in groundwater with high N loading rates. The lignocellulose index (LCI) is the ratio of lignin content to lignin + cellulose. Leaf litter in wetland soils stabilizes at an LCI of 0.8, at which point the organic matter is highly resistant to decomposition under continued anaerobic conditions (DeBusk and Reddy, 1998). Within the denitrification wall, the LCI was initially 0.24 and declined to  $0.4 \pm 0.04$  in the 540 day duration of the study. This indicates that although there is a decline in carbon quality, the carbon is still available for decomposition. Although the carbon quality has declined, there were no detectable reductions in denitrification rate within 540 days. Longer time-frames will be necessary to discern if this reduction in carbon quality will influence denitrification rates. No significant difference was observed in total carbon or fiber properties between media samples collected at the leading edge, midpoint and the center of the denitrification wall.

### **Total Carbon Mass Balance**

A mass balance of carbon losses can aid with determining major carbon export processes and projections of wall longevity. The total carbon mass at the beginning of

the study was  $1.4 \times 10^4 \pm 1.4 \times 10^3$  kg. Oxygen declined from the upgradient well (3.7-3.9 mg L<sup>-1</sup>) to the denitrification wall wells (0.56-0.72 mg L<sup>-1</sup>), which would consume approximately 34-38 kg yr<sup>-1</sup> based on the stoichiometry of the aerobic respiration reaction (Equation 1-1). Assuming the likely scenario that nitrate concentrations are completely depleted within the wall, stoichiometry of the denitrification reaction (Equation 1-2) indicates that the carbon lost as CO<sub>2</sub> by the denitrification process is approximately 315±65 kg yr<sup>-1</sup>. Assuming the TKN increase is due solely to the DNRA process, carbon lost from this reaction would be 48±29 kg yr<sup>-1</sup>).

To determine carbon export as a result of DOC leaching, a first-order exponential decay curve was fit to the DOC concentrations over time (n=29) in the downgradient well with the use of an iterative fit model in JMP<sup>®</sup> 8.0 (SAS Institutes). Based on this model combined with groundwater flowrates, the total mass loss attributed to DOC export in the 540 day duration of the study is approximately 790 kg. At this stage of the denitrification wall, DOC export has been the dominant process removing carbon. The majority of this DOC export occurred in the first few months with export rates as high as 14.5 kg day<sup>-1</sup>. The current DOC export rate of approximately 48 kg yr<sup>-1</sup> is much lower than other carbon-utilizing processes. Long-term field studies have indicated that carbon consumption follows an exponential decay curve, possibly due to the high leaching of DOC after initial installation (Long et al., 2011; Moorman, 2010). Based on all these values, the C loss rate in the denitrification wall is 450±71 kg yr<sup>-1</sup>.

The nitrate reduction rates within the denitrification wall will likely decline before the carbon has been completely depleted, particularly because the lignin fraction of the total carbon pool is recalcitrant to decomposition. Lignin decomposition is thought not to

occur in anaerobic conditions, although lignin is likely a component of the carbon lost as DOC exported in groundwater. The lignin content of the denitrification wall media is  $26 \pm 1.1\%$  of the total fiber composition. Based on carbon loss rates estimated above and assuming the lignin component of the media is entirely recalcitrant, the estimated longevity of the denitrification wall is  $23 \pm 5.9$  years. This estimation is similar to carbon consumption rates measured in New Zealand, where a denitrification wall receiving lower nitrogen loads is on pace to have all of the carbon consumed in approximately 28 years (Long et al., 2011). The denitrification wall will need to be monitored in the future to determine if declines in carbon quality instigate reductions in nitrate removal rates before all carbon is lost.

### **Summary and Recommendations**

In this denitrification wall with a continuously high nitrate loading rate, an elevated removal efficiency relative to other studies was observed. Nitrate removal rates per volume of media were measured as high as  $5.5 \text{ g-N m}^{-3} \text{ day}^{-1}$  in well transects and  $7.68 \text{ g-N m}^{-3} \text{ day}^{-1}$  in the laboratory. Consequently it can be concluded that denitrification walls will rapidly remove nitrate even when placed within the high nitrate loading rate conditions characteristic of groundwater adjacent to major surface water discharges thus confirming Hypothesis 2-1. These rates are higher than those measured in other sand-sawdust denitrification walls, although laboratory analyses indicate that denitrification rates are sufficient to explain the declines in nitrate, verifying Hypothesis 2-2. Due to these high nitrate removal rates and the size of the wall, approximately  $220 \pm 54 \text{ kg}$  of N was removed from over approximately 37 million liters of groundwater per year.

A rapid decline in denitrifying enzymes with short distances and nitrate removal rates in the well transect study indicates that all nitrate was depleted in a fraction of the wall width. The rapid N depletion in the wall indicates that assuming laminar flow of groundwater, the denitrification wall was oversized. Even though the treatment volume was high, nitrate concentration in downgradient wells at the ends of the wall were elevated compared to wells within the wall, indicating that groundwater was likely bypassing the wall. A greater treatment volume could thus be achieved with the same volume of denitrification wall media by installing a thinner permeable barrier over a longer width to minimize bypass discharges and treat a larger volume of groundwater

Further reductions in the size of PRBs could be achieved by decreasing the height of the wall because groundwater converges from above and below the PRBs. In this study, when groundwater elevation was up to 0.7 meters above the wall there was no negative impact on nitrate reductions, thus indicating downward movement into the high permeability zone. Deliberately placing the denitrification wall below the high water table also has the advantage of reducing rapid carbon depletion due to aerobic decomposition that can occur during droughts. This increase in carbon depletion, has been found to considerably reduce the lifespan of the carbon amendment (Long et al., 2011; Moorman et al., 2010). In the current study carbon consumption rates indicate a lifespan of approximately  $23 \pm 5.9$  years (Objective 2-1). These high nitrate removal rates and the implied groundwater convergence, indicate that more efficiently sizing denitrification walls can treat a more significant volume of groundwater.

## CHAPTER 3 EVALUATION OF A DENITRIFICATION WALL TO REDUCE SURFACE WATER NITROGEN LOADS

### **Background**

Nitrogen leached to groundwater underneath agricultural fields can have a cascade of impacts on the biology of aquatic ecosystems as it is transported to surface waters (Galloway et al., 2003). Biological denitrification is a process that removes nitrate from aquatic ecosystems, thus terminating the N cascade. Denitrification is common in riparian ecosystems where shallow groundwater is transported laterally through continuously inundated, anaerobic soils before entering surface waters (Cooper, 1990; Hill, 1996). Nevertheless, denitrification is often limited when much of the groundwater isn't transported through riparian subsoils with suitable biogeochemistry (Cooper, 1990; Hill, 1996; Lowrance, 1992; Schipper and Cooper, 1993). In areas where the water table is relatively close to the surface, there is an opportunity for an enhancement of denitrification by increasing the contact between shallow groundwater and high-carbon areas that can support denitrification.

The earliest research on denitrification walls focused on the feasibility of this technology to reduce nitrate in localized groundwater plumes by determining nitrate reductions in contiguous well transects as was done in Chapter 2 (Robertson and Cherry, 1995; Schipper and Vojvodic-Vukovic, 1998). The long-term success of these walls has shifted the focus towards determining the viability of this technology at an appropriate scale to reduce nitrate loading in surface waters draining agricultural properties. The efficacy of this technology to reduce stream N loading will depend on maximizing the volume of water that can be routed through the carbon substrate with a sufficient detention time to be treated. In this study, to maximize the volume of water

treated, a denitrification wall was located adjacent to a significant seepage stream thus intercepting an area where a large portion of the groundwater was focused. To determine N load reductions at the stream scale, the affected tributary and a control watershed were monitored before and after denitrification wall installation. This tributary monitoring allows for an assessment of the efficacy of the denitrification wall in the larger watershed context to meet surface water N load regulations. The hypotheses of this study are described in the following text:

- Objective 3-1. Determine if targeting a denitrification wall adjacent to surface water discharges can treat disproportionately large groundwater areas
- Hypothesis 3-1. Nitrate loads will decrease in a receiving stream solely as a result of the denitrification wall installation.

## **Materials and Methods**

### **Site Location and Construction**

The wall was installed 14 meters from the headwaters of a small stream (Figure 3-1). The headwaters of the stream begins as a well-defined seep that occurs due to a break in elevation where the shallow groundwater penetrates the surface. The seep is the largest contributor to the discharge of this small tributary, although there are numerous small seepages along the flowpath. To maximize treatment volume, the wall was centered in a groundwater cone of depression where surface water discharges had locally lowered groundwater levels (Figure 3-1). It was thought that this localized depression in the water table indicated that groundwater from a wide area would therefore be directed through this zone.

## Surface Water Monitoring

To determine the influence of the denitrification wall at the watershed scale, surface water N loads were monitored before and after wall installation in two catchments, which drain almost entirely from the property. This monitoring occurred in

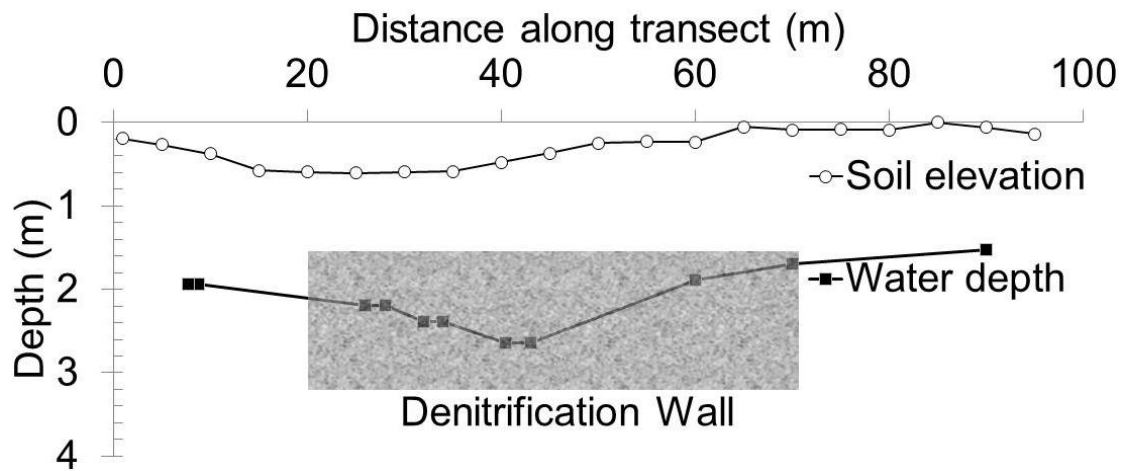


Figure 3-1. A diagram of soil and water table elevation measured before the wall was installed and the approximate location of the wall.

the 'treatment' tributary that was affected by denitrification wall installation and a 'control' watershed with similar land-use, climate, hydrology, fertilizer applications and N concentration that should not be affected by the wall (Figure 3-2). Based on a watershed delineation from sub-meter digital elevation models (DEMs), the denitrification wall only consists of approximately 10-11% of the edge of field perimeter contributing to the 'treatment' watershed (Figure 3-2). Because this small denitrification wall was targeted adjacent to a significant surface water discharge, it is expected to have a disproportional impact on N loading in the receiving stream.

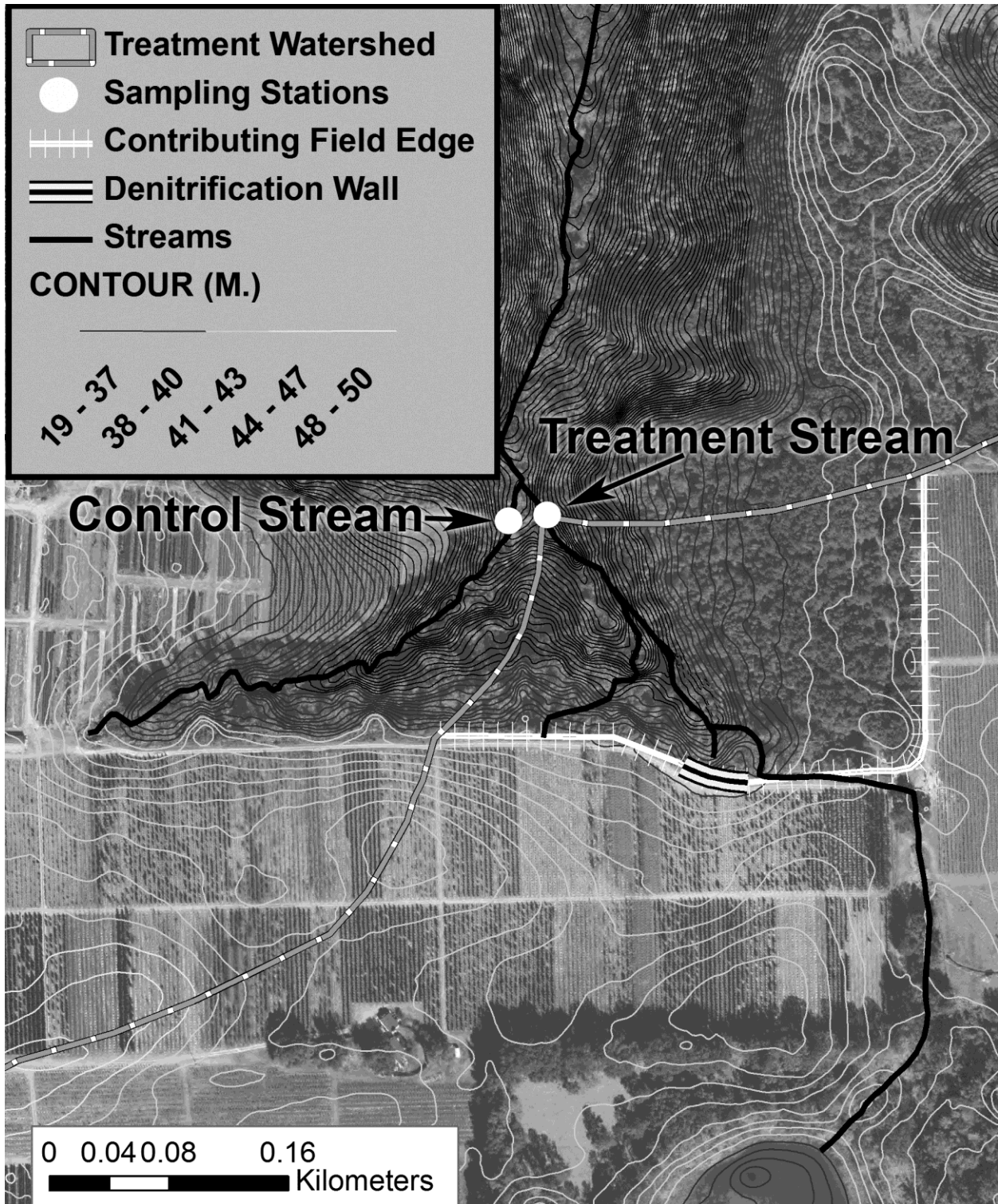


Figure 3-2. Map of the denitrification wall, contributing edge of field perimeter, elevation and N load sampling stations at the treatment and control streams. The denitrification wall only composes approximately 10-11% of the edge of field area contributing to the treatment watershed. Map created by author, using publicly available orthophotographs from (ACPA, 2006)

Weirs, pressure transducers (Instrumentation Northwest Inc., Kirkland, Wa) and dataloggers (Campbell Scientific, Logan, Utah) were installed downstream of the treatment and control catchments to calculate discharge following protocols outlined in USBR (2001). Weirs were a compound v-notch design with a larger compound rectangular weir for short duration high flow events located above a 90 degree v-notch weir used to measure lower volume baseflow conditions. The relationship between stage and discharge for the v-notch portion of these weirs was determined using the Kindsvater-Shen equation and flows through the rectangular portion were calculated using the Kindsvater-Carter equation (USBR, 2001). When water was discharging through the larger rectangular portion of the weir, flows through the v-notch were calculated as an orifice flow using a standard orifice flow equation. The data was collected continuously and reported every five minutes.

At the two sampling stations, discharge-weighted water samples were collected in an autosampler at programmed stream discharge volumes into pre-acidified bottles. Samples were removed from the autosampler weekly, filtered if applicable, refrigerated and analyzed within 28 days. For the first 163 days of sampling, approximately 15-20 flow-weighted samples per week were collected which were composited in to increments of 5 samples for a N load reporting frequency of 3-4 times per week. For the remainder of the monitoring, flow-weighted samples were collected at the same frequency but composited in to one weekly sample for nitrogen analysis, which gives the same average load as the previous method. In addition to the flow-weighted samples, grab samples were collected (n=34) beginning in October, 2008 for 290 days before monitoring of the discharge sampling station began (August, 2009). This extends

the nitrogen concentration record before the wall was installed to 352 days. After the wall was installed, N concentration, discharge and load were monitored for an additional 448 days. Grab samples were carefully collected from the middle of the water column, minimizing sediment disturbance and were immediately filtered if applicable and refrigerated.

Flow-weighted and grab samples were analyzed for nitrate and total Kjeldahl N (TKN). Unfiltered samples were digested with a block digestion and subsequently analyzed colorimetrically for TKN on an autoanalyzer (Seal Analytical, West Sussex, UK). Nitrate samples were prepared by filtering through a 0.45  $\mu\text{m}$  membrane filter (Pall Corporation, Port Washington, NY) and then analyzed colorimetrically after reduction in a cadmium column on an autoanalyzer (Seal Analytical, West Sussex, UK). Nitrogen load was calculated by multiplying the N concentration in the water sample ( $\text{M L}^{-3}$ ) by the discharge between samples ( $\text{L}^3 \text{T}^{-1}$ ). Statistically significant differences in N concentration and load in the two streams before and after denitrification wall installation were determined with a t-test. A change point analysis was done on N concentration and load to determine statistically significant changes in these values at an alpha level of 0.05 with the Change-Point Analyzer<sup>®</sup> software (Taylor Enterprises, Inc.).

Dissolved oxygen (DO) and dissolved organic carbon (DOC) were measured downstream from the seep in response to a bacterial bloom immediately at the stream headwaters. Dissolved oxygen was measured using a multi-probe (556 MPS, YSI Incorporated, Yellow Springs, Ohio) and DOC was determined after filtering through a

0.45 µm membrane filter (Pall Corporation, Port Washington, NY) as non-purgable organic carbon on an infrared gas analyzer (Shimadzu Corp, Kyoto, Japan).

Rainfall was measured with a tipping bucket and potential evapotranspiration was determined using the REF-ET software (Allen, 1999) as a turfgrass reference with the Penman-Monteith equation based on site measurements for solar radiation, air temperature and wind combined with relative humidity measurements (Campbell Scientific, Logan, Utah).

## Results and Discussion

### Stream Oxygen Depletion

Shortly after installation of the denitrification wall, filamentous white bacteria colonized the upper 10 m of the stream located immediately downstream of the seep. This is likely in response to excess carbon export from the wall stimulating bacterial colonization and possibly the activities of chemolithotrophic bacteria such as the *Beggiatoa* genus using reduced H<sub>2</sub>S to gain energy. *Beggiatoa* is known to be present in sulfur-rich seeps and springs and the odor of H<sub>2</sub>S was very strong during this period. The bacteria covered large portions of the stream for 50 days. As a result of this bacterial colonization, dissolved oxygen (DO) and dissolved organic carbon (DOC) were measured immediately downstream of the seep headwaters. Dissolved Oxygen and DOC values were compared to concentrations measured in groundwater within and downgradient from the denitrification wall.

During this period, dissolved organic carbon (DOC) in groundwater not influenced by the wall averaged  $1.78 \pm 0.29 \text{ mg L}^{-1}$ , while DOC concentrations downgradient of the wall regularly exceeded  $70 \text{ mg L}^{-1}$ . DOC concentrations in the stream declined over time from a high of  $5.3 \text{ mg L}^{-1}$  22 days after wall installation, to  $2.3 \text{ mg L}^{-1}$  50 days after

installation when filamentous bacteria were no longer visually detectable (Table 3-1). Similarly to DOC, DO within the stream headwaters rapidly declined 29 days after installation of the denitrification wall and rebounded to levels above background concentrations within fifty days after installation (Table 3-1). Even when DO was below background, spatial sampling indicated that after approximately 20 meters downstream from the headwaters, turbulence in the water column had increased the DO concentration to approximately 3.7 mg L<sup>-1</sup>. Although DO concentrations in the stream headwaters stabilized above background concentrations (2.3 – 2.9 mg L<sup>-1</sup>) within 50 days, DO concentrations within groundwater around the denitrification wall still ranged from 0.6 – 0.8 mg L<sup>-1</sup> 499 days after wall installation. It appears that as DOC leaching from the wall declined or was effectively assimilated by new bacterial growth, BOD at the seep subsequently declined. Therefore DO levels could easily be elevated to background levels upon atmospheric exposure and mixing in the stream. This indicates that when a denitrification wall is added in close proximity to a stream, there may be short-lived negative water quality impacts and temporary mitigating practices should be considered.

Table 3-1. Dissolved oxygen concentration (DO) and dissolved organic carbon (DOC) within receiving surface waters. Normal DO of seepage headwaters in the vicinity range from 2.3 to 2.9 mg L<sup>-1</sup>, while unimpacted groundwater DOC was 1.78 ± 0.29 mg L<sup>-1</sup> during this period

Receiving Stream Headwaters		
Days since installation	DOC (mg L <sup>-1</sup> )	DO (mg L <sup>-1</sup> )
14	4.8	2.4
22	5.3	
29	4.9	1.2
36	3.6	1.6
50	2.3	2.6
499		2.9
660	0.94	2.8

In a synthesis paper on denitrification bioreactors, Schipper et al., 2010b observed that excessive DOC concentrations were found initially in many studies and this could result in depletion of DO in receiving waters. They proposed a variety of preventative measures including pre-leaching the media, installing filters downgradient and maintaining high rates of flow during start-up to ensure nitrate is still present to assist in DOC consumption. The feasibility and cost of these options will need to be weighed against the short-term impacts on surface water quality.

### **Surface Water N Loading Reduction**

The treatment stream receiving discharges from the denitrification wall and an adjacent control stream (Figure 3-2) were monitored before and after wall installation to detect and quantify changes in nitrogen concentration and load due solely to the wall installation. While no two watersheds are exactly the same in hydrology or nitrogen concentration, these two watersheds are sufficiently similar to merit comparison. The two streams discharge from immediately adjacent watersheds whose major headwaters are separated by less than 500 m. As such they both share very similar climates. Both watersheds are almost entirely under the same land-use (container-plant nursery) and fertilizer is applied at the same time of year to both watersheds. Most significantly, before the wall was installed, the relationship in discharge and nitrogen concentration between the two streams is strongly correlated justifying their comparison (Figure 3-3).

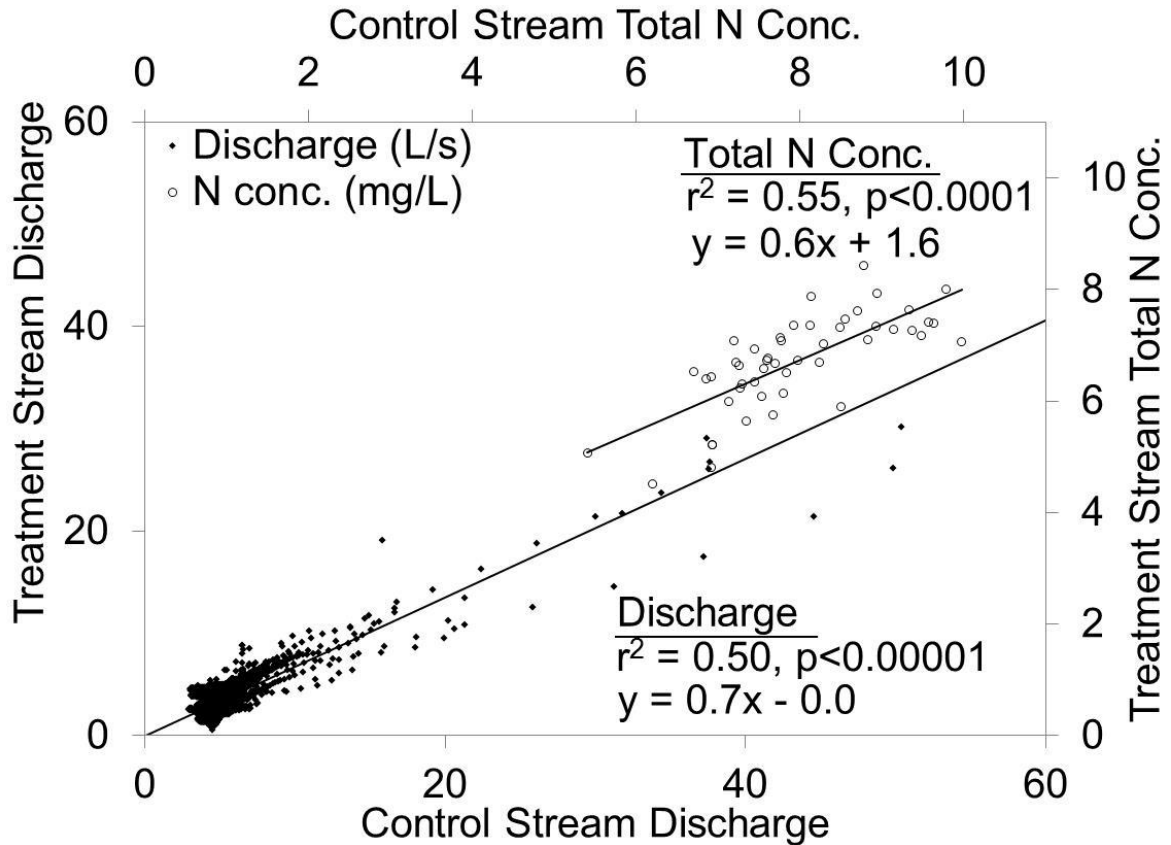


Figure 3-3. The correlation between discharge and N concentration between the control and treatment stream. The correlation between discharge and nitrogen concentration between the two streams is strongly significant, justifying their comparison.

All results are reported as total N, which is the sum of measured nitrate and TKN. TKN only averaged  $0.7 \pm 0.4 \text{ mg L}^{-1}$  and  $0.8 \pm 0$  in the control and treatment streams respectively and this concentration did not significantly change after the wall was installed. Before the denitrification wall was installed, total nitrogen concentrations were stable in both the treatment and control streams and no significant change points occurred (Figure 3-4a). After the wall was installed, the N concentration in the treatment stream immediately diverged from the control stream, with the first change point occurring in the treatment stream 2 days after the wall was installed. Due to the fact that the detention time of the denitrification wall in groundwater was reported in Chapter 2 as

1.7 – 1.9 days, this is strong confirmation of the denitrification wall's immediate impact. Subsequent change points occurred when the concentration appeared to partially rebound higher and then stabilize at an intermediate concentration over the duration of the study. This is plausibly due to an initially high concentration of soluble and labile C sources when the wall was first installed, which instigated elevated N removal rates. After these labile C sources were depleted, the N removal rates appear to have stabilized at a new equilibrium, utilizing consistent C sources. Long-term studies of denitrification walls have indicated that N removal rates stabilize after one year of operation and are predictive of long-term rates (Robertson et al., 2000; Schipper and Vojvodic-Vukovic, 2001; Jaynes et al., 2008, Schipper et al., 2010b). Removing this period of temporarily high N reductions, the total N concentration declined from  $6.7 \pm 1.2$  mg L<sup>-1</sup> before the wall was installed to  $3.9 \pm 0.78$  mg L<sup>-1</sup> in the period after the last change point only. The concentrations observed in the treatment stream after wall installation have no overlap with concentration deviations experienced before wall installation across the range of discharges (Figure 3-4b). This indicates that the concentration reduction in the treatment stream is robust across a variety of discharges. No change points were detected and no subsequent decline was apparent in the control watershed, which significantly increased from  $7.4 \pm 0.91$  mg L<sup>-1</sup> (n=70) before construction to  $7.9 \pm 0.78$  mg L<sup>-1</sup> (n=109) after construction (Figure 3-4a, c).

Corresponding to the N concentration reductions, the N load declined in the treatment stream. Before wall installation, the daily total N loading rate within the treatment stream was  $1.5 \pm 0.32$  kg day<sup>-1</sup> (n=20) (Figure 3-4e). Similarly to N concentration, the initial two-month decline in loading rate was quite high decreasing by

73% to  $0.39 \pm 0.51 \text{ kg day}^{-1}$  ( $n=70$ ) for an annual average reduction of approximately  $391 \text{ kg yr}^{-1}$ . Mass loads of any constituent are very strongly driven by discharge. It is therefore difficult to extrapolate the impact of the denitrification wall on N loading beyond the initial period after construction because seasonal shifts in precipitation and evapotranspiration over longer time frames modify discharge and thus stream N load (Figure 3-4f). Unfortunately as the change point analysis of N concentration revealed, the initial N reductions were temporarily elevated and after three months they stabilized at a new equilibrium. An analysis of the climatically similar periods before and immediately after the wall was installed will likely yield artificially high estimates of long-term load reduction. Nitrogen loading rate over the entire 15 month monitoring period after wall installation was  $0.82 \pm 1.59 \text{ kg day}^{-1}$  ( $n=119$ ) but much of this load is driven by rain events and declines in evapotranspiration, which increase discharges (Figure 3-4f). For example, N loading increased during the winter months, largely due to a 50-year storm in January and seasonally-reduced evapotranspiration creating even greater discharges (Figure 3-4f).

One method for discerning long-term rate reductions is to compare the same seasons before and after wall installation. During a subsequent summer/fall period one year after wall installation, where there was no significant difference in rainfall, evapotranspiration or discharge from the previous year, the total N loading rate in the treatment watershed was  $0.52 \pm 0.26 \text{ kg day}^{-1}$  ( $n=15$ ). Comparing this stabilized N loading rate a year after construction to the same time of year before wall construction ( $1.46 \pm 0.32 \text{ kg day}^{-1}$ ) indicates a large cumulative N load reduction of 65% for an average load reduction of approximately  $340 \pm 130 \text{ kg}$  of N per year.

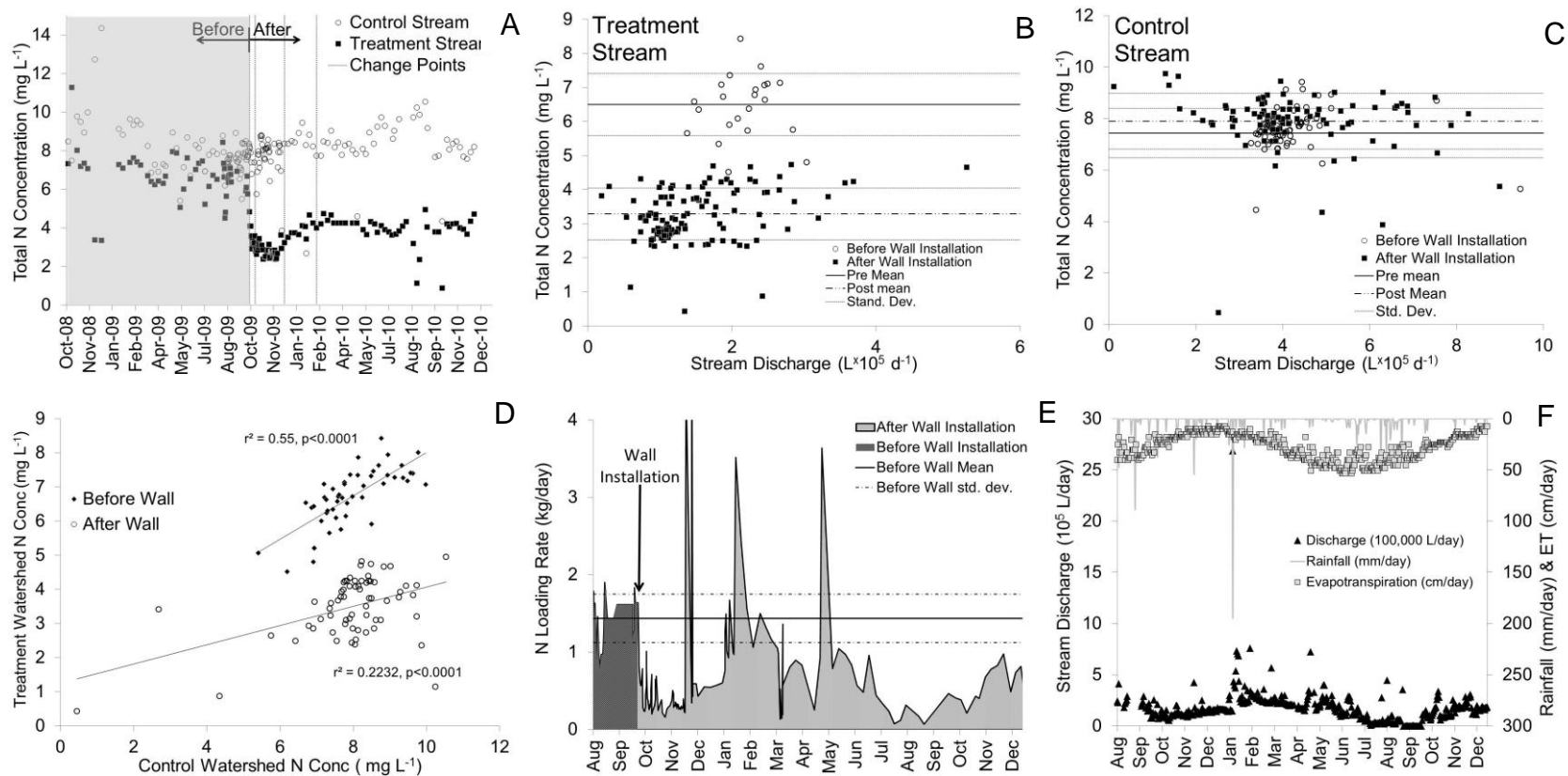


Figure 3-4. N concentration, load and hydrology values for the treatment and control stream before and after wall implementation. Shown in the figures are (A) N concentrations in the control and treatment stream before and after wall installation with significant change points indicated, N concentrations across the range of discharges measured for the (B) treatment and (C) control stream, (D) N concentration relationships between the control and treatment stream before and after wall installation and (E) N load in the treatment stream before and after wall installation, and (F) watershed rainfall, evapotranspiration and treatment stream discharge.

## Nitrogen in groundwater versus surface water

The average discharge of the stream within the treatment watershed is  $17.4 \times 10^4 \pm 16.4 \times 10^4$  L day<sup>-1</sup>. This high variability in daily discharges attests to the strong seasonal variability of the stream. Based on the findings in Chapter 2, the denitrification wall treats approximately  $10 \times 10^4 \pm 2.7 \times 10^4$  liters of groundwater per day (~60% of stream discharge). Based on rates measured one-year after construction, N load in the stream has been reduced by approximately  $0.94 \pm 0.36$  kg d<sup>-1</sup>, while reductions quantified in groundwater from Chapter 2 were only  $0.68 \pm 0.17$  kg d<sup>-1</sup>. Based on these values the reduction in groundwater N load resulting from water passing through the denitrification wall is on average lower than the N load reductions in the stream, although there is overlap in the variability measured. Two possible explanations for this discrepancy are measurement uncertainties, or that the denitrification wall has increased in-situ N reductions either in groundwater outside the footprint of the well transects or within the stream itself. The former explanation is an inevitable limitation of assessing complicated groundwater and surface water discharges, while the latter hypothesis has intriguing implications.

There is some evidence that at least initially, excess carbon spiraling within the watershed was stimulating N loss and transformations within the stream. For a duration of five months after wall installation, grab samples from the stream below the seep were collected and analyzed for nitrate. During this period, nitrate reductions at the stream seep were significantly lower ( $33 \pm 13\%$ , n=25) than what was observed in flow-weighted samples collected 155 meters downstream of the seep at the surface water sampling station ( $57 \pm 12\%$ , n=92). While it is entirely reasonable to assume that some of the effluent from the denitrification wall bypassed the main seep and discharged at

seepages downstream, it is plausible that increased DOC loads resulting from the wall had stimulated further nitrate reductions. Before wall installation, significant in-situ nitrate reductions as a result of denitrification were observed where stream morphology facilitates high organic carbon and hypoxia (Frisbee, 2007).

Although the DOC loading rate downstream of the wall declined from that initial 5-month period when grab samples were collected at the main headwaters, the DOC concentration in groundwater is still elevated above background conditions. One-year after wall installation, the DOC concentration had increased between the upgradient and downgradient well from  $0.94 \pm 0.61$  to  $3.1 \pm 1.2$  mg L<sup>-1</sup> (n=14) and the DOC loading rate was 1.04 kg day<sup>-1</sup> higher as a result. Assuming the DOC is bioavailable and there are hypoxic pockets in smaller seeps or within the stream itself where denitrification can occur, the stoichiometry of the denitrification reaction can be used to estimate potential further nitrate reductions in the stream. Based on this stoichiometry, the excess carbon loading has the potential of removing an additional 0.97 kg N day<sup>-1</sup>, which would be more than sufficient to explain the difference between reductions measured in groundwater as compared to those measured in surface waters. Actual nitrate reductions as a result of denitrification within the stream are likely to be less than this total potential value as a result of hydrological and biogeochemical limitations on the denitrification reaction. Additionally it is possible that the increased carbon in the stream instigated increased N assimilation rates. Nevertheless, the increased DOC concentration above background indicates that the impact of a denitrification wall on nitrate reductions potentially extends far beyond the footprint of the wall and could

influence N cycling much further downgradient of the wall. Further work would need to be done to confirm this hypothesis.

### **Summary of results**

Installation of denitrification walls adjacent to streams enables reductions in groundwater nitrate before reaching sensitive surface water bodies. Even in relatively fast moving groundwater ( $1.7 \text{ m day}^{-1}$ ) with short detention times ( $1.7 - 1.9$  days) within the denitrification wall, annual N load was dramatically reduced in a receiving stream. Although the small denitrification wall only composed 10-11% of the edge of field area contributing to the treatment stream, the denitrification wall treated 60% of the stream volume and total N load declined from 65 – 73% for a total reduction of  $345 - 391 \text{ kg yr}^{-1}$ . The total N concentration in the stream declined from  $6.7 \pm 1.2 \text{ mg L}^{-1}$  before the wall was installed to  $3.9 \pm 0.78 \text{ mg L}^{-1}$ . Surface water reductions as a result of denitrification wall installations have never been reported before and this work verifies that targeting denitrification walls can have a disproportionate impact on downstream N loading. Because there was no corresponding decline in concentration or load in the control stream, the N load reductions are solely as a result of the denitrification wall installation, thus confirming Hypothesis 3-1. While this denitrification wall was sufficient to markedly reduce N load in one stream, it represents only approximately 10% of the total nitrate load discharged from a 160 acre agricultural property. The success of this denitrification wall indicates the possibility of using similar techniques to achieve N load reductions in all four tributaries draining this property.

The effect of the denitrification wall on groundwater biogeochemical cycling appeared to extend beyond the immediate confines of the wall cross section. Initially high pulses of DOC and possibly  $\text{H}_2\text{S}$  contributed to declines in surface water DO and a

bloom of bacteria in the receiving stream for approximately 50 days. This increase in DOC loading likely facilitated additional denitrification and N assimilation within the groundwater and stream. Hence N possibly continues to be removed in groundwater downgradient from the wall and/or within the stream itself.

### **Nitrogen load treatment costs**

The cost of materials and construction of the denitrification wall were approximately \$20,000. This could be reduced by using on-site sand at a cost reduction of approximately \$3,000 and utilizing trenching equipment, which is usually owned by agricultural landowners. This trenching equipment could pragmatically be used to construct a series of narrow walls each adding up to the desired flow length. Nevertheless, assuming a conservative 15 year life-span and stable nitrate removal rates measured one year after installation, the total cost per kilogram of N removal over the 15-year period with the current study design is \$0.79 per kg. This is a conservative estimate as the carbon longevity of the denitrification wall is estimated to be  $23 \pm 5.9$  years (Chapter 2) and the longevity of a carefully monitored denitrification wall in operation for 15 years is estimated to be 28 years total (Long et al., 2011). Estimates of nitrogen removal costs within the Mississippi basin for other N removal treatments are generally an order of magnitude higher (CENR, 2000). Municipal wastewater treatment is estimated to cost  $\$40 \text{ kg}^{-1}$ , treatment wetland costs are  $\$8.90 \text{ kg}^{-1}$  and riparian buffers cost are  $\$26 \text{ kg}^{-1}$  (CENR, 2000). Scaling this groundwater bioremediation up to target all four streams discharging from the agricultural property could therefore be a cost-effective method to markedly reduce N load to downstream aquatic systems.

CHAPTER 4  
MODELING THE EFFECTS OF TEMPERATURE, HYDRAULICS AND MEDIA  
PHYSICOCHEMICAL PROPERTIES ON DENITRIFICATION BIOREACTOR  
PERFORMANCE

**Background**

The long-term success of denitrification bioreactors to efficiently remove nitrate from groundwater with no maintenance, indicates this technology is a feasible option to achieve significant improvements in water quality (Long et al., 2011, Moorman et al., 2010; Robertson, 2008). For denitrification bioreactors to be used on a wide-scale, generalizable conclusions on the performance of different media types will be useful for providing design guidelines in a range of groundwater temperatures and velocities. A wide variety of media have been used for denitrification bioreactors including vegetable oil, ethanol, newspaper, jute pellets, wheat straw, alfalfa straw, sawdust, wood pulp (cellulose) and cotton (Hunter and Follett, 1997; Patterson and Grassi, 2002; Volokita et al., 1996b; Wakatsuki and Esumi, 1993; Vogan et al., 1992; Volokita et al., 1996a; Boussaid and Martin, 1988). Cameron and Schipper (2010) observed that although very labile media (maize cobs, wheat straw, green waste) initially had higher nitrate removal rates than hardwood or softwood sawdust, they also had the greatest declines in nitrate removal rates within the 10 months of the study. Due to the long-term sustainability of wood media as compared to more initially labile forms, the consensus in the field is that wood sawdust or woodchips are the most utilitarian bioreactor media. As a result of these factors, the effects of two different types of wood (hardwood and softwood) on bioreactor performance were evaluated, although there are likely other carbon sources that could sustainably reduce nitrate in bioreactors.

Bioreactor performance has also been hampered by reductions in hydraulic conductivity due to excavation and media installation. Resulting from the hydraulic bypass of a denitrification wall that used fine wood media (Schipper et al., 2004), the focus of the field has shifted towards using coarser wood particles (Robertson, 2010). As a result, the more recent bioreactors have been constructed from coarser wood media (Jaynes et al., 2008; Schipper et al., 2010a). Contrastingly, recent research indicated that the hydraulic bypass observed in the Schipper et al., (2004) study was a result of wet-mixing poorly sorted aquifer material below the water table and was not necessarily due to the use of fine sawdust (Barkle et al., 2008). It is feasible that finer media would have higher denitrification rates resulting from an inherently higher surface area to volume ratio providing more area for enzyme degradation and microbial attachment. Excluding finer media types could therefore possibly eliminate an efficient bioreactor media source. To test these hypotheses, the nitrate removal rates and hydraulic properties of three different sizes of bioreactor media (fine pine sawdust, coarse pine sawdust and large shredded pine) were evaluated in this study. Additionally the surface area of all the media was quantified to establish if there is a more direct connection between media surface area and denitrification rates.

Denitrification walls have been constructed with wood:sand volume ratios of approximately 20% (Robertson and Cherry, 1995; Schipper et al., 2004), 50% (Schipper et al., 1998) and even 100% (Fahrner, 2002). While it is reasonable to assume that increases in wood amount will result in increased nitrate removal rates, at least one denitrification wall has been consistently shown to be nitrate and not carbon limited (Long et al., 2011; Schipper et al., 2005). If there are differential nitrate removal rates

resulting from increasing wood volumes, it will be important to quantify for providing bioreactor design guidelines. Additionally, the hydraulic impacts of increasing wood:sand volume ratios will be important to understand to minimize hydraulic bypass. In this study, the impact on bioreactor denitrification rates and hydraulic performance from increasing the wood volume will be discerned.

Denitrification walls constructed of wood media continue to remove greater than 60-90% of nitrate for at least 15 years (Long et al., 2011, Moorman et al., 2010; Robertson, 2008). To verify the long-term sustainability of the different wood treatments (wood type, wood size and wood volume), changes in total carbon and carbon quality will be determined over time. Changes in carbon quality occur as a result of microbial processes but as was observed in the field-scale denitrification wall in Chapters 2 and 3, a majority of the initial carbon loss is through dissolved organic carbon (DOC) export. This DOC export can also detrimentally impact receiving waters, therefore the DOC leaching of each of the treatments were quantified in this study. Increases in total Kjeldahl N (TKN) were also observed as a result of denitrification wall installation. As opposed to denitrification, nitrate that is converted to TKN is still bioavailable and can impact receiving bodies. Because TKN and DOC can impact adjacent waterbodies, their export rates from the different treatments will be quantified.

While it is possible to use these qualitative predictors of bioreactor media (wood type, wood size and wood volume) as pragmatic guidelines, parameterizing the physicochemical drivers of denitrification rate will allow for a greater customization towards the variety of potential bioreactor media. Determining the specific media properties which drive denitrification rate, may elucidate potential media sources with

high denitrification efficiency and improve our understanding of denitrification in natural settings. Although it is clear that very labile media (maize cobs, wheat straw, green waste) have higher denitrification rates (Cameron and Schipper, 2010), the quantitative relationship between measurable predictors of carbon quality and media surface area on denitrification rate has not been well established. Lastly, the role of temperature in denitrification rates will be evaluated to inform the scaling of bioreactor designs to different climates. The objective of this last portion of the study is to determine which physicochemical properties of bioreactor media influence nitrate removal rates and create a predictive model across a range of temperatures and groundwater hydraulics to facilitate design. The hypotheses and objectives of this research are described in the following list:

- Objective 4-1. Infer denitrification wall performance from qualitative and quantitative predictors to guide design
- Hypothesis 4-1. Nitrogen reduction rates will increase with greater wood volume ratios and smaller wood sizes.
- Hypothesis 4-2. Hydraulic conductivity will decrease with declining wood sizes.
- Hypothesis 4-3. Nitrogen reduction rates will be higher in bioreactor media with greater total carbon content, bioavailable fiber components and surface areas.

## **Materials and Methods**

### **Mesocosm Installation**

To examine the effects of wood media size, percent volume, surface area, temperature and carbon quality on the biogeochemical, physical and hydraulic properties of reactor media, a continuous flow-through mesocosm experiment was conducted. Groundwater from underneath an agricultural property with an average nitrate concentration of  $7.5 \pm 0.73 \text{ mg L}^{-1}$  continuously flowed through the different

treatments for a duration of 246 days. Groundwater was pumped (Mini Typhoon® DTW, Proactive Environmental Products, Bradenton, FL) from a well to a 200 L collapsible bladder (Navimo USA Inc, Sarasota, Florida) contained within a water-filled displacement tank approximately 2 m. off the ground (Figure 4-1). Using a sealed bladder excluded atmospheric exposure, which could affect dissolved oxygen content and therefore the denitrification rate of the groundwater. The groundwater well pump was controlled by float switches (SMD Fluid Controls, Wallingford, CT) triggered by changes in the water displacement volume caused by the expansions and contractions of the collapsible bladder. This allowed for a relatively consistent head gradient between the bladder and the mesocosms. The pumps were powered by solar panels (Sunforce Products Inc, Montreal West, QC, Canada) connected to deep cell marine batteries. Once in the bladder, the groundwater flowed via passive head gradients in to the bottom of each mesocosm packed with the reactor media treatments and out the top. This vertical flow-through design was used to minimize the impact of hydraulic short-circuiting above the media, which would occur as media compacted in a horizontal flow-through system.

Each mesocosm consisted of PVC pipes 15.2 cm in diameter and 1.52 meters long for a total volume of approximately 28000 cm<sup>3</sup> each. At the bottom (influent) and top (effluent) portions of the mesocosm a nylon filter fabric (Aquatic Ecosystems, Inc., Apopka, Florida) with a pore size of 0.105 mm was glued to the PVC to prevent the fluidized reactor media from mobilizing. Additionally at the bottom (influent) portion of the mesocosm, a 1.3 cm layer of gravel was added to evenly distribute flow and prevent short-circuiting. The thirty mesocosms were packed with 10 different treatments in

triplicate. Each treatment was prepared in batches by thoroughly mixing the wood product with a commercially available (Edgar Minerals, Inc., Edgar, Florida) washed and sieved quartz sand (particle size = 0.106 – 0.15 mm) and small aliquots of local A-horizon soils to seed the reactor media with denitrifying bacteria. The reactor media were then added to each PVC mesocosm and tamped down with a consistent pressure approximately every 0.3 meters. Subsamples of each mixed media type were collected in duplicate at the beginning of the study for further analysis. PVC caps were placed on the top and bottom with ½ inch i.d. tubing entering and exiting the mesocosm.

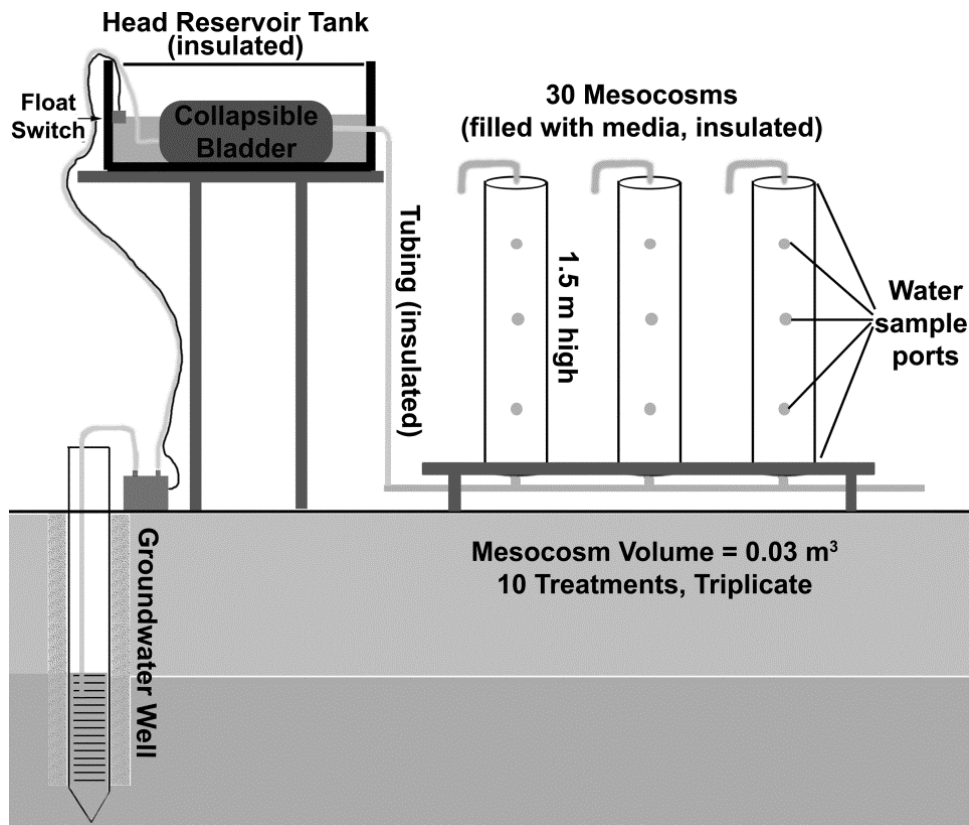


Figure 4-1. A diagram of the continuous-flow mesocosm experiment used to test the impact of various treatments on nitrate removal rates. Thirty mesocosms were filled with ten different bioreactor media in triplicate. Groundwater from underneath an agricultural property continuously flowed through the media for 246 days. Groundwater was protected from exposure to oxygen and temperature increases.

The displacement tank and each individual mesocosm were wrapped with a reflective and insulating material to reduce temperature change from conditions in the groundwater. Additionally the entire apparatus was covered in a tent, which was covered with this material. Temperature of the influent and effluent water was measured at each sampling event with a thermometer and over longer time periods using a thermochron ibutton<sup>®</sup> equipped with a datalogger (Maxim, Sunnyvale, CA).

The treatments included different particle sizes, wood types as well as different volumes of wood media (Table 4-1). Additionally control mesocosms with sand-alone were monitored. All wood treatments were free of bark. The ‘wood media volume treatment’ consisted of different volumetric percentages of coarse and fine pine sawdust to sand (0, 10, 25, 50%) as well as hardwood ratios of 25 and 50%. The two ‘wood type treatments’ tested were a fine hardwood sawdust and a fine softwood/pine sawdust mixed in 25% and 50% volumetric percentages. The ‘wood media size’ treatment consisted of a 25% mixture by volume of the fine pine sawdust, a coarse pine sawdust and a large shredded pine.

Table 4-1. A summary of the bioreactor media treatments.

Wood Type	Wood:Sand Volume Ratio	Diameter (D <sub>25</sub> , D <sub>50</sub> , D <sub>75</sub> )	Species
Fine Pine Sawdust (FPS)	10%		
Fine Pine Sawdust (FPS)	25%	(0.35, 0.53, 0.55 mm)	
Fine Pine Sawdust (FPS)	50%		<i>Pinus taeda</i> , <i>Pinus</i>
Coarse Pine Sawdust (CPS)	10%		<i>elliottii</i>
Coarse Pine Sawdust (CPS)	25%	(1.4, 2.5, 4 mm)	
Coarse Pine Sawdust (CPS)	50%		
Shredded Pine	25%	(3.5, 6.3, 7.8 mm)	
Hardwood Sawdust	25%		<i>Quercus nigra</i> ,
Hardwood Sawdust	50%	(0.25, 0.28, 0.25 mm)	<i>Quercus virginiana</i>
Control sand	0%	(0.11 - 0.2 mm)	

The particle diameter distributions of each treatment are shown in Figure 4-2. It is important to note that the three reactor media used in the 'wood media size' treatment represent a broad range of particle diameters, while the fine hardwood and fine softwood sawdust used in the 'wood media size' treatment have similar particle diameter compositions, thus enabling controlled comparisons.

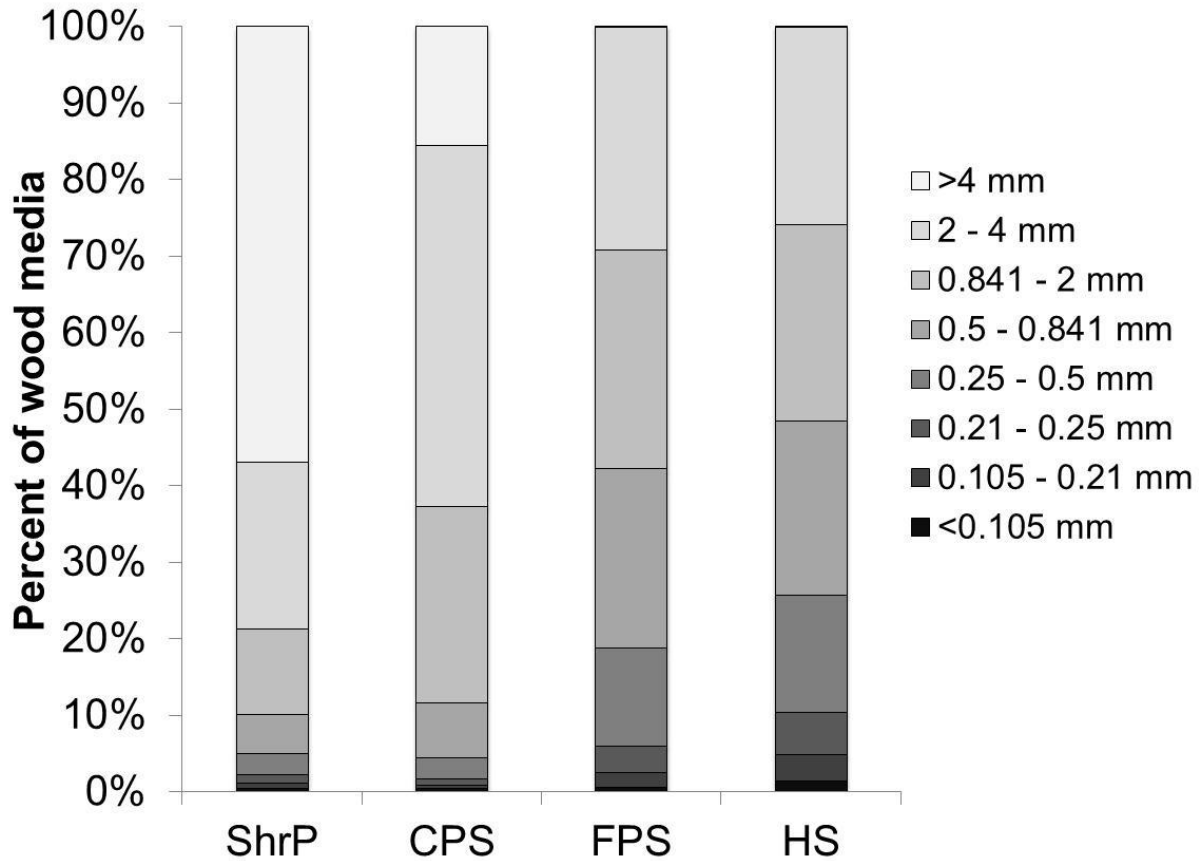


Figure 4-2. A particle size analysis of the different wood media showing the percentages of wood mass within a given particle diameter range.

To track N and C transformations with flow distance in the mesocosms, water sampling ports were installed every 38 cm by drilling a hole and placing a stopcock valve with nylon filter fabric. This will allow for a determination of whether reaction rates were zero order or first order with respect to declining nitrate concentrations and to ensure nitrate does not become limiting before sampling. Combined with the influent

and effluent of the mesocosms, this allowed for water samples to be collected at 5 different locations within each mesocosm. To determine if there is an even distribution of nitrate within the mesocosm by height or if short-circuiting is occurring, nine randomly distributed sampling ports were duplicated by installing an adjacent water sampling port at the same level. For further quality assurance, six duplicate samples were taken during each sampling event.

### **Media Physical Properties**

Bulk density was quantified by weighing the media before mesocosm introduction on a field-scale (Defender 3000, Ohaus, Parsippany, NJ) and dividing this mass by the total mesocosm volume. The different media treatments compressed over time, therefore the total volume was adjusted at the end of the study by subtracting the volume of empty space above the media from each mesocosm. Effective porosity was determined for each treatment. The effective porosity measures only the pores that transmit water, thus excluding dead-end pores and pores internal to the wood particles (Fetter, 2001). Effective porosity was determined as the volume of water that drained due to gravity from previously saturated mesocosms, which is a measure of field capacity (Ahuja et al., 1984; Timlin et al., 1999). This measure of effective porosity has been shown to be a more accurate predictor of the mobile groundwater volume in reactor media than total porosity (Barkle et al., 2008).

### **Media Hydraulic Conductivity**

Hydraulic conductivity ( $K_{sat}$ ) was measured over time ( $n = 11$ ) using a constant head method (ASTM, 2006) and quantified with a modified form of Darcy's Law using Equation 4-1.

$$K_{sat} = QL/hA \quad (4-1)$$

In this equation,  $K_{sat}$  is the saturated hydraulic conductivity ( $L T^{-1}$ ),  $Q$  is mesocosm discharge ( $L^3 T^{-1}$ ),  $L$  is the length of reactor media the water travels through ( $L$ ),  $h$  is the head difference from the bladder outflow to the mesocosm outflow and  $A$  is the cross-sectional area of the mesocosm.

### **Water Sampling and Analysis**

Water samples were collected from the sampling ports nine times over the duration of the experiment and analyzed for nitrate, total Kjeldahl N (TKN) and dissolved organic carbon (DOC). Each sample was collected as both an unfiltered, acidified sample and a sample that was passed through a 0.45  $\mu m$  membrane filter (Pall Corporation, Port Washington, NY), then acidified. All samples were immediately stored on wet ice and transported to the laboratory where they were placed in a refrigerator at 4°C until analysis. Unfiltered samples were processed using a block digestion and subsequently analyzed colorimetrically for TKN (EPA Method 351.2) with an autoanalyzer (Seal Analytical, West Sussex, UK). Nitrate-nitrite was analyzed colorimetrically (EPA Method 353.2) after cadmium reduction using an autoanalyzer (Seal Analytical, West Sussex, UK). Total Organic Carbon was quantified using EPA Method 415.1, after combustion as non-purgable organic carbon with an infrared gas analyzer (Shimadzu Corp, Kyoto, Japan).

### **Media Sampling and Analysis**

Reactor media collected before the experiment were compared to media samples collected at the end of the study to determine changes in total carbon and carbon quality (C:N ratio, fiber analysis) as a result of groundwater exposure and microbial denitrification. This analysis will be useful in inferring the longevity of each treatment type. Additionally microbial properties of the reactor media were analyzed by quantifying

microbial biomass carbon (MBC) and potential denitrification rate in the laboratory.

Lastly, total media surface area was quantified.

Media sampling was conducted at the end of the study by cutting open each mesocosm and collecting samples at several locations. Preliminary sampling was done by collecting media samples every 5 cm on four mesocosms representing the range of treatments. Based on these preliminary results, it was determined that the portion near the influent (0-10 cm portion) had unique soil properties, while the remaining portion of the mesocosm (10-152 cm) was similar. As a result, samples were collected at 0 and 10 cm, and in triplicate within the remaining portions of the mesocosms at 38, 76 and 114.3 cm. Samples were immediately placed in wet ice and brought back to the laboratory to be stored at 4°C until analysis. Samples were analyzed for total carbon, MBC and fiber components.

### **Total Carbon and Carbon Quality**

The gravimetric moisture content was quantified on subsamples of reactor media by weighing a fresh, field-moist subsample in a forced air drying oven at 105°C for 48 hours. These oven-dried samples were then homogenized and ground with a plant grinder for fiber analysis (Thomas Scientific, Swedesboro, NJ). Neutral detergent fiber (NDF), hemicellulose, cellulose and lignin were quantified as mass loss after a sequential neutral detergent-acid digestion technique (Van Soest et al., 1991) in a fiber analyzer (ANKOM, Fairport, New York). Ash content was calculated after 4 hours in a 550°C muffle furnace as the mass loss on ignition (LOI). Sub-samples of dried and ground media were further prepared by grinding with a ball-mill and analyzed for total C and total N using a thermal conductivity detector after dynamic flash combustion (Flash EA<sup>®</sup> 1112, Thermo Fisher Scientific, Miami, OK).

### **Microbial Biomass Carbon**

Moist media samples were analyzed for microbial biomass carbon (MBC) by the 24 hr. chloroform fumigation-extraction method within 4 days (Vance et al., 1987). Samples were extracted with 25 mL of 0.5 M  $K_2SO_4$  and filtered through 2.5  $\mu m$  filter paper (Whatman, Maidstone, UK). Total organic carbon (TOC) was measured as described previously. MBC was determined as the difference between untreated and chloroform-fumigated media. An extraction efficiency ( $k_{EC}$ ) factor of 0.37 was applied based on previous determinations (Sparling et al., 1990).

### **Media Denitrification Rate**

Media samples collected at 38 cm within each mesocosm were analyzed for potential denitrification rate using the acetylene block technique (Yoshinari and Knowles, 1976) within 4 days after sampling. Potential denitrification rate analysis involved measuring the denitrification rate of sample slurries inundated in the influent groundwater to the mesocosms. Samples were prepared for potential denitrification rate analysis by homogenizing media samples and then adding approximately 3 g of media into a glass serum bottle sealed with a rubber septa and aluminum crimp cap. Five mL of the influent groundwater was purged with 99.99%  $O_2$ -free  $N_2$  gas and added to the media with a syringe. Headspace air within the serum bottle was evacuated and replaced with  $N_2$  gas and then approximately 15% of the headspace  $N_2$  was replaced with acetylene gas ( $C_2H_2$ ) (Balderston et al., 1976; Yoshinari and Knowles, 1977). Serum bottles were shaken with a longitudinal shaker for an hour and stored at a constant temperature of 22°C for the duration of the analysis. Headspace gas was sampled after four hours and then hourly for the next five hours. Potential denitrification rate was quantified by fitting a least-squares regression line to the cumulative  $N_2O$

production. The denitrification rates were calculated as a rate per reactor media volume using bulk density measurements.

Nitrous-oxide production in headspace gas samples was quantified with a gas chromatograph that was equipped with a  $3.7 \times 10^8$  (10mCi)  $^{63}\text{Ni}$  electron capture detector (300C) (Shimadzu GC-14A, Kyoto, Japan). A stainless steel column (1.8 m long by 2 mm i.d.) packed with Poropak<sup>TM</sup> Q (0.177-0.149 mm; 80-100 mesh) was used (Supelco, Bellefonte, PA). The operating temperatures of the instrument were 120, 30 and 230°C for the injector, column and detector respectively. All values were modified to account for  $\text{N}_2\text{O}$  dissolution into the aqueous phase employing Bunsen absorption coefficients (Tiedje, 1982).

### **Particle Surface Area**

Total micropore (<2nm) surface area was quantified using  $\text{CO}_2$  sorptometry on an autosorb<sup>®</sup> (Quantachrome, Boynton Beach, Florida) with methodology outlined in Mukherjee et al. (2011). Briefly, bioreactor media was de-gassed under vacuum for 24 h at 180°C prior to analysis. Surface area and pore volume measurements were based on  $\text{CO}_2$  adsorption isotherms measured at 273 K and a partial pressure range of 0.001-0.15 and interpreted following protocol outlined in Jagiello and Thommes (2004).

### **Statistical and Data Analysis Methods**

Mean hydraulic conductivity was compared between treatments using a two-way ANOVA, followed by pairwise comparisons using a t-test. Different media types may change in hydraulic conductivity as a result of preferential flow-paths, compaction and media decomposition. As a result, the rate of change in hydraulic conductivity for the treatments was determined by fitting a least squares regression (LSR) line between hydraulic conductivity and time for each mesocosm. Subsequently, the LSR slope of

each treatment was compared using a two-way ANOVA and pairwise t-tests. Contrasts in carbon and fiber consumption between the beginning and end of the study were discerned between treatments on a pool of individual mesocosm differences (matched pairs analysis).

Nitrate removal rates within the mesocosms were determined as daily mass nitrate loss per volume of reactor media modified from Schipper and Vojvodic-Vukovic (2000) using Equation 4-2.

$$Nr = Q\Delta_n/V_s \quad (4-2)$$

In this equation,  $Nr$  is the nitrate mass removal rate per volume of reactor media [ $\text{g-N m}^{-3} \text{d}^{-1}$ ],  $Q$  is the mesocosm discharge [ $\text{L}^3 \text{T}^{-1}$ ],  $\Delta_n$  is the change in nitrate N concentration [ $\text{M L}^{-3}$ ] and  $V_s$  is the mesocosm volume the nitrate travels through [ $\text{L}^3$ ].

Dissolved organic carbon and TKN export rates were determined using the same methods. Due to the non-linear nature of DOC export rates over time, these values were fit to an exponential decay model in JMP<sup>®</sup> 8.0 (SAS Institute Inc., Cary, NC) with Equation 4-3

$$C_t = C_o e^{-rt} + \theta \quad (4-3)$$

In this equation,  $C_t$  is the DOC export rate per volume of media at time  $t$  [ $\text{M L}^{-3} \text{T}^{-1}$ ],  $C_o$  is the initial DOC export rate at time = 0,  $r$  is the exponential rate constant and  $\theta$  is the asymptote rate. The variable  $\theta$  was manually fit as the average DOC export rate in the final two sampling events.

The nitrate reduction rates between treatments were modeled as an analysis of covariance (ANCOVA), with a covarying quadratic temperature interaction using the PROC GLM procedure (SAS<sup>®</sup> 9.2, SAS Institute Inc., Cary, NC). To develop a multiple

regression model between the predictor variables (groundwater temperature, carbon quality, hydraulic conductivity, surface area) and nitrate reduction rates, a mixed forward and backward stepwise multiple linear regression was initially used to select the dominant predictor variables. Non-linear relationships were modeled using the fit model platform. Lastly, a multiple regression was done based on the predictors selected by the stepwise regression process to create the final model. All analyses were done at an alpha level of 0.05 and pairwise t-tests were analyzed with a bonferroni correction to the alpha level. Except where mentioned, all analyses were done using the software JMP<sup>®</sup> 8.0 (SAS Institute Inc., Cary, NC).

## Results

### Hydraulic Conductivity

The addition of woody material both increased and decreased the mean hydraulic conductivity ( $K_{sat}$ ) relative to the control sand in differing treatments (Figure 4-3). All bioreactor treatments including the control increased in hydraulic conductivity over time, likely as a result of preferential flow channels (Table 4-2). Increasing the volume of all wood types (0%, 10%, 25% and 50% by volume) had no consistent effect on the mean or rate of change in hydraulic conductivity (Table 4-2). The higher wood volume treatments tended to have a greater rate of increase in hydraulic conductivity although the differences were not significant. It is therefore difficult to predict the hydraulic conductivity of a reactor media from the amount of wood added alone.

The addition of large shredded pine and fine pine sawdust as bioreactor media markedly increased the mean hydraulic conductivity above the intermediate-size coarse pine sawdust media. The fine pine sawdust had a rate of increase in hydraulic conductivity much greater than the control, while the coarse pine sawdust had the

lowest rate of increase. Therefore, the hydraulic conductivity does not decrease with smaller media sizes. Increasing the wood media size above or below the coarse pine sawdust increased the mean and rate of change. A possible explanation for this discrepancy is that the coarse pine sawdust had a wide range of particle sizes. Soils with a wide range of particle sizes are more likely to fill varying poresizes (Fetter, 2001). The 75th percentile range of particle diameters for the coarse pine sawdust was 2.6 mm but only 0.2 mm for the fine pine sawdust. Although the shredded pine media had the highest particle diameter range (75th percentile range = 4.3 mm), the large wood pieces likely did not fill porespaces. As a result, the hydraulic conductivity of the shredded pine media treatment remained high.

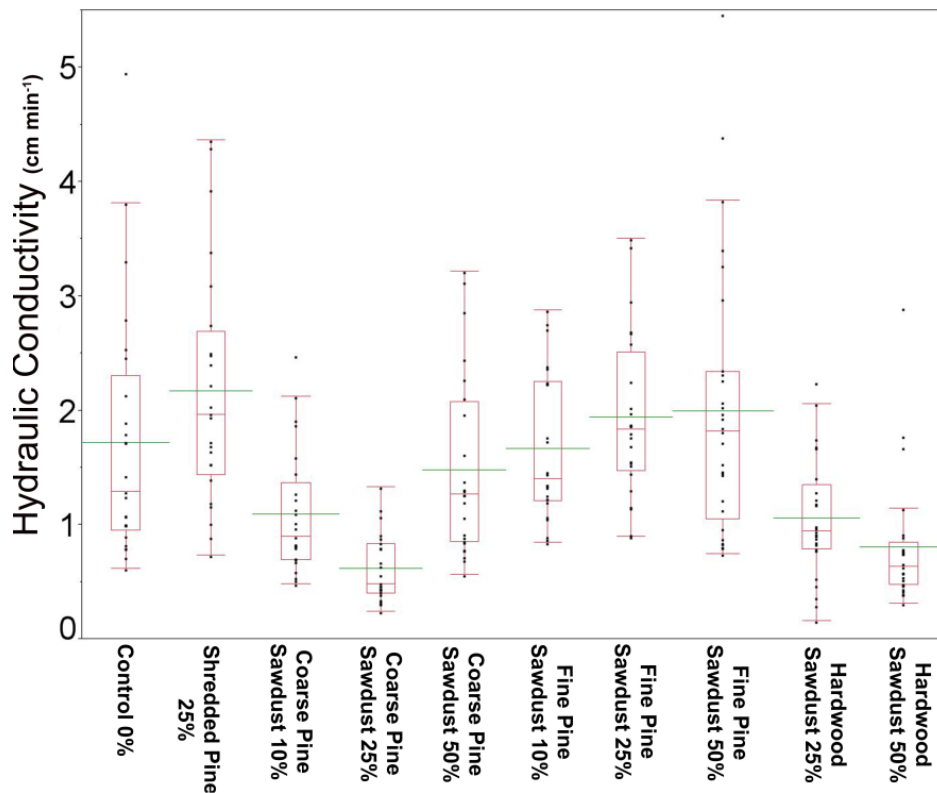


Figure 4-3. The saturated hydraulic conductivity for all treatments (wood volume, wood type and wood size) averaged over all sampling times. The percentage values after the treatment name, indicates the percent wood volume mixed with sand. The mean line is displayed in green and box plots of the quantiles are displayed for the treatments.

Table 4-2. A statistical analysis on the hydraulic conductivity mean and rate of change (slope) from varying the wood volume and particle size. Means  $\pm$  1 S.D. for the 246 day duration of the study are presented.

Saturated Hydraulic Conductivity ( $K_{sat}$ ) by Treatment							
Vol (%)	Wood Volume Treatment			Wood Size Treatment			
	Mean (cm min <sup>-1</sup> )	ANOVA		Wood Size	Mean (cm min <sup>-1</sup> )	ANOVA	
0	1.9 $\pm$ 0.7		A	Shred	2.06 $\pm$ 0.6		A
10	1.55 $\pm$ 0.5	F(3,17)=0.6 p<0.651	A	Coarse	0.62 $\pm$ 0.3	F(3,8)=4.3 p<0.043	B
25	1.38 $\pm$ 1.0		A	Fine	2.14 $\pm$ 0.7		A
50	1.86 $\pm$ 0.8		A	Control	1.91 $\pm$ 0.7		A
Rate of Change of Saturated Hydraulic Conductivity by Treatment ( $\Delta K_{sat}$ yr <sup>-1</sup> )							
0	2.5 $\pm$ 0.2		A	Shred	2.04 $\pm$ 1.1		AB
10	1.7 $\pm$ 1.2	F(3,20)=0.3 3p<0.799	A	Coarse	0.55 $\pm$ 0.5	F(3,8)=5.0 0p<0.029	B
25	2.3 $\pm$ 2.1		A	Fine	4.36 $\pm$ 2.1		A
50	2.6 $\pm$ 1.8		A	Control	2.52 $\pm$ 0.2		AB

ANOVA results indicate a significant difference within the treatment. Treatments with different letters are significantly different from each other at p<0.05.

### Dissolved Organic Carbon and Total Kjeldahl Nitrogen export

The DOC export rate was calculated for each of the eight sampling events as the mass load of DOC per volume of reactor media and modeled over time. Initially the DOC export rate was high for all treatments except the control and rapidly declined to a much lower asymptotic rate after approximately 50-150 days following an exponential decay curve (Figure 4-4). Generally the total DOC export rate increased with increasing wood volume (Table 4-3). The hardwood sawdust treatments were an exception to the increase in DOC export rate with increasing wood volume. The hardwood volume doubled from 25 to 50%, although the DOC export rate was slightly lower in the latter treatment. Similarly to any mass load, the DOC export rate is calculated from the concentration of the analyte and the hydraulic loading rate, so a positive relationship between the hydraulic and mass-loading rate is inherent. The lower hydraulic conductivity of the 50% hardwood volume treatment (Figure 4-3) explains the lower

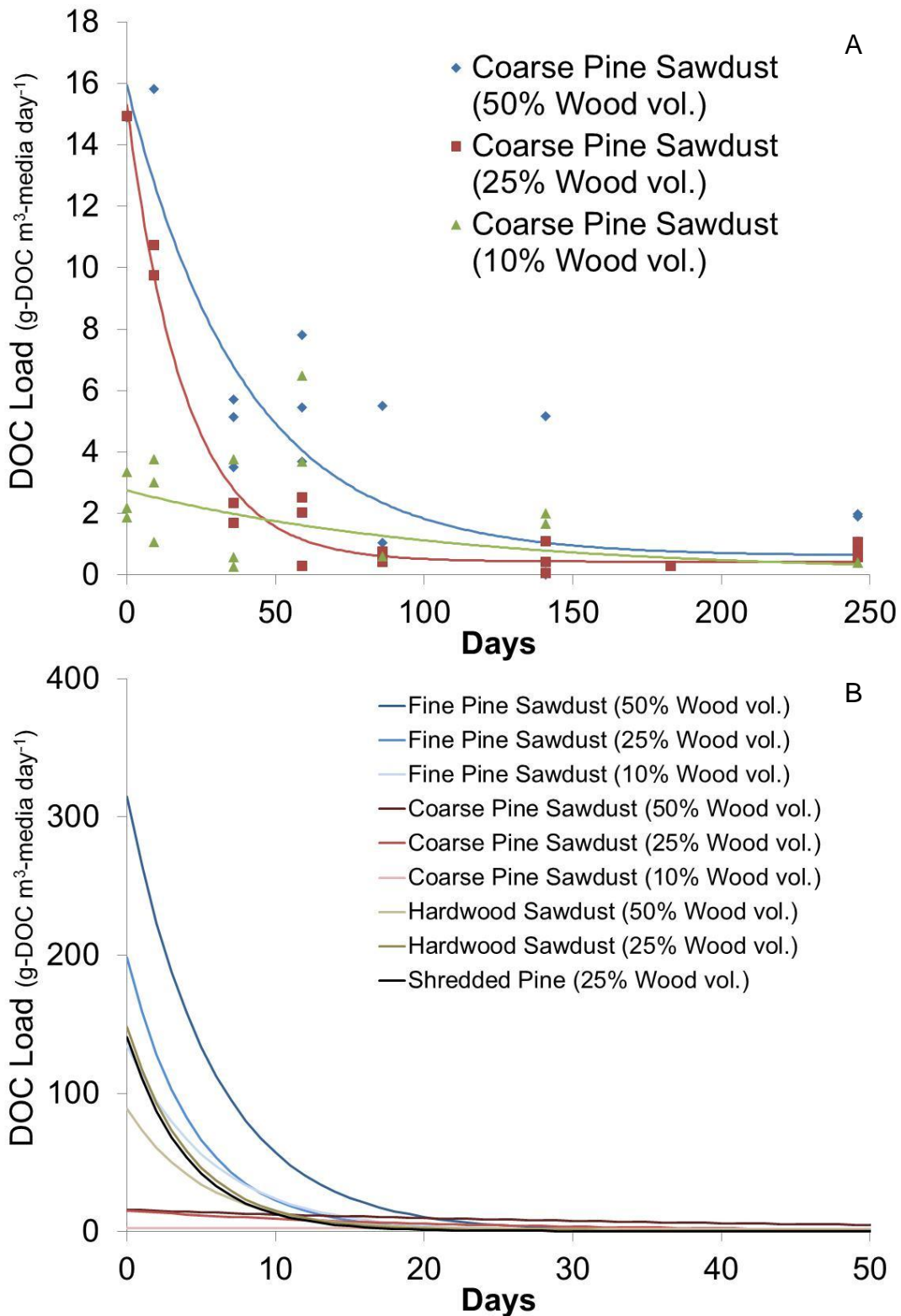


Figure 4-4. Actual and modeled data for dissolved organic carbon (DOC) export rate per volume of bioreactor media over time for all treatments. Shown in the figure are the (A) coarse pine sawdust treatment as an example and (B) modeled data for all the treatments.

DOC export rates with increasing wood volume for the hardwood sawdust. It should be noted that the long-term or asymptotic loading rate of the 50% hardwood volume treatment is over 1.5 times greater than the 25% hardwood volume treatment (Table 4-3). This indicates that the 50% hardwood sawdust had more leachable carbon remaining at the end of the study. Therefore it is possible that over longer time periods, the 50% hardwood treatment would export a greater mass of carbon albeit at a lower concentration and loading rate. Similarly, the coarse pine sawdust had lower DOC exports rates over time than the other treatments, largely resulting from the lower hydraulic conductivity.

The TKN export rate was calculated using the same methods as the DOC export rate. Similarly to DOC export, the TKN export rate was initially highest on the first sampling at day zero (TKN export rate =  $2.2 \pm 2.0 \text{ g m}^{-3} \text{ d}^{-1}$ ). In contrast, there was no significant declining trend with TKN over time as demonstrated by the fact that the second highest TKN export rate occurred at the end of the study on day 246 (TKN export rate =  $1.4 \pm 0.8 \text{ g m}^{-3} \text{ d}^{-1}$ ). It is likely that initially the TKN export was due to organic N present within leached DOC fractions, although the high export rate at the end of the study belies a biological source, such as dissimilatory nitrate reduction to ammonium (TKN) or net ammonium mineralization (ammonification). In anaerobic conditions, net ammonium mineralization generally occurs with organic matter C:N ratios greater than 100 (Reddy and Delaune, 2008). At ratios lower than this, the microbial community retains ammonium to maintain their internal C:N ratio of 10 (Reddy and Delaune, 2008). In this study the C:N ratio of all media types stayed above 100 initially averaging  $194 \pm 38$  and declining to  $103 \pm 37$  over the duration of the study.

Table 4-3. Results from the first order decay model of dissolved organic carbon (DOC) over time for the treatments. The total DOC export per volume of media over the 246 day period is reported as is the asymptote DOC export rate to indicate long-term export rates. The equation parameters as well as the root mean squared error (RMSE) of the model fit are reported.

Wood Type (% wood volume)	DOC conc. (mg L <sup>-1</sup> )	DOC Export (g m <sup>-3</sup> of media)	Asymptote rate (g m <sup>-3</sup> of media d <sup>-1</sup> )	<i>C<sub>o</sub></i>	<i>r</i>	<i>θ</i>	RMSE
Fine Pine Sawdust (10%)	35.7	942	0.49	133.81	0.18	0.49	12.5
Fine Pine Sawdust (25%)	46.1	1220	1.00	197.4	0.22	1.00	29.1
Fine Pine Sawdust (50%)	54.2	2109	0.53	313.9	0.17	0.53	64.9
Coarse Pine Sawdust (10%)	5.3	268	0.40	2.7	0.01	0.06	1.6
Coarse Pine Sawdust (25%)	25.2	394	0.43	14.9	0.05	0.43	0.7
Coarse Pine Sawdust (50%)	31.3	748	0.67	15.3	0.03	0.62	2.2
Hardwood Sawdust (25%)	44.3	914	0.95	147.1	0.24	0.95	5.6
Hardwood Sawdust (50%)	42.5	820	1.47	87.4	0.20	1.47	17.6
Shredded Pine (25%)	42.6	725	0.32	140.6	0.24	0.32	27.5

Table 4-4. A statistical analysis of the effects on total Kjeldahl N (TKN) export rate from varying the wood volume, type and particle size. Means ± 1 S.D. of TKN export rate are presented as export rate per volume of media.

Wood Volume Treatment			Wood Type Treatment				Wood Particle Size Treatment				
Vol (%)	TKN export (gm <sup>-3</sup> d <sup>-1</sup> )	ANOVA	Wood type	TKN export (gm <sup>-3</sup> d <sup>-1</sup> )	ANOVA	Group	Wood Size	TKN export (gm <sup>-3</sup> d <sup>-1</sup> )	ANOVA		
0	0.02±0.1		B	Soft	1.76±0.7	F(2,12)=13p <0.001	A	Fine	1.56±0.8	A	
10	0.49±0.3	F(3,14)=4p	B	Hard	0.82±0.2		B	Shred	1.22±0.9	F(3,8)=3p	AB
25	0.87±0.6	<0.031	AB	Cont.	0.02±0.1		B	Coarse	0.78±0.7	<0.010	AB
50	1.24±0.5		A					Control	0.02±0.2		B

ANOVA results indicate a significant difference within the treatment. Treatments with different letters are significantly different from each other at p<0.05

Therefore it is likely that net ammonium mineralization is not a likely source of TKN and other processes such as DNRA are the source of TKN after the excessive DOC leaching has declined. As a result of the variability in TKN export rates, no trend was modeled to the TKN export rate over time. The TKN export rate increased with greater wood volumes, plausibly as a result of greater DOC leaching with higher wood volumes (Table 4-4). Additionally the fine pine sawdust had a significantly greater TKN export rate than the hardwood sawdust, which is likely to be driven largely by the greater hydraulic conductivity of the former. There were no consistent trends between TKN export rate and wood particle size.

### **Reaction Order**

If the denitrification rate is affected by changes in nitrate concentration, the reaction follows first order kinetics with respect to nitrate. Contrastingly, if the rate isn't affected by nitrate concentration then nitrate reduction rate is independent of nitrate (zero order) and is controlled by other parameters (labile carbon, reduction-oxidation potential, microbial surface area, enzyme kinetics). Nitrate concentration naturally decreases as groundwater flows through the mesocosms resulting from denitrification. Therefore, if the nitrate reduction rate changes by location within the mesocosm, it can be predicted that this rate is a function of nitrate concentration. Contrastingly, it is possible that denitrification rate is a function of other parameters such as the reduction-oxidation (redox) potential or dissolved oxygen (DO) concentration. Since denitrification only occurs under when DO is limited, it is plausible that DO and redox potential will be too high near the inflow and therefore denitrification rates will have an initial lag phase and will need to be modeled accordingly. Using a paired t-test ( $\alpha = 0.5$ ) no significant differences were found between the nitrate removal rate and the four sampling locations

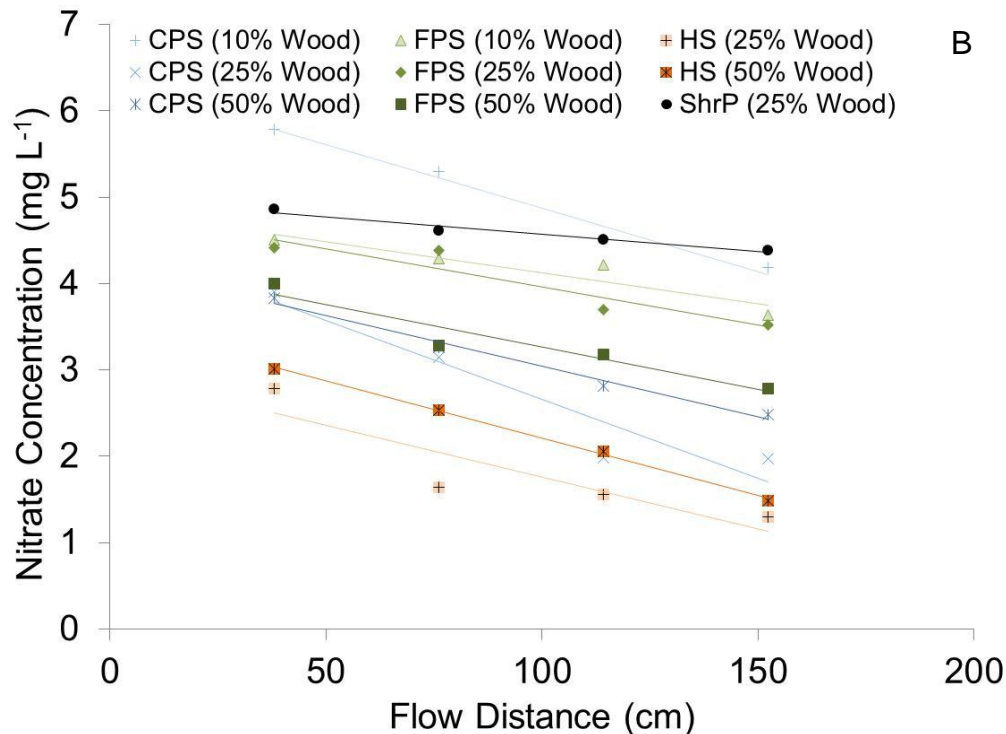
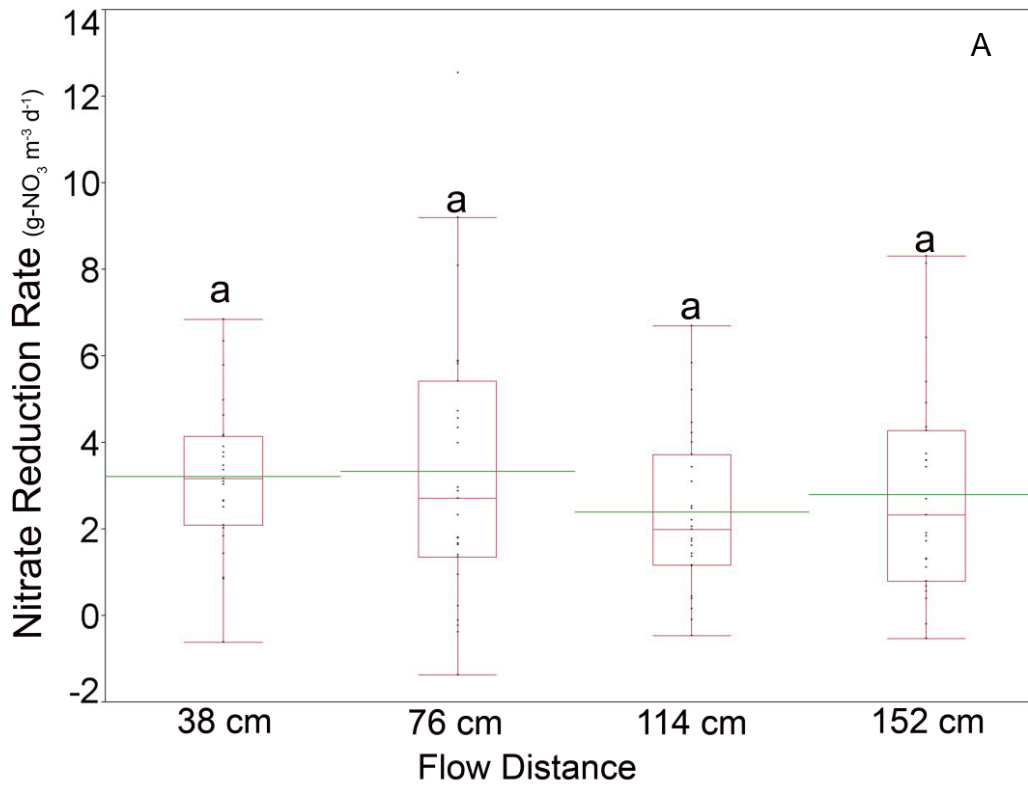


Figure 4-5. Figures demonstrating the zero order reaction kinetics of denitrification in this experiment. (A) Nitrate reduction rate by flow distance averaged over all treatments. Distances with the same letter are not significantly different from each other. (B) Average NO<sub>3</sub> concentration by flow distance for the treatments.

within all the mesocosms (Figure 4-5A). Within all of the treatments the nitrate concentration by flow-distance was strongly linear (Figure 4-5B). It is plausible that at very low nitrate concentrations the reaction rate declines correspondingly, but due to the distances between sampling locations this was undetected in the present study. The results of this study indicate that within the ranges of nitrate concentration measured and the spatial scales involved, the reaction rate follows zero order kinetics and the data will be analyzed accordingly. This is consistent with the research of Robertson (2010), who found that the nitrate reduction rate was best modeled with zero order reaction kinetics in wide concentration ranges from 3.1 to 48.8 mg L<sup>-1</sup>. Additionally the lack of an initial lag phase indicates that denitrification was not initially limited by DO or redox.

### **Denitrification Rate**

The relationship in nitrate concentrations between duplicated ports installed within the same mesocosm at the same flow distance had a slope of 1.0 and an  $r^2$  of 0.93. This indicates that short-circuiting did not occur within the mesocosms. Initial rates of denitrification were quite high. During the first three sampling events at days 0, 9 and 36, the nitrate reduction rate was sufficient that no nitrate was present in even the first sampling port located 38.1 cm from the inflow. The initial flow-rate for the mesocosms averaged  $64.9 \pm 27.2$  cm d<sup>-1</sup> and the temperature of the influent water averaged  $26.0 \pm 0.28$ °C through these first three sampling events. This entails that influent groundwater with a nitrate concentration of  $7.2 \pm 0.6$  mg L<sup>-1</sup> is completely denitrified in a little over half a day. Due to the nitrate limitation before the first sampling port, no accurate reduction rate could be calculated. Although nitrate reduction rates would be higher than  $38$  g m<sup>-3</sup> d<sup>-1</sup> in at least one of the mesocosms with an average rate greater than  $9.3 \pm 6.2$  g m<sup>-3</sup> d<sup>-1</sup> over all the mesocosms. During this time period, the DOC concentration

averaged  $148 \pm 180 \text{ mg L}^{-1}$  and therefore these high denitrification rates are likely as a result of the presence of high concentrations of labile carbon during the initial start-up period. After 50 days, the DOC concentrations had dramatically declined and stabilized in all of the treatments (Figure 4-4). As a result of these temporarily high DOC concentrations and the difficulty in accurately quantifying rates, the data from the first 60 days was excluded from this analysis. Temporarily high nitrate removal rates were observed over a similar timespan in the field-scale denitrification wall as discussed in Chapter 3. By removing the data from the first 60 days, these analyses will be more representative of stabilized long-term N reduction rates. After the first 60 days, the flow-rate was increased to  $289 \pm 146 \text{ cm d}^{-1}$  for the duration of the study so that nitrate was still present in the sampling ports and an accurate nitrate removal rate could therefore be calculated.

Over the sampling period the average temperature of the groundwater in the mesocosms ranged from  $7.9 - 24.1^\circ\text{C}$  and the absolute value of the average change in temperature between influent and effluent of the mesocosms averaged  $3.3 \pm 2.1^\circ\text{C}$ . The wide range of temperatures these aboveground mesocosms were exposed to allowed for a thorough analysis of nitrate reduction rates by temperature. The effect of temperature on the denitrification reaction for all treatments is quite strong ( $r^2=0.87$ ) with reaction rates more than doubling over the temperature range ( $15 - 22^\circ\text{C}$ ) found within the field-scale denitrification wall discussed in Chapters 2 and 3 (Figure 4-6). The  $Q_{10}$  value across the temperature range of measurement ( $7.9 - 24.1^\circ\text{C}$ ) is 4.74. The  $Q_{10}$  of many other denitrification bioreactor studies ranged from 0.16-2 (Cameron and Schipper, 2010; Elgood et al., 2010; Warneke et al., 2011), although the only other

study to measure rates over a comparably wide temperature range (6 - 22°C) as the present study had a very similar  $Q_{10}$  of 4.95 with an  $r^2=0.96$  (Robertson et al., 2008). Additionally the exponential rate constant (0.16) of the Robertson et al., (2008) study and the present work are equivalent, providing strong confirmation of the shape of this exponential relationship. Due to this strong temperature interaction, the nitrate reduction rates of the different treatments (wood volume, wood type and wood size) were compared, controlling for the covariate temperature using an analysis of covariance (ANCOVA).

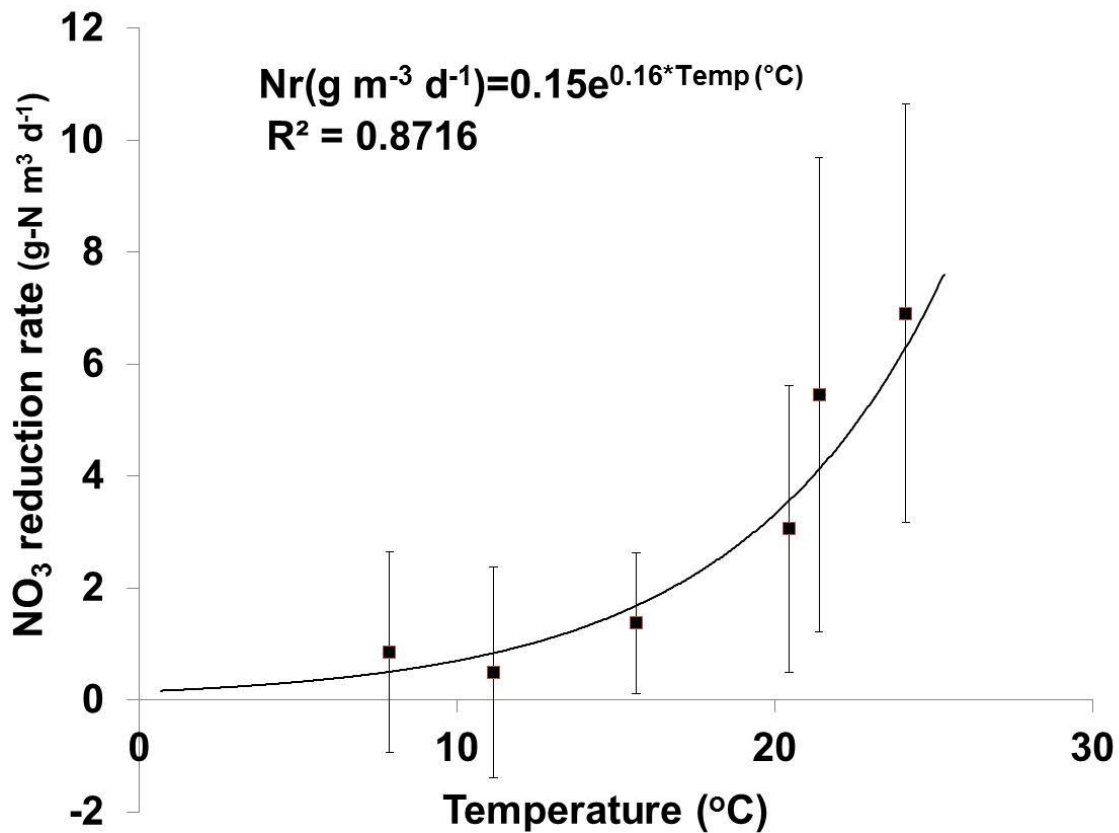


Figure 4-6. The nitrate reduction rate as a function of groundwater temperature for all the mesocosms treatments.

The effect of treatment was significant for all three comparisons (wood volume, wood type and wood size) (Table 4-5). Taking temperature in to account the temperature\*treatment interaction was significant for all three treatments  $F(3,156)=6.8$ ,

$p < 0.001$ ;  $F(2,68)=5.8$ ,  $p < 0.005$  and  $F(3,60)=12$ ,  $p < 0.0001$  respectively. This justifies including temperature in the model. The whole model was strongly significant for all three studies ( $p < 0.0001$ ) and the model explained 52, 56 and 73% of the variability for the wood volume, wood type and wood particle size treatments respectively. The results of the ANCOVA for the three studies across the range of temperatures measured are shown in Figure 4-7. The relationship between temperature and nitrate removal rates within a given treatment for this statistical model can be calculated based on Equation 4-4.

$$N_r = \alpha + bx + cx^2 \quad (4-4)$$

In this equation,  $N_r$  is the nitrate reduction rate per volume of reactor media [ $\text{g-N m}^{-3}$  of media  $\text{d}^{-1}$ ] which is described in Equation 4-2,  $\alpha$  is the intercept,  $b$  is the estimated temperature regression coefficient,  $x$  is the temperature and  $c$  is the estimated temperature quadratic term. The values of these coefficients are shown in table 4-5. In general this model provided a good fit to the actual data and the model is relatively homoscedastic, indicating the model accuracy is generally equivalent across the range of nitrate reduction rates and temperature values measured (Figure 4-8).

The hardwood treatment had slightly higher nitrate reduction rates particularly at low temperatures, although the differences from softwood sawdust were not significant overall. Similarly, although the fine pine sawdust had higher measured nitrate reduction rates across the majority of the temperature range than the coarse pine sawdust or shredded pine, the differences between all the particle sizes were not significant. Similarly, previous researchers have found no significant differences in nitrate removal rates between softwood and hardwoods and different particle sizes (Cameron and

Table 4-5. A statistical analysis of the effects on nitrate reduction rate (Equation 4-2) from varying the wood volume, type and particle size. Least squares means  $\pm$  1 S.D. of nitrate reduction rate are presented as rate mass loss per volume of reactor media. The equation coefficients for each treatment are also displayed.

Wood Volume Treatment			Wood Type Treatment				Wood Size Treatment				
Wood (%)	NO <sub>3</sub> Removal Rate (g m <sup>-3</sup> d <sup>-1</sup> )	ANOVA	Wood type	NO <sub>3</sub> Removal Rate (g m <sup>-3</sup> d <sup>-1</sup> )	ANOVA	Pine size	NO <sub>3</sub> Removal Rate (g m <sup>-3</sup> d <sup>-1</sup> )	ANOVA			
0	-0.14 $\pm$ 2.0	A	Control	-0.08 $\pm$ 1.9	A	Control	-0.07 $\pm$ 1.4	A			
10	1.24 $\pm$ 2.1	F(8,157)=19	Soft	3.00 $\pm$ 2.0	F(6,69)=15	B Shred	1.86 $\pm$ 1.4	F(8,61)=15			
25	2.32 $\pm$ 2.0	p<0.0011	Hard	3.61 $\pm$ 2.1	p<0.001	B Coarse	1.64 $\pm$ 1.5	p<0.0001			
50	3.68 $\pm$ 2.1	D				Fine	2.47 $\pm$ 1.5	B			
Model	r <sup>2</sup> = 0.52	F(8,157)=21 p<0.0001	Model	r <sup>2</sup> = 0.56	F(6,69)=15 p<0.001	Model	r <sup>2</sup> = 0.73	F(8,157)=21 p<0.0001			
	<i>a</i>	<i>b</i>	<i>c</i>	<i>a</i>	<i>b</i>	<i>c</i>	<i>a</i>	<i>b</i>	<i>c</i>		
10	4.33	-0.58	0.021	Soft	-0.76	0.06	0.009	Shred	0.42	-0.25	0.018
25	1.37	-0.34		Hard	1.53	-0.04		Coarse	2.05	-0.36	
50	3.84	-0.41						Fine	-0.09	-0.19	

ANOVA results indicate a significant difference within the treatment. Treatments with different letters in the group column are significantly different from each other at p<0.05

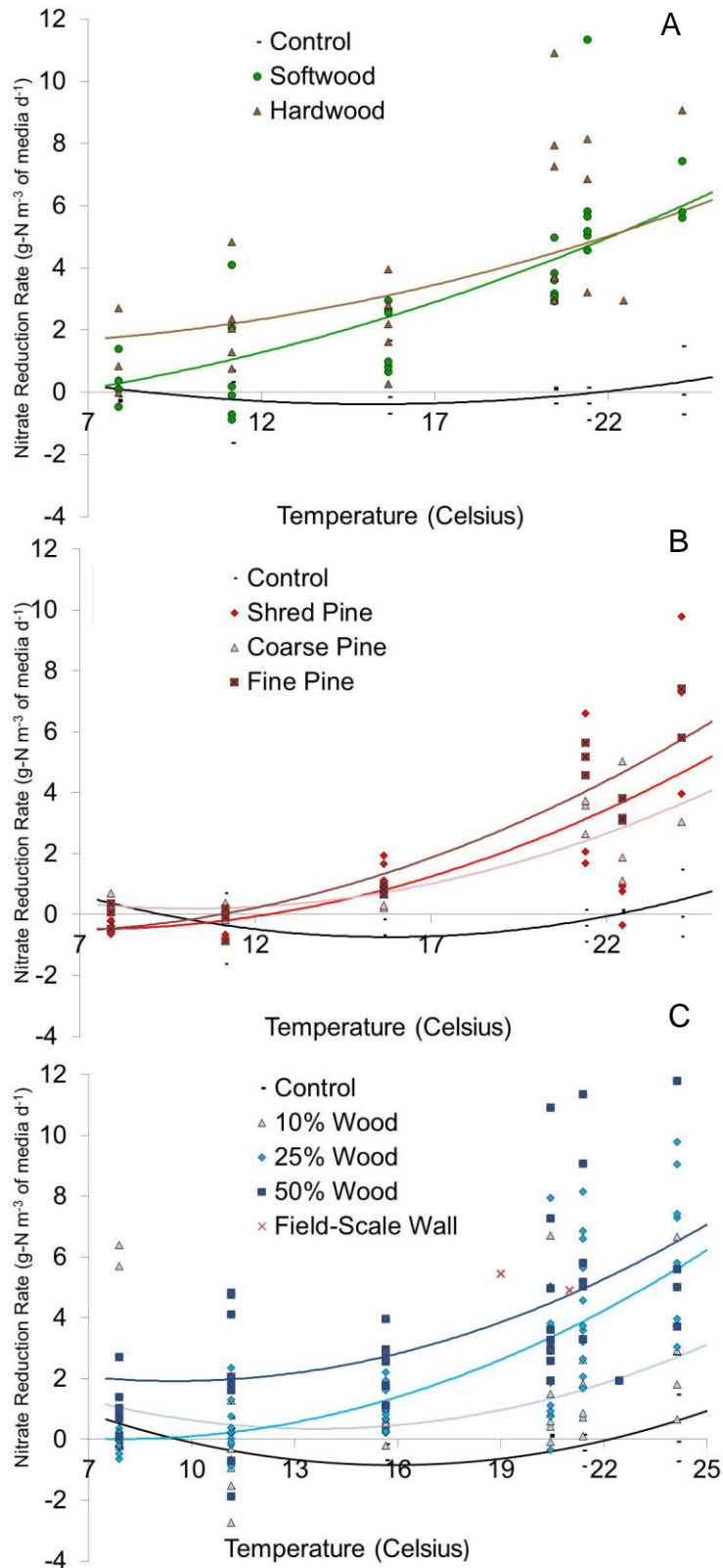


Figure 4-7. The results of the ANCOVA model comparing nitrate reduction rates across a range of temperatures. Comparisons shown include the (A) wood volume, (B) wood type and (C) wood particle size treatments respectively.

Schipper, 2010). When all the various wood types and sizes were grouped together in to a wood volume treatment, significant differences were found. All the treatments were significantly different from the control with the exception of the 10% wood volume (Table 4-5). This 10% wood volume treatment only had high denitrification rates at temperatures ( $>22^{\circ}\text{C}$ ) unlikely to be encountered in many geographical areas. Using 10% sawdust would require longer detention times for complete nitrate removal and is likely not desirable as bioreactor media. The nitrate reduction rates of the 25 and 50% wood volume treatments are significantly different from each other and the 10% treatment. Therefore the wood volume treatment is a good indicator of bioreactor performance. All the wood types and sizes are pooled in to these treatments, so this model can be used as a guide for bioreactor design using a variety of different wood media. The difference between the 25 and 50% wood volume treatments appears to be most significant at the low to intermediate temperatures and converges at higher temperatures. The nitrate reduction rate of the 50% treatment ranges from 140 to 14% higher than the 25% wood volume across the temperature range of the field-scale denitrification wall discussed in Chapters 2 and 3 ( $15 - 22^{\circ}\text{C}$ ). This convergence could indicate an upper limit to the denitrification reaction brought on by kinetic and/or nitrate limitation at high temperatures.

The results of the denitrification wall discussed in Chapter 2 and other denitrification walls which have temperature, wood volume and nitrate removal rates reported can be used to verify the accuracy of this wood volume model (Table 4-6). The predictions of this model indicate that the expected nitrate removal rate across the range of temperatures observed in groundwater measured in Chapter 2 ( $15 - 22^{\circ}\text{C}$ ),

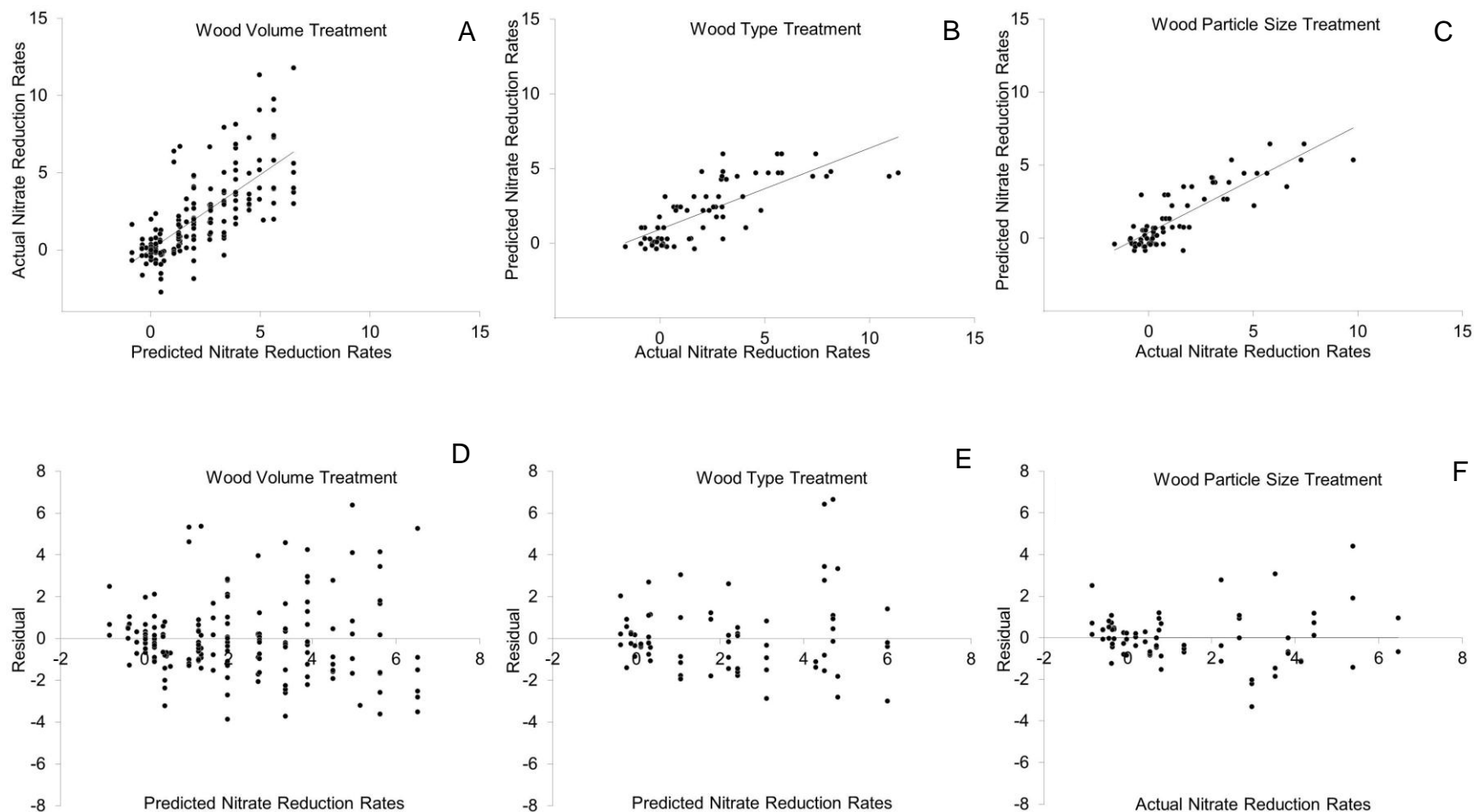


Figure 4-8. Figures detailing the goodness of fit between the actual and predicted nitrate reduction rates of the ANCOVA statistical model. Values are shown for the (A) wood volume treatment, (B) wood type treatment and (C) wood particle size treatment. The residuals across the range of predicted values of the (D) wood volume treatment, (E) wood type treatment and (F) wood particle size treatment are also shown.

would be  $2.57 - 5.27 \text{ g-N m}^{-3} \text{ d}^{-1}$ . When the porewater velocity and direction were directly measured with the groundwater flowmeter, the actual denitrification rates were  $4.91 - 5.46 \text{ g-N m}^{-3} \text{ d}^{-1}$  and the model predicted rates were  $3.86 - 4.76 \text{ g-N m}^{-3} \text{ d}^{-1}$ . This indicates that the wood volume model is a relatively good indicator of the field-scale denitrification wall discussed in Chapters 2 and 3, although the model slightly underpredicts the field data. The rates measured in the field-scale wall are shown in Figure 4-7C. These field-rates are well within the range of the equivalent 50% wood volume ratio mesocosm treatment, further justifying this experiment as an accurate representation of field conditions. The observed data from other denitrification walls with reported nitrate reduction rates, temperatures and wood volumes are also shown in Table 4-6. The denitrification wall from Schipper et al., (2000) was reported by the authors to be a strongly nitrate limited system. This statistical model predicts that rates would be higher (Schipper et al., 2000) if the denitrification wall was receiving higher nitrate loads. In this instance, the nitrate is rapidly depleted and the denitrification wall is oversized (Schipper et al., 2000). The rates reported in this model could be useful towards determining the effective detention time required to remove the existing nitrate loads, thus improving the efficiency of design. Later, the authors artificially spiked this same denitrification wall with higher loads of nitrate and the previously measured rate ( $0.4 \pm 0.45 \text{ g m}^{-3} \text{ d}^{-1}$ ) increased upwards ( $1.4 \text{ g m}^{-3} \text{ d}^{-1}$ ) towards the rate predicted ( $2.1 \text{ g m}^{-3} \text{ d}^{-1}$ ) by this model (Schipper et al., 2005). The authors concluded that even though the wall was spiked with high nitrate loads, it was still nitrate limiting and the results of this statistical model provide confirmation of that assessment (Schipper et al., 2005). The final study reported in the literature had higher nitrate reduction rates ( $1.7 \text{ g m}^{-3} \text{ d}^{-1}$ )

than would be predicted ( $0.8 \text{ g m}^{-3} \text{ d}^{-1}$ ) by the model (Robertson et al., 2000). This is a denitrification wall receiving septic system wastewater which has correspondingly high amounts of dissolved organic carbon. It is therefore plausible that this denitrification wall is behaving more similarly to walls with higher wood content because the carbon in the septic system effluent is fueling increases in denitrification rate. Although further data would need to be collected to confirm model accuracy, using this model to guide predictions based on wood volume alone will provide reasonably accurate estimates of bioreactor denitrification rates to guide their design.

Table 4-6 – A comparison of actual and predicted nitrate removal rates of other denitrification walls based on the model created in this study. Wood volume and groundwater temperature are the inputs to the model, which is detailed in Equation 4-4 and Table 4-5.

Source	Temperature Average (°C)	Wood volume	Actual rate	Predicted rate
Schmidt (this study)	19	50%	4.9	3.9
	21		5.5	4.8
Schipper et al. (2000)	14	50%	0.18	2.4
	15		0.17	2.6
	16		0.30	2.8
	17		0.19	3.1
	16		1.2	2.8
Schipper et al. (2005)*	12		1.4	2.1
Robertson et al. (2000) $\alpha$	14	20%	1.7	0.80

\* For this study, an existing denitrification wall was spiked with higher nitrate loads to determine a maximum nitrate removal rate.

$\alpha$  This is the rate for this study as reported in a synthesis paper on bioreactors (Schipper et al., 2010b).

### Carbon Quality Transformations

Total carbon concentration and fiber composition were quantified on the bioreactor media at the beginning and end of the study to determine media quality changes as a result of carbon leaching and the denitrification reaction. Based on this analysis it should be possible to make inferences on the longevity of the different media types.

Throughout the duration of the study (246 days), total carbon and non-lignin fiber content significantly declined by  $0.9 \pm 0.8\%$  and  $0.9 \pm 1.3\%$  of the total reactor volume respectively. This represents a very small decline in the total carbon and total fiber pool (Figure 4-9). Although the carbon declined due to DOC export and microbial consumption, the nitrogen content of the media increased from 0.028% to 0.038%. The microbial community generally has a C:N ratio of 10. Therefore when C:N ratios of organic matter are high (C:N=194±38) as is the case with the present study, nitrogen is retained in the microbial pool to maintain the microbial ratio even though carbon is lost as CO<sub>2</sub> (Equation 1-2) (Reddy and Delaune, 2008).

In the duration of the study, there were consistent and statistically significant reductions in the less recalcitrant components, NDF ( $-0.57 \pm 0.37$ , n=27, p<0.001), hemicellulose ( $-0.56 \pm 0.54$ , n=27, p<0.001) and cellulose ( $-0.58 \pm 1.59$ , n=27, p<0.035), while ash and lignin content ( $1.1 \pm 1.9$ , n=27, p<0.025) significantly increased. Lignin decomposition is strongly limited in anaerobic conditions, so it is included with the ash fraction. There were no significant differences in fiber consumption between fiber fractions with differing lability (NDF, hemicellulose, cellulose) indicating an even microbial consumption and export rate for all fiber components at least over the short-term. The lignocellulose index (LCI) is a ratio of the total lignin content to lignin + cellulose and is a good indicator of organic matter bioavailability under anaerobic conditions (Debusk and Reddy, 1998). Organic matter in wetland soils stabilizes at an LCI of 0.8, after which the organic matter is highly recalcitrant under continued anaerobic conditions (DeBusk and Reddy, 1998). Within the mesocosm treatments, the LCI was initially  $0.25 \pm 0.10$  and declined to  $0.44 \pm 0.13$  in the 246 day duration of the

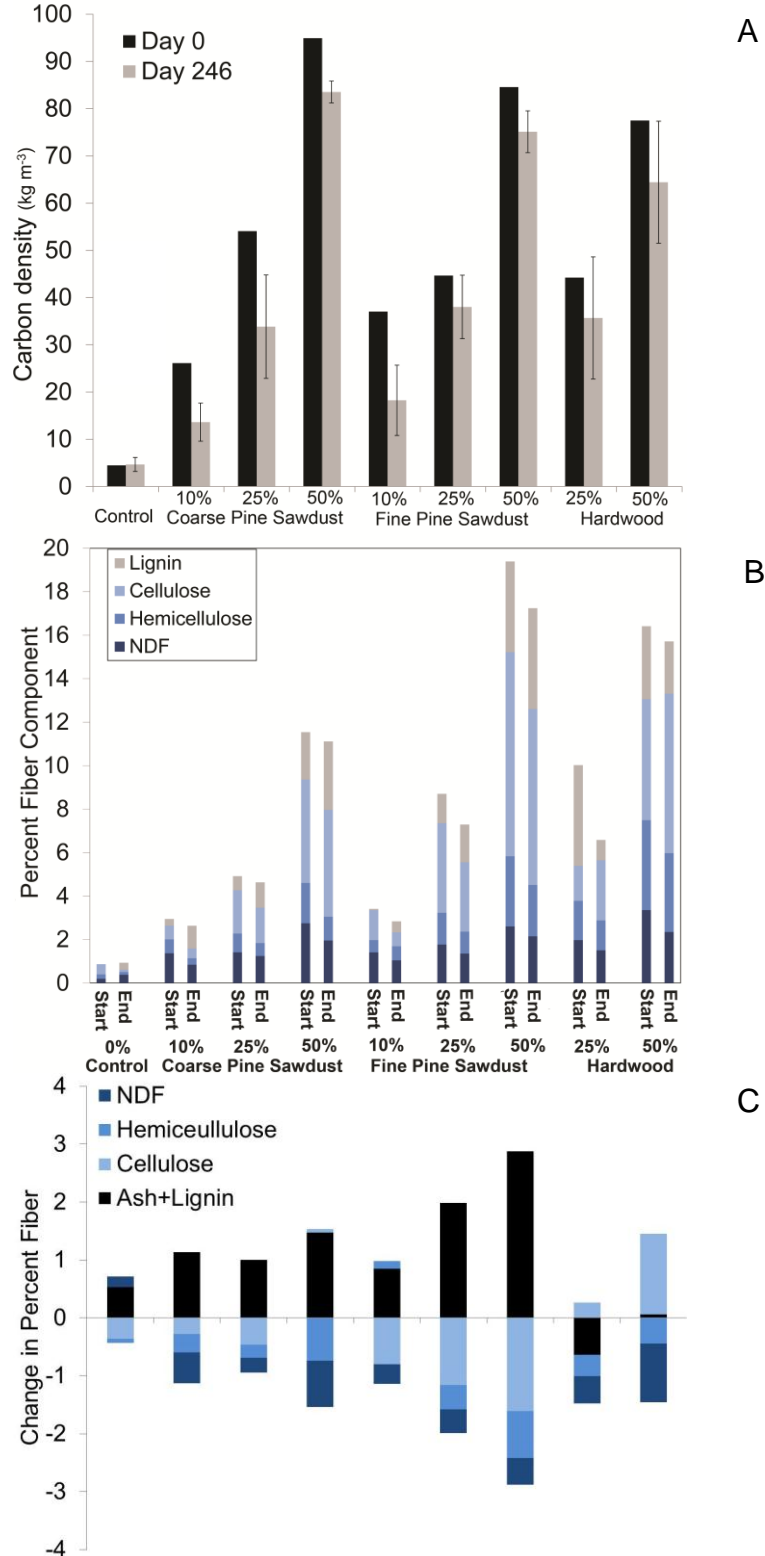


Figure 4-9. Carbon quantity and quality values of the bioreactor media and changes in these values in the duration of the study. Values shown are (A) Total carbon and (B) fiber content of the media at the start and end of the study and (C) Change in percentage for all fiber components and ash.

study. These mesocosm values are very similar to the before (0.24) and after ( $0.4 \pm 0.04$ ) LCI values in the field-scale denitrification wall discussed in Chapter 2. Both in the field and in the mesocosms there was a gradual increase in media recalcitrance as indicated by the increase in LCI, although the LCI remains above the stable ratio of 0.8 indicating continued bioavailability.

Comparing between the wood type treatments (hardwood vs. softwood), there were some significant differences in the loss of fiber components with time but no differences in total carbon (Table 4-7). The lignin fraction of the hardwood sawdust decreased over time, while this fraction increased in all the other treatments (Figure 4-9C). While anaerobic lignin decomposition in the hardwood media is not likely, the effluent from the hardwood treatments were much darker in color than the other treatments, which could indicate the leaching of soluble lignin-rich humified compounds (Figure 4-10). Additionally the hardwood reactor media tended to increase within the cellulosic fraction, while all other treatments saw declines in cellulose.

Due to a higher hydraulic conductivity (Figure 4-3), the fine pine sawdust treatment had a greater volume of water transmitted through the reactor and the leaching of DOC in this treatment was also higher than the coarse pine sawdust (Figure 4-4). Additionally it should be noted that similarly to the DOC export rates, there were greater declines in total fiber in the 25% volume hardwood sawdust treatment rather than the 50% hardwood sawdust treatment. This is also likely driven by differences in hydraulic conductivity between the two treatments. Therefore, the consumption and export of carbon appears to be higher in denitrification bioreactors with greater hydraulic and/or nitrate loading rates. This indicates that denitrification walls receiving high loads, will

possibly have a decline in lifespan. Although the lifespan of the field-scale denitrification wall discussed in Chapter 2 ( $23 \pm 5.9$  years), is comparable to a denitrification wall (28 years) with lower hydraulic loading rates (Long et al., 2011). Due to the low total C and fiber consumption of each treatment, the longevity of all the wood types is likely to be long enough for each wood type to be a sustainable option.



Figure 4-10. A photograph of the bioreactor effluent from the first sampling indicating the dark color of the hardwood treatment. The treatments from left to right are hardwood sawdust 25%, hardwood sawdust 50%, fine pine sawdust 50% and coarse pine sawdust 25%. The darker color of the hardwood treatments could indicate the loss in soluble lignin components.

Table 4-7. Changes of neutral detergent fiber (NDF), hemicellulose, cellulose, lignin and carbon within the study.

Fiber type	Fiber change by wood volume				Fiber change by wood type			
	Vol	Change in %	ANOVA	Group	Type	Change in %	ANOVA	Group
NDF	0	+0.18±0.1		B	Ctrl	+0.18±0.2		B
	10	-0.43±0.3	F(3,17)=5.0	A	Soft	-0.43±0.1	F(2,12)=11	A
	25	-0.33±0.3	p<0.011	AB	Hard	-0.74±0.4	p<0.002	A
	50	-0.62±0.4		A				
Hemicell.	0	-0.08±0.2		B	Ctrl	-0.08±0.1		B
	10	-0.10±0.3	F(3,17)=4.5	B	Soft	-0.46±0.1	F(2,10)=4.6	AB
	25	-0.32±0.2	p<0.017	AB	Hard	-0.56±0.1	p<0.04	A
	50	-0.78±0.6		A				
Cellulose	0	-0.36±0.1		A	Ctrl	-0.36±0.1		AB
	10	-0.54±0.3	F(3,17)=0.2	A	Soft	-1.39±1.1	F(2,12)=8.4	A
	25	-0.81±0.8	p<0.862	A	Hard	+0.82±1.0	p<0.005	B
	50	-0.78±1.4		A				
Lignin	0	+0.31±0.5		A	Ctrl	+0.31±0.5		B
	10	+0.58±0.6	F(3,17)=0.9	A	Soft	+0.66±0.4	F(2,12)=9.8	B
	25	+0.50±0.2	p<0.448	A	Hard	-2.0±2	p<0.003	A
	50	+0.69±0.7		A				
%Carbon	0	0			Ctrl	0		
	10	-0.99±0.3	F(2,15)=0.5	A	Soft	-0.62±0.8	F(1,10)=0.5	A
	25	-0.67±0.9	p<0.601	A	Hard	-1.02±1.2	p<0.507	A
	50	-1.0±0.7		A				

ANOVA results indicate a significant treatment effect. Treatments with different letters in the Group column are significantly different from each other at p<0.05

## Predictors of Denitrification Rate

Providing design guidelines for bioreactors requires determining important predictors of denitrification rates. If these predictors are easily measurable, they can be used to make practical inferences about the denitrification potential of a given bioreactor media and support design specifications. The utility of using wood volume alone as a predictor was demonstrated previously. Using more specific predictors will allow for general conclusions to be made on the importance of the physical and chemical drivers of denitrification rate. Many of the measured indicators of carbon quality had significant correlations with nitrate reduction rates averaged over all sampling events (Table 4-8). It is important to note that the correlations listed in Table 4-8 are correlations of average nitrate reduction values across the range of temperatures the mesocosms were exposed to (7.9 - 24.1°C). Therefore, these values indicate the correlations between media physicochemical properties and denitrification rate independent of groundwater temperature. The two most bioavailable fiber components NDF and hemicellulose were strong ( $R > 0.50$ ) predictors of nitrate reduction rate. Neutral detergent fiber is a measurement of the loss of readily bioavailable starches as a result of amylase enzymes, although this fraction does not represent any specific cellular component (Van Soest et al., 1991). Although there was a high degree of correlation between many of these predictor variables, it should be noted that these labile fiber components (NDF and hemicellulose) were stronger predictors of nitrate reduction rate than measurements of total wood volume alone (%carbon and %LOI). This indicates the quality and bioavailability of the carbon is more important than the wood volume alone. Because NDF is a very commonly measured fiber component for feed analysis it would

be a useful indicator of media denitrification potential. Surprisingly, the C:N ratio was not significantly correlated with measured denitrification rate.

Table 4-8. Correlations between measured predictors and nitrate reduction rate ( $\text{g m}^{-3} \text{d}^{-1}$ ) as determined from Equation 4-2 over all temperatures. The Pearson correlation coefficients indicate the strength and the direction of the regression, while the p-value determines the significance of the relationship. Pearson coefficients greater than 0.50 are considered strong correlations.

Carbon Quality Predictor	Pearson Correlation Coefficient	p-value
NDF	0.75	<.0001
Surface area	0.73	<.0001
Hemicellulose	0.70	<.0001
Microbial Biomass C	0.56	0.0044
%Carbon	0.48	0.0126
Lignin	0.47	0.0158
Loss on Ignition	0.47	0.0163
Cellulose	0.45	0.0207
Potential DN Rate	0.35	0.0891
C:N Ratio	-0.18	0.3769

The surface area was also a strong predictor ( $R>0.50$ ) of nitrate reduction rates. This is possibly a result of a larger spatial area for extracellular enzyme contact. Although surface area is a difficult property to measure and requires specialized equipment, it is likely that there is a relationship between surface area and particle size within a given wood type. In the present study, there is a weak relationship between *Pinus spp.* particle diameter and surface area, although pure hardwood sawdust has over twice the surface area of the pure fine pine sawdust so each wood type would have to be measured separately. It is important to note that the two laboratory procedures (microbial biomass carbon and potential denitrification rate) had mixed success in predicting nitrate removal rates. Microbial biomass carbon was a strong indicator of nitrate reduction rates, while potential denitrification rate was not. The lack of a relationship between potential denitrification rate and actual denitrification rate

indicates the utility of in-situ studies as opposed to laboratory analyses for accurately quantifying small differences in denitrification rate.

To predict actual nitrate reduction rates, an empirical model was developed relating these measurable parameters and nitrate reduction rates. Besides the measurements of carbon quality, it is known that temperature and possibly the  $K_{sat}$  affect the nitrate reduction rates, so they are included in the model as well. To minimize the number of predictor variables and to choose unique predictors which aren't strongly correlated with each other, a mixed forward and backward stepwise multiple linear regression was used. The results of this procedure indicate that NDF, LOI, surface area, temperature and  $K_{sat}$  alone most fit these criteria. With the exception of the surface area as previously discussed, these predictors are often reported in literature or are relatively easily measurable. A multiple least-squares linear regression was then used to model the best linear relationship between the predictor variables and nitrate reduction rates. As was previously observed, temperature has an exponential relationship with nitrate reduction rates (Figure 4-6). Additionally, although surface area has a positive correlation with nitrate reduction rates, at high surface areas the slope of this relationship declines indicating a logarithmic relationship. Therefore the overall linear model was modified with these parameters included as the appropriate non-linear relationships. This multiple regression can be used to calculate nitrate removal rates from measured predictor variables with Equation 4-5.

$$N_r = b_1X_1 + b_2X_2 + b_3 \ln X_3 + b_4X_4 + b_5e^{rX_5} + a \quad (4-5)$$

In this equation,  $N_r$  is the nitrate reduction rate per volume of reactor media [ $\text{g m}^{-3} \text{d}^{-1}$ ] described in Equation 4-2,  $X_1 - X_5$  are the actual measurements of LOI [%], NDF [%],

surface area [ $L^2 M$ ],  $K_{sat}$  [ $L T^{-1}$ ] and temperature [ $^{\circ}C$ ] respectively,  $b_1 - b_5$  are the constant coefficients of the respective predictors and  $a$  is the constant intercept term.

The results of the whole model were significant  $F(5,133)=36.3$ ,  $p<0.0001$  and the equation containing these variables explained approximately 56% of the variability (Figure 4-11A). Beta weights (standardized multiple regression coefficients) and uniqueness indices are presented in Table 4-9, along with the  $b$  coefficients and intercept term for the equation. The equation above can be used to predict actual nitrate reduction rates although it is important to note that the magnitude of the  $b$  coefficient is not an indicator of the strength of the relationship because the predictor variables are measured on different scales. For example, loss on ignition and NDF are measured as percentages. The beta weights are standardized coefficients that can be used to determine the strength and direction of the predictor on the response variable. Each of the predictor variables displays significant beta weights (Table 4-9). These beta weights indicate that temperature is the strongest predictor of denitrification rate, followed by NDF. The beta weight for hydraulic conductivity is negative indicating a negative linear relationship. Additionally, the LOI has a negative beta weight. Similarly to the %C predictor variable, LOI has a weakly positive relationship to nitrate reduction rates. But at very high values of LOI, the nitrate reduction rate declines possibly due to changes in hydraulic properties at high wood volumes. As a result, LOI acts as a suppressor variable for NDF, thus minimizing the variability of this decline in nitrate reduction rates at high wood volumes.

While many of these predictor variables are correlated with each other, the uniqueness index values indicate the proportion of variance explained by that predictor

variable alone, without including the other predictors. Similarly to beta weights, the uniqueness indices for each predictor variable are significant (Table 4-9). Temperature alone explains approximately 43 out of the 56% of total variability in nitrate reduction rates of the model, followed by NDF, which predicts an additional 10% of the total variance. The other predictor variables account for 1 – 2% of the variability. This indicates that with the exception of groundwater temperature and NDF, the model can be simplified with a small decline in predictive capability, by removing one or more of the predictor variables if it is unknown. Pragmatically, if the NDF and the groundwater temperature alone are known, relatively strong predictions on bioreactor performance can be made. It is possible that over time NDF will decline in importance for predicting N reduction rate as this bioavailable component is depleted. Although as discussed previously, all fiber components (NDF, hemicellulose, cellulose) had equivalent rates of degradation and leaching. Additionally, in this study bioreactor performance was only analyzed after the media had been leached for 60 days, which would exclude many temporarily, labile carbon sources.

One of the mesocosm treatments is the same as the field-scale denitrification wall discussed in Chapters 2 and 3. Therefore comparing actual to predicted nitrate removal rates of the denitrification wall can be used to test if this experimental model is relevant to field conditions. Based on this model, the predicted nitrate removal rates of the field-scale denitrification wall would be  $4.3 - 7.6 \text{ g-N m}^{-3} \text{ d}^{-1}$  across the temperature range observed in the groundwater of  $15 - 22^\circ\text{C}$ , with an average of  $5.7 \text{ g-N m}^{-3} \text{ d}^{-1}$  ( $19^\circ\text{C}$ ). More specifically, when porewater velocities were measured in the denitrification wall with the groundwater flowmeter in May and July, the actual denitrification rate ranged

from 4.9 – 5.5 g-N m<sup>-3</sup> d<sup>-1</sup> respectively and the predicted denitrification rate of the model would be 5.7 - 6.8 g-N m<sup>-3</sup> d<sup>-1</sup>, providing a reasonably accurate fit, albeit an overestimate. This indicates that this experiment provides a framework for understanding bioreactor denitrification rates in the field. Further confirmations would be required to verify the accuracy of this model.

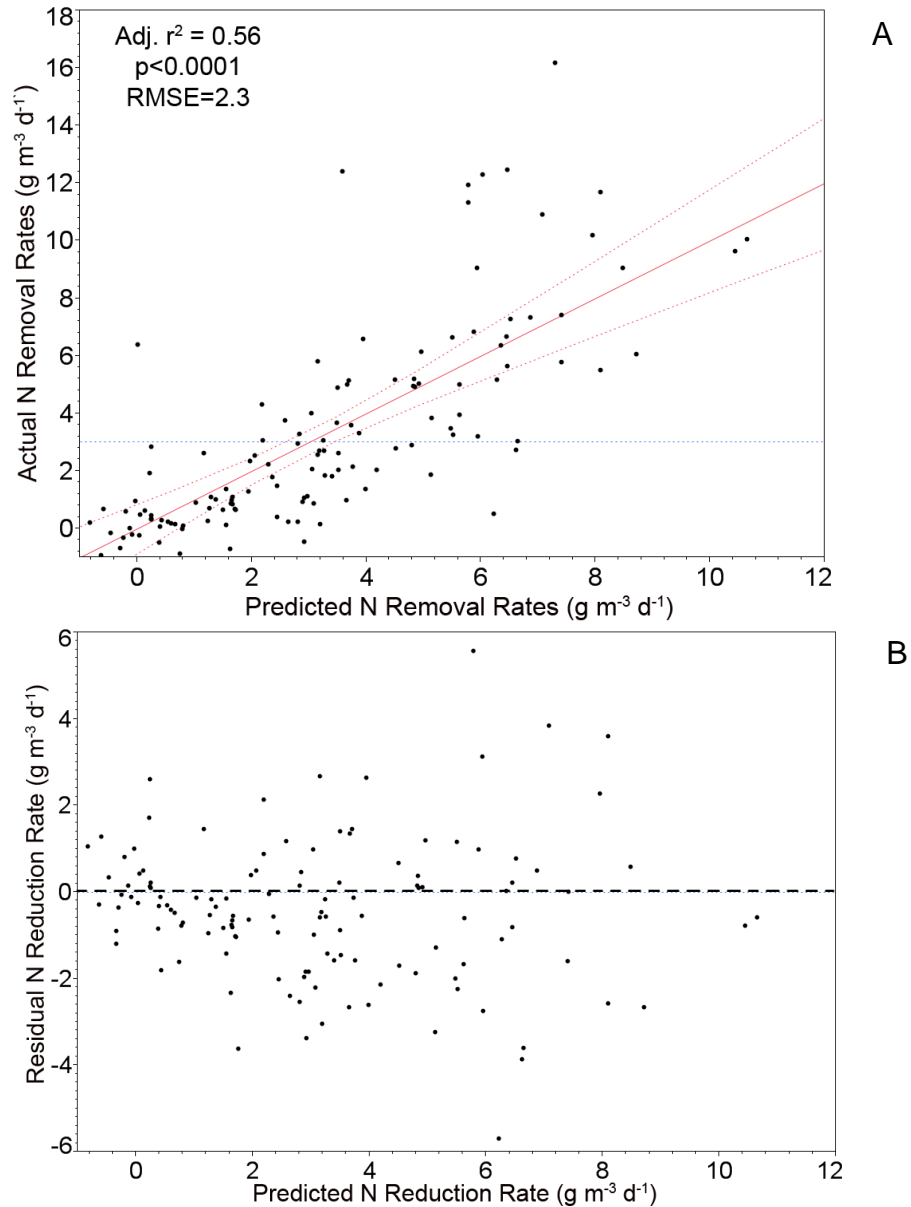


Figure 4-11. Graphs detailing the accuracy of the multiple regression model. The relationship between (A) actual and predicted values and (B) residuals by predicted values for the model are reported.

Table 4-9. Parameters of the multiple regression model predicting nitrate removal rates as a function of temperature and media physicochemical properties. Nonstandardized coefficients of the equation (*b* Coefficient), the standardized coefficient (Beta weight) and uniqueness index of the predictor variables are reported. The exponential constant (*r*) and the intercept term (*a*) of the nonstandardized equation are also shown.

Predictor	<i>b</i> Coeffic.	SE <i>b</i> Coeffic.	Beta weight.	t	Uniqueness index	<i>r</i>	<i>a</i>
Temp	0.1272	0.1	0.62	10.6**	0.43**	0.165	-0.94
NDF	190.4	0.7	0.33	2.6*	0.10*		
LOI	-14.94	5.4	-0.28	-2.8*	0.01*		
Surface Area	1.144	0.3	0.25	2.4*	0.02*		
<i>K<sub>sat</sub></i>	-0.3199	0.2	-0.12	-2.1*	0.001*		

Note: \**p*<0.05. \*\**p*<0.001

### Summary

In some instances, generalizations on denitrification bioreactors can be made based on categorical and coarsely quantified predictors such as wood volume, particle size and type. This is particularly true for the wood volume treatment as significant differences in nitrate reduction rates were observed between the 10, 25 and 50% wood volumes. The equation of this relationship can be used to guide bioreactor design across a range of groundwater temperatures for a given wood volume. It is difficult to infer hydraulic properties as well as carbon and TKN export rates based on these broad categories alone. The hydraulic conductivity did not decrease with smaller particle sizes thus Hypothesis 4-2 is not confirmed. The hydraulic properties of a given bioreactor media depend on a complex sorting of the range of wood particle sizes and will therefore be difficult to predict. The carbon and TKN export rates over time are a function of the hydraulic conductivity and therefore the determination of a bioreactor medium's hydraulic properties is important for a number of reasons.

By quantifying some of the relatively easily measurable predictor variables of NDF, LOI, temperature, surface area and  $K_{sat}$ , robust predictions can be made on media denitrification rates. The model produced in this study accurately predicts the denitrification rate and more broadly elucidates the relative importance of groundwater temperature and the hydraulic and carbon quality components of bioreactor media. Temperature alone is an important predictor variable that will most predominantly shape the dimensions of denitrification bioreactors and limit their geographical extent. Denitrification bioreactors should therefore be designed primarily for the expected minimum groundwater temperature. This strong temperature relationship may limit the geographic extent or seasonal impact of denitrification walls. Although, in the absence of impractical heating systems, the groundwater is usually a fixed parameter and the physicochemical properties of the chosen media become important. This is demonstrated by the strong correlations between media physicochemical properties and average denitrification rate across all temperatures measured (Table 4-7). Within a given temperature regime of a specified location, the carbon quantity, quality and surface areas of the bioreactor media all influence denitrification rate thus confirming Hypothesis 4-3. Bioreactor media with greater proportions of bioavailable components and a higher surface area to volume ratio, will yield greater denitrification rates thus reducing the size and volume of denitrification bioreactors.

## CHAPTER 5 CONCLUSIONS AND RECOMMENDATIONS

### Summary of Research

Denitrification walls have been proven to be an effective, long-term method for remediating nitrate in groundwater underneath agricultural properties. Efficiently sizing denitrification walls to achieve meaningful nitrate reductions requires accurate estimates of nitrate removal rates in a wide variety of conditions. A large denitrification wall receiving continuously high nitrate loads was evaluated using an array of well transects for hydraulic flow and water quality measurements and media were collected from within the denitrification wall to evaluate enzyme activity. Groundwater flow through the wall was relatively rapid ( $1.7 \text{ m day}^{-1}$ ) with short detention times (1.7 – 1.9 days), yet the denitrification wall effectively treated approximately  $10 \times 10^4$  liters of groundwater per day, effectively removing  $220 \pm 54 \text{ kg yr}^{-1}$  of nitrate from groundwater. Maximum nitrate removal rates per volume of media ( $4.9 - 5.5 \text{ g-N per m}^{-3} \text{ day}^{-1}$ ) were higher than other sand-sawdust walls even though the wall was receiving high nitrate loads with short detention times. In fact, rapid reduction of potential denitrification rates in media samples from  $4.89 \text{ g N m}^{-3} \text{ day}^{-1}$  to undetectable rates within a quarter of the wall length suggests that all nitrate was removed in an even shorter detention time than could be assessed by the monitoring well array used in this study. Even with the rapid porewater velocity and high nitrate removal rates, no significant decrease in total media carbon could be measured after 18 months. The study results demonstrate that denitrification walls have the potential to markedly reduce groundwater nitrate with a smaller underground footprint than was previously estimated.

While nitrate contamination in groundwater is often diffuse, one objective of the denitrification wall study was to maximize treatment volume. This was accomplished by locating a small denitrification wall where a large groundwatershed was funneled towards a seepage slope that formed the headwaters of a stream. This method was used to markedly impact not only groundwater but also the surface water draining the property. Nitrogen load was constantly measured in a 'treatment' stream receiving discharges from the denitrification wall and an immediately adjacent 'control' stream with the same land-use and climate but without influence of the denitrification wall. Beginning two days after the denitrification wall was installed, nitrogen concentration in the treatment stream declined over the long-term from  $6.7 \pm 1.2$  to  $3.9 \pm 0.78$  mg L<sup>-1</sup> and total N loading rate declined by 65% for an annual reduction of approximately 391 kg (0.4 tons) with no corresponding decline in the control watershed. This denitrification wall only composes 10-11% of the edge of field area contributing to the treatment watershed, yet it treated approximately 60% of the total stream discharge. This finding confirms the effectiveness of using a targeted approach. At a larger scale, this N load reduction observed in the treatment stream is 10% of the total from all four streams draining the 160-acre agricultural property, indicating a wider treatment area would be required for more substantial impacts. The total load reduction measured at the watershed scale ( $391 \text{ kg yr}^{-1}$ ) was higher than that estimated in the well transect study ( $249 \pm 61 \text{ kg yr}^{-1}$ ). This indicates the possibility of an extended impact of the carbon exported beyond the boundaries of the wall. This extended impact was inauspiciously confirmed when dissolved oxygen (DO) levels at the headwaters of the receiving stream declined for approximately 50 days, then stabilized at previous levels. This research

indicates that targeting denitrification walls adjacent to streams or headwaters can effectively reduce N loading in receiving waters, although with a potentially short-term impact on stream biological oxygen demand and dissolved oxygen. Overall, this study indicates that utilizing denitrification walls to supplement nitrogen management on agricultural properties can be an effective and sustainable solution to reduce downstream nitrogen loads.

Among the selected range of media, bioreactor performance is not strongly affected by wood type (hardwood, softwood) or wood particle size. The amount of wood used in the bioreactor media is a strong predictor of nitrate reduction rates and this parameter can be used to provide robust predictions of denitrification rate to guide wall design. Each of these treatments (size, type, wood volume ratio) effectively reduced nitrate with a minimal loss of total carbon and fiber, thus indicating a long-term sustainability of bioreactors containing the selected media. In the duration of the study, there was a small, but measurable decline in carbon quality as indicated by a decrease in bioavailable fiber components and an increase in the lignocellulosic index (LCI). These declines in carbon quality did not affect stabilized denitrification rates in the duration of the study, indicating the carbon compounds are still bioavailable. Although there were some differences between the export of dissolved organic carbon and total Kjeldahl nitrogen between the treatments, this was largely driven by the hydraulic conductivity of the media. The greater the hydraulic loading through a denitrification bioreactor, the greater the export of these constituents. This indicates that the hydraulic conductivity is an important parameter to consider in bioreactor design for water quality reasons, particularly when located next to sensitive water bodies. The hydraulic

conductivity is also an important parameter to quantify to ensure that groundwater flows through the denitrification bioreactor. Unfortunately, the hydraulic conductivity was difficult to predict based on wood size or amount alone. Therefore, a careful assessment of the hydraulic conductivity of selected media is important towards determining the success of a bioreactor installation. The results of this research indicate that denitrification rate is driven by water temperature, carbon quality and media surface area. The groundwater temperature is the most important consideration when designing bioreactors, although within a given temperature regime, increases in carbon quality will improve bioreactor performance at least over the short-term.

### **Recommendations and Guidelines**

Denitrification walls are a permeable reactive barrier (PRB) used to treat continuously saturated groundwater for nitrate. The treatment media consists of mixtures of sawdust/wood chips to sand. As evidenced by this research, it is preferable to use a ratio of wood to sand of at least 25% for effective nitrogen removal. While 100% wood media have been used in some installations, the sand maintains the soil matrix as the wood decomposes, which allows PRBs to be structurally stable with no loss of productive land. The sand can either be used from the excavated trench or imported from other locations. In order to maintain permeability, the wood media mixture needs to be sufficiently porous and resistant to compaction to ensure that groundwater is transported through the media and not around it. Denitrification walls have been hampered when the hydraulic conductivity of the media was lower than the surrounding aquifer and the groundwater was transported around the wall (Schipper et al., 2004, Barkle et al., 2007). Hydraulic conductivity should therefore be measured on the media and the surrounding aquifer before installation. Hydraulic conductivity of the surrounding

aquifer can be measured with either dye tracer studies or slug and pump tests within existing wells (Fetter, 2001). To avoid hydraulic clogging resulting from the installation itself, the sawdust or wood chip should always be mixed with sand above ground and then added to the excavated trench (Barkle et al., 2007). To minimize sorting of the buoyant wood as groundwater begins to enter the recently excavated hole, the mixed media should be added immediately after excavation.

Since denitrification walls rely on anaerobic processes, the wall should be located under consistently saturated conditions. The microorganisms will not produce the enzymes for denitrification if the location of wall installation is not below the water table for long durations. To improve the efficacy of treatment, care should be taken to ensure that the entire contaminated water table is captured. The bottom of the denitrification wall is usually installed to a clay-rich confining layer (aquitard) to prevent untreated groundwater from going under the wall. If a confining layer is too deep for practical installation, the treatment of surficial groundwater can likely still instigate meaningful nitrogen load reductions even without penetrating the confining layer. The top of the denitrification wall should generally be installed around the mean high water table, which can be determined from indicators in the soil and/or well water level monitoring. Installing the denitrification wall slightly below the mean water table is not a significant concern. When the hydraulic conductivity of the denitrification wall is higher than the surrounding aquifer, groundwater converges from above and below the wall to be treated. This convergence increases in distance and magnitude, the greater the hydraulic conductivity of the denitrification wall is above the surrounding aquifer (Benner et al., 2001; Robertson et al., 2005). In the present study, there was no reduction in the

nitrate removal rate when the groundwater level was up to 0.7 m above the top of the wall, even though the hydraulic conductivity of the wall was only 1.3 - 3 times higher than the surrounding aquifer. Additionally, when the water table drops below the top of the denitrification wall, aerobic decomposition proceeds, which reduces carbon much more rapidly than under continuously saturated conditions. This depletion in carbon stores occurs to such an extent that the wall longevity in the upper portion has been lowered by an order of magnitude (Long et al., 2010; Moorman et al., 2010). These results indicate that the top of the wall should generally be located slightly below the mean high water table, although strictly matching the upper bounds of the denitrification wall to the exact high water table is not crucial.

The greatest reductions in nitrogen load in groundwater or receiving surface waters will be achieved by maximizing the capture volume of the denitrification wall. Gaining a more thorough understanding of site hydrology and groundwater transport will strongly support the success of a project. In the present study, a denitrification wall with a width spanning only 10-11% of the edge of field area made a disproportionately large impact on nitrogen load reductions in a receiving stream. This was achieved by locating the denitrification wall adjacent to the headwaters of a stream, where large volumes of groundwater were focused. Therefore when possible, denitrification walls should ideally be located in areas where groundwater transport is rapid, as long as sufficient detention time for nitrate removal is possible. This can often occur adjacent to streams and ditches, particularly where groundwater is seen rapidly seeping to the surface. Unfortunately when placing sawdust in the ground adjacent to surface water bodies, there may be a short-term impact on receiving waters from excessive carbon leaching.

The excessive carbon leaching can reduce the dissolved oxygen of the receiving stream, thus impacting aquatic organisms and stream health. This detrimental impact needs to be considered in relation to the sensitivity of the receiving stream/ditch and compared to the much longer-term improvement in water quality to be gained from the denitrification wall. In many situations, groundwater transport and discharges are evenly dispersed over wide areas and major surface water discharges are not present, therefore a targeted approach will not work. In these instances, efficiently sized denitrification walls should ideally be installed along the entire downgradient edge of the property. This will ensure that the entire volume of contaminated groundwater passes through the denitrification wall to be treated before leaving the property.

Efficiently sizing denitrification walls for full removal of nitrate necessitates ensuring that the groundwater has a sufficient detention time within the denitrification wall. In the present study, the length (L) of the wall in the direction of groundwater flow was 1.7 m. and this wall was oversized because nitrate was removed long before exiting the wall. Particularly when a denitrification wall is installed along the entire edge of an affected property, oversizing of denitrification walls can be costly. Once the groundwater velocities of a proposed denitrification wall are known, design guidelines for this flow length (L) can be finalized based on the results from the present study. It is important to note that meeting the flow length (L) requirements for a given nitrogen reduction doesn't require this wall length to be continuous. For instance, trenching equipment can be used to create a series of thinner denitrification walls as long as the total length (L) of these thinner walls fulfills the design guidelines. The nitrate reduction rates in this study are reported in units ( $\text{g-N m}^3 \text{ of media d}^{-1}$ ) intended to normalize rates

for the dimensions of reactor media. Therefore, these rates can be used as guidelines for sizing bioreactors. Based on influent nitrate concentrations and site-specific hydraulics, the desired size of the denitrification bioreactor can be computed based on rates and models in this paper with Equation 5-1.

$$L = \frac{\Delta[N]\phi}{N_r} * v \quad (5-1)$$

In this equation,  $L$  is the denitrification wall length [L],  $\Delta[N]$  is the desired concentration reduction [ $M L^{-3}$ ],  $N_r$  is the reported nitrate removal rate [ $g-N m^{-3}$  of media  $d^{-1}$ ],  $\phi$  is the total pore volume transmitting groundwater (effective porosity) [ $L^3 L^{-3}$ ] and  $v$  is the porewater velocity [ $L T^{-1}$ ]. Installing one or more wells in the vicinity of the proposed denitrification wall will aid in determining the influent nitrogen concentration  $\Delta[N]$ , and the porewater velocity ( $v$ ) and direction. Porewater velocity ( $v$ ) and direction can be determined from head gradients between wells utilizing Darcy's equation, from heat-pulse groundwater flowmeters or from dye tracer studies.

The nitrate removal rate ( $N_r$ ) used as a guideline in the design of a specific bioreactor will depend firstly on groundwater temperature. To achieve complete nitrate reduction year-round, the minimum expected groundwater temperature should guide the design. Chapter 4 provided two methods for inferring the relationship between the nitrate reduction rates of a chosen bioreactor media and groundwater temperature. A model (Equation 4-4; Table 4-5) was developed between wood volume and nitrate reduction rates across a variety of temperatures, which is summarized in Table 5-1. Relating wood volume to nitrate reduction rates has great utility for providing design guidelines (Figure 5-1). If the influent N concentration and groundwater temperature are known, a detention time for complete nitrate removal can be quantified from Figure 5-1.

The flow length [L] of the wall can be calculated by multiplying the groundwater velocity [L T<sup>-1</sup>] by the detention time [T] deduced from this figure. Additionally, a model was developed to incorporate relatively easily measurable predictor variables (NDF,  $K_{sat}$ , LOI, surface area) to nitrate reduction rates using Equation 4-5. These nitrate reduction rates ( $N_r$ ) can be used in Equation 5-1, to provide flow length (L)

Table 5-1. A design guideline table relating the volumetric nitrate reduction rate ( $\text{g m}^{-3} \text{d}^{-1}$ ) to the groundwater temperature for three wood volumes measured.

Temp (°C)	Wood Volume		
	10%	25%	50%
7			1.14
8			1.31
9			1.48
10			1.65
11		0.22	1.82
12		0.37	1.99
13		0.56	2.19
14	0.35	0.80	2.36
15	0.39	1.08	2.57
16	0.47	1.40	2.83
17	0.59	1.77	3.13
18	0.76	2.18	3.47
19	0.97	2.63	3.86
20	1.22	3.12	4.29
21	1.51	3.66	4.76
22	1.85	4.24	5.27
23	2.23	4.86	5.83
24	2.65	5.53	6.43
25	3.12	6.23	7.07

Since the actual NO<sub>3</sub> reduction rates were variable at low temperatures, likewise the model was variable at these temperatures. Other researchers have measured denitrification at low temperatures with long detention times. Due to the short detention time of this experiment ( $0.36 \pm 0.78$  days), nitrate reductions at low temperatures were often not detected. Reduction rates were accurately measured at 7 and 11°C in the 50% wood volume and these values were regressed. Nitrate reduction wasn't measured in the 25% wood volume treatment until the temperature reached 11°C, while no accurate predictions on the 10% wood volume can be made until the temperature reaches 14°C.

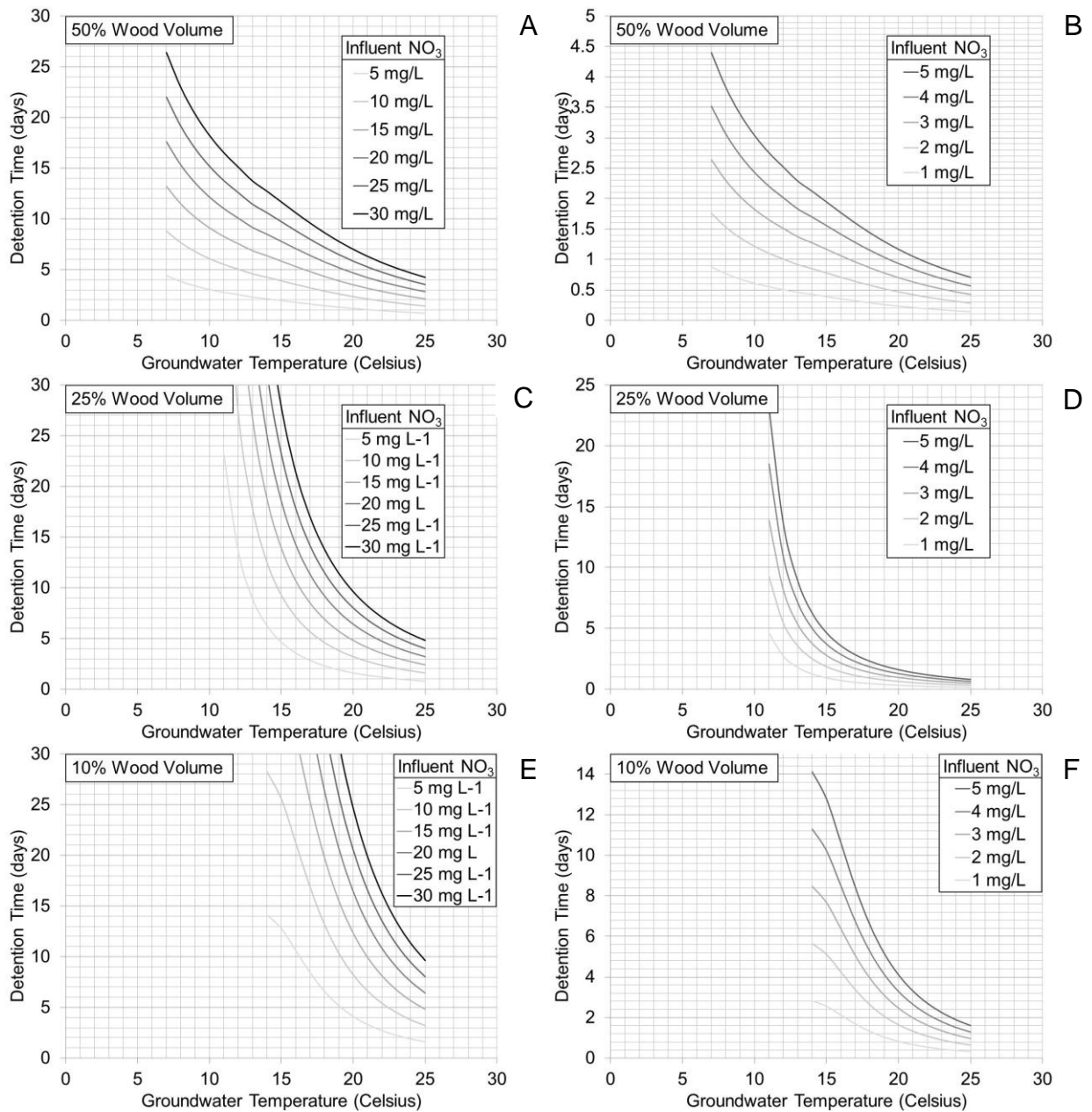


Figure 5-1. Design guidelines relating the time required to completely remove influent  $\text{NO}_3$  concentrations as a function of groundwater temperature. Shown in the figures are the relationship between groundwater temperature and detention time for high (5-30 mg L<sup>-1</sup>) and low (<5 mg L<sup>-1</sup>) influent  $\text{NO}_3$  concentration ranges for denitrification bioreactors using 50% wood (A, B), 25% wood (C,D) and 10% wood (E,F) respectively.

Denitrification walls can be a low-cost, sustainable and effective means to reduce nitrogen loading in groundwater. The site of a proposed denitrification wall should be thoroughly assessed, often with professional help if necessary. Care should be taken to ensure that a denitrification wall is installed in continuously saturated conditions, with a sufficiently conductive wood-sand media and that large volumes of groundwater are treated. Utilizing this technology in combination with efficient source control has a realistic potential to aid in meeting water quality regulations such as total maximum daily loads (TMDLs) and numeric nutrient criteria in rivers and lakes.

## LIST OF REFERENCES

- Addy, K.L.; Gold, A.J.; Groffman, P.M.; Jacinthe, P.A. 1999. Ground water nitrate removal in subsoil of forested and mowed riparian buffer zones. *JEnvironQual.* 28:962-970.
- Ahuja, L.R.; Naney, J.W.; Green, R.E.; Nielsen, D.R. 1984. Macroporosity to Characterize Spatial Variability of Hydraulic Conductivity and Effects of Land Management. *Soil Science Society of America Journal* Vol48. July-August:17 Ref.
- Alachua County Property Appraisers [ACPA], 2006. ACPA\_NC\_1ft. Aerial Imagery. Alachua County, Fl.
- Alden, A.S.; Munster, C.L. 1997. Field test of the in situ permeable ground water flow sensor. *Ground Water Monitoring & Remediation.* 17:81-88.
- Allen, R.G. 1999. REF-ET: A reference evapotranspiration software. Available at <http://www.kimberly.uidaho.edu/ref-et/> (verified 29 July 2011)
- Andersen, L.J.; Kristiansen, H. 1984. Nitrate in groundwater and surface water related to land use in the Karup basin, Denmark. *EnvironGeol.* 5:207-212.
- Babcock, B.A.; Blackmer, A.M. 1992. The value of reducing temporal input nonuniformities. *Journal of Agricultural and Resource Economics.* 17:335-347.
- Barkle, G.F.; Schipper, L.A.; Burgess, C.P.; Painter, B.D.M. 2007. In situ Mixing of Organic Matter Decreases Hydraulic Conductivity of Denitrification Walls in Sand Aquifers. *Ground Water Monitoring and Remediation.* 28:57-64.
- Benner, S.G.; Blowes, D.W.; Molson, J.W.H. 2001. Modeling preferential flow in reactive barriers: Implications for performance and design. *Ground Water.* 39:371-379.
- Blowes, D.W.; Robertson, W.D.; Ptacek, C.J.; Merkle, C. 1994. Removal of agricultural nitrate from tile-drainage effluent water using in-line bioreactors. *JContamHydrol.* 15:207-221.
- Bohlke, J.K.; Denver, J.M. 1995. Combined use of groundwater dating, chemical, and isotopic analyses to resolve the history and fate of nitrate contamination in two agricultural watersheds, Atlantic Coastal Plain, Maryland. *Water Resources Research.* 31:2319-2339.
- Boussaid, F.; Martin, G.; Morvan, J.; Collin, J.J.; Landreau, A. 1988. Denitrification In-Situ of Groundwaters With Solid Carbon Matter. *Environmental Technology Letters ETLEDB* Vol9:8 ref.

- Breemen, N.; Boyer, E.W.; Goodale, C.L.; Jaworski, N.A.; Paustian, K.; Seitzinger, S.P.; Lajtha, K.; Mayer, B.; van Dam, D.; Howarth\*, R.W.; Nadelhoffer\*, K.J.; Eve\*, M.; Billen\*, G. 2002. Where did all the nitrogen go? Fate of nitrogen inputs to large watersheds in the northeastern U.S.A. *Biogeochemistry*. 57-58:267-293.
- Cameron, S.G.; Schipper, L.A. 2010. Nitrate removal and hydraulic performance of organic carbon for use in denitrification beds. *EcolEng*. 36:1588-1595.
- Committee on environment and natural resources [CENR], 2000. Integrated assessment of hypoxia in the northern Gulf of Mexico. National Science and technology council. Washington, D.C. Available at [http://oceanservice.noaa.gov/products/hypox\\_ia.pdf](http://oceanservice.noaa.gov/products/hypox_ia.pdf). (verified 11-15-11)
- Cooper, A.B. 1990. Nitrate depletion in the riparian zone and stream channel of a small headwater catchment. *Hydrobiologia*. 202:13-26.
- Cowell, B.C.; Dawes, C.J. 2006. Seasonal Comparisons of the Phytoplankton and Decline in Water Transparency in the Spring-Fed Rainbow River, Florida. *Journal of Freshwater Ecology*. 23:169-178.
- DeBusk, W.F.; Reddy, K.R. Turnover of detrital organic carbon in a nutrient-impacted Everglades marsh. *Soil SciSocAmJ*. 62:1460-1468; 1998
- Edwards, T.M.; Guillette, L.J. 2007. Reproductive characteristics of male mosquitofish (*Gambusia holbrooki*) from nitrate-contaminated springs in Florida. *Aquatic Toxicology*. 85:40-47.
- Edwards, T.M.; Miller, H.D.; Guillette, L.J. 2006. Water quality influences reproduction in female mosquitofish (*Gambusia holbrooki*) from eight Florida springs. *Environmental healthperspectives*. 114 Suppl 1:69-75.
- Elgood, Z.; Robertson, W.D.; Schiff, S.L.; Elgood, R. 2010. Nitrate removal and greenhouse gas production in a stream-bed denitrifying bioreactor. *EcolEng*. 36:1575-1580.
- Elser, J.J.; Andersen, T.; Baron, J.S.; Bergstroem, A.-K.; Jansson, M.; Kyle, M.; Nydick, K.R.; Steger, L.; Hessen, D.O. 2009. Shifts in Lake N:P Stoichiometry and Nutrient Limitation Driven by Atmospheric Nitrogen Deposition. *Science* (Washington). 326:835-837.
- Elser, J.J.; Bracken, M.E.S.; Cleland, E.E.; Gruner, D.S.; Harpole, W.; Hillebrand, H.; Ngai, J.T.; Seabloom, E.W.; Shurin, J.B.; Smith, J.E. 2007. Global analysis of nitrogen and phosphorus limitation of primary producers in freshwater, marine and terrestrial ecosystems. *Ecology Letters*. 10:1135-1142.

- Fetter, C.W. 2001. Applied hydrogeology. United States (USA): Prentice-Hall, Upper Saddle River, NJ, United States (USA).
- Florida Department of Environmental Protection [FDEP], 1997-98. Available at <http://www.fgdl.org> (verified 11-07-11). drainage\_basins\_1997\_areas.zip. Drainage basins. Tallahassee, Fl.
- Freeze, R.A.; Cherry, J.A. 1979. Groundwater / R. Allan Freeze, John A. Cherry.
- Galloway, J.N.; Aber, J.D.; Erisman, J.W.; Seitzinger, S.P.; Howarth, R.W.; Cowling, E.B.; Cosby, B.J. 2003. The Nitrogen Cascade. *Bioscience*. 53:341-356.
- Gardner, L.M.; White, J.R. 2010. Denitrification Enzyme Activity as an Indicator of Nitrate Movement through a Diversion Wetland. *Soil SciSocAmJ*. 74:1037-1047
- Goolsby, D.A.; Battaglin, W.A. 2000. Nitrogen in the Mississippi Basin; estimating sources and predicting flux to the Gulf of Mexico. United States (USA): U. S. Geological Survey, Reston, VA, United States (USA).
- Gradwell, M.W.; Birrell, K.S. 1979. Methods for physical analysis of soils. New Zealand (NZL): Department of Scientific and Industrial Research (DSIR), Lower Hutt, New Zealand (NZL).
- Greenan, C.M.; Moorman, T.B.; Kaspar, T.C.; Parkin, T.B.; Jaynes, D.B. 2006. Comparing Carbon Substrates for Denitrification of Subsurface Drainage Water. *JEnvironQual*. 35:824 p.
- Grierson, P.F.; Comerford, N.B.; Jokela, E.J. 1999. Phosphorus mineralization and microbial biomass in a Florida Spodosol: Effects of water potential, temperature and fertilizer application. *Biology and Fertility of Soils*. 28:244-252.
- Groffman, P.M.; Tiedje, J.M. 1989. Denitrification in north temperate forest soils: Relationships between denitrification and environmental factors at the landscape scale. *Soil BiolBiochem*. 21:621-626.
- Hallberg, G.R. 1989. Nitrate in Ground Water in the United States. IN: Nitrogen Management and Ground Water Protection Developments in Agricultural and Managed-Forest Ecology 21 Elsevier, New York, NY 1989 p 35-74, 11 fig, 4 tab.
- Hill, A.R. 1983. Denitrification: Its Importance in a River Draining an Intensively Cropped Watershed. *Agriculture, Ecosystems and Environment* Vol10. August:36 Ref.
- Hill, A.R. 1996. Nitrate Removal in Stream Riparian Zones. *JEnvironQual*. 25:743-755.
- Hong, N.; Scharf, P.C.; Davis, J.G.; Kitchen, N.R.; Sudduth, K.A. 2007. Economically Optimal Nitrogen Rate Reduces Soil Residual Nitrate. *JEnvironQual*. 36:354-362.

- Howarth, R.; Anderson, D.; Cloern, J.; Elfring, C.; Hopkinson, C.; Lapointe, B.; Malone, T.; Marcus, N.; McGlathery, K.; Sharples, A.; Walker, D. 2000. Nutrient Pollution of Coastal Rivers, Bays, and Seas. *Issues in Ecology*.
- Hudak, P.F. 2000. Regional trends in nitrate content of Texas groundwater. *Journal of hydrology*. 228:37-47.
- Hunter, W.J.; Follett, R.F.; Cary, J.W. 1997. Use of vegetable oil to remove nitrate from flowing groundwater. *TransASAE*. 40:345-354.
- Jacinte, P.-A.; Groffman, P.M.; Gold, A.J.; Mosier, A. 1998. Patchiness in microbial nitrogen transformations in groundwater in a riparian forest. *JEnvironQual*. 27:156-164.
- Jacinte, P.A.; Groffman, P.M.; Gold, A.J. 2003. Dissolved Organic Carbon Dynamics in a Riparian Aquifer: Effects of Hydrology and Nitrate Enrichment. *JEnvironQual*. 32:1365-1374.
- Jaynes, D.B.; Kaspar, T.C.; Moorman, T.B.; Parkin, T.B. 2008. In Situ Bioreactors and Deep Drain-Pipe Installation to Reduce Nitrate Losses in Artificially Drained Fieldss. *JEnvironQual*. 37:429 p.
- Lewis Jr, W.M.; Wurtsbaugh, W.A. 2008. Control of Lacustrine Phytoplankton by Nutrients: Erosion of the Phosphorus Paradigm. *International Review of Hydrobiology*. 93:446-465.
- Long, L.M.; Schipper, L.A.; Bruesewitz, D.A. 2010. Long-term nitrate removal in a denitrification wall. *Agriculture, Ecosystems & Environment*. 140:514-520; 2010
- Lowrance, R. 1992. Groundwater nitrate and denitrification in a coastal plain riparian forest. *JEnvironQual*. 21:401-405.
- Mackenzie, F.T.; Mackenzie, J.A. 1995. *Our changing planet; an introduction to Earth system science and global environmental change*. United States (USA): Prentice-Hall, Inc., Englewood Cliffs, NJ, United States (USA).
- Moorman, T.B.; Parkin, T.B.; Kaspar, T.C.; Jaynes, D.B. 2010. Denitrification activity, wood loss, and N<sub>2</sub>O emissions over 9 years from a wood chip bioreactor. *EcolEng*. 36:1567-1574.
- Mukherjee, A.; Zimmerman, A.R.; Harris, W. 2011. Surface chemistry variations among a series of laboratory-produced biochars. *Geoderma*. 163:247-255
- Nolan, B.T. 1999. Nitrate behavior in ground waters of the Southeastern USA. *JEnvironQual*. 28:1518-1527.

- Nolan, B.T. 2001. Relating nitrogen sources and aquifer susceptibility to nitrate in shallow ground waters of the United States. *Ground Water*. 39:290-299.
- Nolan, B.T.; Stoner, J.D. 2000. Nutrients in groundwaters of the conterminous United States, 1992-1995. *Environmental Science & Technology, ES & T*. 34:1156-1165.
- Parkin, T.B. 1987. Soil microsites as a source of denitrification variability. *Soil SciSocAmJ*. 51:1194-1199.
- Patterson, B.M.; Grassi, M.E.; Davis, G.B.; Robertson, B.S.; McKinley, A.J. 2002. Use of polymer mats in series for sequential reactive barrier remediation of ammonium-contaminated groundwater; laboratory column evaluation. *Environmental Science & Technology, ES & T*. 36:3439-3445.
- Puckett, L.J. 1995. Identifying the Major Sources of Nutrient Water Pollution. *Environmental Science & Technology [EnvironSciTechnol]*. 29.
- Puckett, L.J.; Cowdery, T.K.; Lorenz, D.L.; Stoner, J.D. 1999. Estimation of nitrate contamination of an agro-ecosystem outwash aquifer using a nitrogen mass-balance budget. *JEnvironQual*. 28:2015-2025.
- Quinlan, E.L.; Philips, E.J.; Donnelly, K.A.; Jett, C.H.; Sleszynski, P.; Keller, S. 2008. Primary producers and nutrient loading in Silver Springs, FL, USA. *Aquatic Botany*. 88:247-255.
- Rabalais, N.N. 2002. Nitrogen in Aquatic Ecosystems. *Ambio*. 31:102-112.
- Reddy, K.R.; DeLaune, R.D. 2008. Biogeochemistry of wetlands : science and applications / K. Ramesh Reddy and Ronald D. DeLaune.
- Refsgaard, J.C.; Thorsen, M.; Jensen, J.B.; Kleeschulte, S.; Hansen, S. 1999. Large scale modelling of groundwater contamination from nitrate leaching. *Journal of hydrology*. 221:117-140.
- Robertson, W.D. 2010. Nitrate removal rates in woodchip media of varying age. *EcolEng*. 36:1581-1587.
- Robertson, W.D.; Blowes, D.W.; Ptacek, C.J.; Cherry, J.A. 2001. Long-term performance of in situ reactive barriers for nitrate remediation. *Ground Water*. 38:689-695.
- Robertson, W.D.; Murphy, A.M.; Cherry, J.A. 1995. Low-cost on-site treatment of landfill leachate using infiltration beds; preliminary field trial. *Ground Water Monitoring & Remediation*. 15:107-115.

- Robertson, W.D.; Ptacek, C.J.; Brown, S.J. 2009. Rates of Nitrate and Perchlorate Removal in a 5-Year-Old Wood Particle Reactor Treating Agricultural Drainage. *Ground Water Monitoring and Remediation*. 29:87-94.
- Robertson, W.D.; Vogan, J.L.; Lombardo, P.S. 2008. Nitrate Removal Rates in a 15-Year-Old Permeable Reactive Barrier Treating Septic System Nitrate. *Ground Water Monitoring & Remediation*. 28:65-72.
- Robertson, W.D.; Yeung, N.; vanDriel, P.W.; Lombardo, P.S. High-Permeability Layers for Remediation of Ground Water; Go Wide, Not Deep. *Ground Water*. 43:574-581; 2005
- Schindler, D.W. 1977. Evolution of phosphorus limitation in lakes. *Science*. 195:260-262.
- Schipper, L.; Vojvodic-Vukovic, M. 1998. Nitrate removal from groundwater using a denitrification wall amended with sawdust; field trial. *JEnvironQual*. 27:664-668.
- Schipper, L.A.; Barkle, G.F.; Hadfield, J.C.; Vojvodic-Vukovic, M.; Burgess, C.P. 2004. Hydraulic constraints on the performance of a groundwater denitrification wall for nitrate removal from shallow groundwater. *JContamHydrol*. 69:263-279.
- Schipper, L.A.; Barkle, G.F.; Vojvodic-Vukovic, M. 2005. Maximum Rates of Nitrate Removal in a Denitrification Wall. *JEnvironQual*. 34:1270-1276.
- Schipper, L.A.; Cameron, S.C.; Warneke, S. 2010a. Nitrate removal from three different effluents using large-scale denitrification beds. *EcolEng*. 36:1552-1557.
- Schipper, L.A.; Cooper, A.B.; Harfoot, C.G.; Dyck, W.J. 1993. Regulators of denitrification in an organic riparian soil. *Soil BiolBiochem*. 25:925-933.
- Schipper, L.A.; Robertson, W.D.; Gold, A.J.; Jaynes, D.B.; Cameron, S.C. 2010b. Denitrifying bioreactors--An approach for reducing nitrate loads to receiving waters. *EcolEng*. 36:1532-1543.
- Schipper, L.A.; Vojvodic-Vukovic, M. 2000. Nitrate removal from groundwater and denitrification rates in a porous treatment wall amended with sawdust. *EcolEng*. 14:269-278.
- Schipper, L.A.; Vojvodic-Vukovic, M. 2001. Five years of nitrate removal, denitrification and carbon dynamics in a denitrification wall. *Water Res*. 35:3473-3477.
- Seitzinger, S.; Harrison, J.A.; Boehlke, J.K.; Bouwman, A.F.; Lowrance, R.; Peterson, B.; Tobias, C.; Van Drecht, G. 2006. Denitrification across landscapes and waterscapes: A synthesis. *Ecological Applications*. 16:2064-2090.

- Smil, V. 2001. Enriching the earth : Fritz Haber, Carl Bosch, and the transformation of world food production / Vaclav Smil.
- Smil, V. 2002. Nitrogen and Food Production: Proteins for Human Diets. *Ambio*. 31:126-131.
- Sparling, G.P.; Feltham, C.W.; Reynolds, J.; West, A.W.; Singleton, P. 1990. Estimation of soil microbial C by a fumigation-extraction method: Use on soils of high organic matter content, and a reassessment of the  $k_{sub}(EC)$ -factor. *Soil BiolBiochem*. 22:301-307.
- Tiedje, J.M. 1982. Denitrification. p.1011-1026. *In* A.L. Page et al. (ed.). *Methods of soil analysis*. Part 2. 2<sup>nd</sup> ed. Agron. Monogr. 9. ASA and SSSA, Madison, WI.
- Tiedje, J.M.; Simkins, S.; Groffman, P.M. 1989. Perspectives on Measurement of Denitrification in the Field Including Recommended Protocols for Acetylene Based Methods. *Plant and Soil*. 115:261.
- Timlin, D.J.; Ahuja, L.R.; Pachepsky, Y.; Williams, R.D.; Gimenez, D.; Rawls, W. 1999. Use of Brooks-Corey parameters to improve estimates of saturated conductivity from effective porosity. *Soil SciSocAmJ*. 63:1086-1092.
- Trachtenberg, E.; Ogg, C. 1994. Potential for Reducing Nitrogen Pollution Through Improved Agronomic Practices. *Water Resources Bulletin*. 30:1109 p.
- U.S. Geological Survey [USGS], 2006. Available at <http://www.fgdl.org>. (verified 11-07-11). NHD24Line\_May06. National Hydrography Dataset – Linear Hydrographic Landmarks 1:24K. Reston, Va.
- Van Soest, P.J.; Robertson, J.B.; Lewis, B.A. 1991. Methods for dietary fiber, neutral detergent fiber, and nonstarch polysaccharides in relation to animal nutrition. *Journal of dairy science*. 74:3583-3597.
- Vance, E.D.; Brookes, P.C.; Jenkinson, D.S. 1987. An extraction method for measuring soil microbial biomass C. *Soil BiolBiochem*. 19:703-707.
- Vitousek, P.M.; Aber, J.D.; Howarth, R.W.; Likens, G.E.; Matson, P.A.; Schindler, D.W.; Schlesinger, W.H.; Tilman, D.G. 1997. Human alteration of the global nitrogen cycle: Sources and consequences. *Ecological Applications*. 7:737-750.
- Vogan, J.; Robertson, W.; Gillham, R.; Cherry, J.; 1992. Society of Environmental Toxicology and Chemistry, P.U. A field trial of emplaced denitrifying layers to promote nitrate removal from septic system effluent.

- Volokita, M.; Abeliovich, A.; Soares, M.I.M. 1996a. Denitrification of groundwater using cotton as energy source. *Water quality international '96 : selected proceedings of the 18th Biennial Conference of the International Association on Water Quality, held in Singapore, 23-28 June 1996.* Oxford [England] ; Tarrytown, New York;
- Volokita, M.; Belkin, S.; Abeliovich, A.; Soares, M.I.M. 1996b. Biological denitrification of drinking water using newspaper. *Water Res.* 30:965-971.
- Wakatsuki, T.; Esumi, H.; Omura, S. 1993. High performance and N & P-removable on-site domestic waste water treatment system by multi-soil-layering method. *Water SciTechnol.* 27:31-40.
- Warneke, S.; Schipper, L.A.; Bruesewitz, D.A.; McDonald, I.; Cameron, S. 2011. Rates, controls and potential adverse effects of nitrate removal in a denitrification bed. *EcolEng.* 37:511-522.
- White, J.R.; Reddy, K.R. 1999. Influence of nitrate and phosphorus loading on denitrifying enzyme activity in Everglades wetland soils. *Soil SciSocAmJ.* 63:1945-1954.
- White, J.R.; Reddy, K.R. 2003. Nitrification and Denitrification Rates of Everglades Wetland Soils along a Phosphorus-Impacted Gradient. *JEnvironQual.* 32:2436-2443.
- Yoshinari, T.; Hynes, R.; Knowles, R. 1977. Acetylene Inhibition of Nitrous Oxide Reduction and Measurement of Denitrification and Nitrogen Fixation in Soil. *Soil Biology and Biochemistry* Vol 9:23 ref.

## BIOGRAPHICAL SKETCH

I was born amongst the whispering pines and shivering aspens of Spokane Washington. The expansive forest provided inspiration for my inquisitiveness and my parents supportive acquiescence allowed me to make many mistakes and subsequently learn from them. As a child, observing the interconnected and obsessive struggle for life on a visit to the Hoh Rainforest in western Washington sparked a lifelong love of science and a drive for answers. I attended the University of Washington in Seattle, WA and earned a Bachelor of Science degree in biology with a track focused on evolution, ecology and conservation biology. I also earned an intensive minor in Fisheries and Aquatic Sciences. I received a Master of Science degree from the University of Florida in Gainesville FL majoring in Soil and Water Sciences. My research dealt with examining the impacts on alluvial floodplain soil biogeochemistry and vegetative succession resulting from decades of land-use conversion. I received the State of Florida Alumni Award which provided funds for a Ph.D. and so I re-enrolled in the Soil and Water Science Department at the University of Florida. During this tenure, I worked with a team to analyze metal contamination and the potential for future mobility and bioavailability of sediments deposited on New Orleans, LA after hurricane Katrina. This was a natural extension from my master's work because the hurricane had turned the entire city in to a floodplain. After this period, I made a large shift in focus to work on permeable reactive barriers for the bioremediation of nitrate in groundwater, for my Ph.D. I finished my Ph.D. from the University of Florida in December, 2011.